

CHARACTERIZATION OF PF/PVAC HYBRID ADHESIVE-WOOD  
INTERACTION AND ITS EFFECT ON WOOD STRAND  
COMPOSITES PERFORMANCE

By

YANG CAO

A thesis submitted in partial fulfillment of the requirements for the degree of  
MASTER OF SCIENCE IN CIVIL ENGINEERING

WASHINGTON STATE UNIVERSITY  
Department of Civil and Environmental Engineering

AUGUST 2010

To the Faculty of Washington State University,

The members of the Committee appointed to examine the thesis of YANG CAO  
find it satisfactory and recommend that it be accepted.

---

Vikram Yadama, Ph.D, Co-Chair

---

Jinwen Zhang, Ph.D, Co-Chair

---

Karl Englund, Ph.D

## ACKNOWLEDGEMENTS

There are so many individuals that I would like to express my gratitude to. I could not be more thankful to my advisor and committee co-chair, Dr. Vikram Yadama for his meaningful guidance, invaluable insight and always positive encouragement. I am grateful to him for bringing me into this project, as I learned so much from him and enjoyed studying and working with him. My special thanks also go to my committee co-chair Dr. Jinwen Zhang, for his support whenever I needed it, as well as my committee member Dr. Karl Englund, for his encouragement and help.

I am also grateful to the CMEC personnel for their countless support and help. Thank you to Robert Duncan, Scott Lewis and Brent Olson, for their experienced and valuable support and suggestions for my experiments. I would also like to thank the staff at CMEC, including Judy Edmister, Pat Smith and Janet Duncan.

Many thanks go to Dr. Michael Knoblauch, Valerie Lynch-Holm, and Christine Davitt at FMIC, for their kind help on my microscopy experiments whenever I needed it. Thank you also to Dr. Rich Alldredge of the Statistics department, who gave me quick and helpful advice on data analysis.

Thank you also to graduate students Yi Wang and Christopher Voth, for your helpful assistance with OSB fabrication, and making the manufacturing process much more efficient with their previous experience. I would also like to thank Derek Tsai, who continues to give me valuable suggestions on my experiments. I am also grateful for my colleges and friends at the lab, including Helen, Amir, Wenbo, Fang, Amy, Greg, and William. I value greatly the fun time we

had together. I extend many thanks to my lovely roomie Mora, my friends Jieni, Shuai, Ding, Maggie Yu, and all my other friends in Pullman; my life would not be so colorful without you guys.

I would love to express my exceptional thanks to my Mum and Dad, for their unconditional love and support, as well as bright advice in every aspect. Finally, I am thankful to my great friends back in China for their sincere and supportive help.

CHARACTERIZATION OF PF/PVAC HYBRID ADHESIVE-WOOD -  
INTERACTION AND ITS EFFECT ON WOOD STRAND  
COMPOSITES PERFORMANCE

**ABSTRACT**

by Yang Cao, M.S.

Washington State University

August 2010

Co-Chairs: Vikram Yadama  
Jinwen Zhang

A multifunctional hybrid adhesive system developed for profiled composite manufacturing was examined in this study. A binary adhesive system, phenol formaldehyde (PF)/ polyvinyl acetate (PVAc), offers initial adhesion to improve wood-strand mat handling during the first stage of composite processing, after which a durable bond is achieved through curing of PF resin under heat and pressure. Before effectively applying this adhesive, it is important to understand adhesive-wood interaction at different scales.

This thesis evaluated the physical properties of PF and PVAc resin blend as individual resin proportions were varied, and then characterized the interactions between the PF/PVAc hybrid adhesive and the wood substrate by evaluating bond strength at macro-scale, and gross adhesive penetration at micro-scale in sugar maple (tangential and radial surfaces). The bond performance and adhesive penetration of PF/PVAc were found to be comparable with that of neat PF when PVAc content was less than 50% in the resin blend, while they underwent an

obvious deterioration when PVAc content rose beyond 50%.

Results regarding wood strand composite performance using a response surface model indicate that addition of PVAc does not significantly affect MOE. However, PVAc content has a positive effect on MOR, IB under normal conditions, water absorption and thickness swelling; whereas, under changing environmental conditions, increase in PVAc content beyond optimum ratio has a negative effect on MOR. In general, applying PF first during the blending process in manufacturing wood-strand composites leads to improved performance in terms of mechanical and physical properties. Results indicate a percentage-dependent effect of PVAc on the interference between PF and wood strands. Because PVAc has good deformability, it can evenly transfer stress from strand to strand, increasing bond strength. However, there is an inverse effect of PVAc under severe RH treatment because of the poor water resistance of PVAc. A PF/PVAc ratio range from 1:0.6 to 1:0.77 is suggested as an optimized ratio in hot-pressing of wood-strand composites.

# TABLE OF CONTENTS

<b>ACKNOWLEDGEMENTS .....</b>	<b>III</b>
<b>ABSTRACT .....</b>	<b>V</b>
<b>TABLE OF CONTENTS .....</b>	<b>VII</b>
<b>LIST OF FIGURES .....</b>	<b>X</b>
<b>LIST OF TABLES.....</b>	<b>XIII</b>
<b>CHAPTER 1 INTRODUCTION.....</b>	<b>1</b>
PREVIOUS RESEARCH REGARDING HYBRID ADHESIVES .....	2
OBJECTIVE OF THE THESIS.....	3
ORGANIZATION OF THE THESIS.....	5
REFERENCES .....	7
<b>CHAPTER 2 CHARACTERIZATION OF PF/PVAC-WOOD INTERACTION: BOND PERFORMANCE AND ADHESIVE PENETRATION QUANTIFICATION.....</b>	<b>8</b>
INTRODUCTION .....	8
OBJECTIVE.....	9
BACKGROUND .....	10
Phenol Formaldehyde (PF) and Polyvinyl Acetate (PVAc) Resin.....	10
Characteristics of wood .....	11
Adhesive bonding .....	13
Adhesive penetration .....	16
MATERIALS AND METHODS.....	25
Experimental Design.....	25
Materials .....	25

pH Testing .....	27
Viscosity and Morphology of PF/PVAc Resin Blends .....	27
Shear Strength.....	28
Penetration Quantification .....	32
<b>RESULTS AND DISCUSSION .....</b>	<b>37</b>
pH Value.....	37
Viscosity and Dispersion of Resin Blends .....	38
Shear Block Strength of Neat Sugar Maple .....	42
Bond Performance and Adhesive Penetration of binary adhesives.....	43
<b>SUMMARY AND CONCLUSIONS.....</b>	<b>52</b>
<b>REFERENCES .....</b>	<b>54</b>
 <b>CHAPTER 3 INFLUENCE OF THE PF/PVAC RATIO AND ADHESIVE APPLICATION SEQUENCE ON WOOD STRAND COMPOSITE PERFORMANCE .....</b>	 <b>57</b>
INTRODUCTION .....	57
OBJECTIVE .....	58
BACKGROUND .....	59
Adhesive Blend for Wood Composite .....	59
Characteristics of Wood Composites Performance.....	61
MATERIALS AND METHODS.....	66
Experimental Design.....	66
Materials .....	67
Wood Composite Manufacturing.....	69
Testing for Mechanical and Physical Properties.....	71
RESULTS AND DISCUSSION .....	75
Density Profile .....	75
Density Effect as a Covariate.....	76
Effects of PF/PVAc ratios.....	78



Effects of Resin Application Sequence .....	81
Optimization .....	93
SUMMARY AND CONCLUSIONS .....	95
REFERENCES .....	97
<b>CHAPTER 4 PROJECT SUMMARY, CONCLUSIONS AND FURTHER WORK .....</b>	<b>100</b>
SUMMARY AND CONCLUSIONS .....	100
FURTHER WORK .....	102
REFERENCES .....	103
<b>APPENDIX A HOT PRESS SCHECULE.....</b>	<b>104</b>
<b>APPENDIX B STATISTICS ON BOND PERFORMANCE.....</b>	<b>105</b>
<b>APPENDIX C STATISTICS ON PROPERTIES OF WOOD STRAND COMPOSITES.....</b>	<b>107</b>

## LIST OF FIGURES

Figure 1-1 Structure of the thesis.....	5
Figure 1-2 Structure of the thesis.....	6
Figure 2-1 Chemical reaction of phenol formaldehyde (Frihart 2005a).....	11
Figure 2-2 Chemical formula of PVAc (Kim and Kim 2006).....	11
Figure 2-3 Macroscopy of wood structure (Marra, 1992) .....	12
Figure 2-4 Micrograph of hardwood Red Oak, X100; Softwood, Eastern white pine, X150 (Hoadley 1990) .....	13
Figure 2-5 Chain-link analogy for adhesion in wood (Marra 1992).....	14
Figure 2-6 PF-Sugar maple adhesion interphase taken by FEI 200F SEM .....	20
Figure 2-7 Principles of fluorescence atoms (“Nobel Web, The Fluorescence Microscope” 2010) .....	21
Figure 2-8 Key point for confocal microscopy-pinhole (Confocal tutorial 2010).....	24
Figure 2-9 Glued wood specimen for neat wood shear block test.....	28
Figure 2-10 Clamp procedure for shear bonding, tangential to tangential surface.....	30
Figure 2-11 Specimens cutting from assembly joint .....	31
Figure 2-12 Shear block test conducted with Instron 4400R.....	32
Figure 2-13 Bond line of neat PVAc without dye after heating at 150 °C, Tangential surface of sugar maple glued with radial surface, taken by Leica Fluorescence Microscopy .....	33
Figure 2-14 A 80 µm Section Cut from Sliding Microtome.....	34
Figure 2-15 Images of adhesive penetration Left-hand, binary adhesive bond line taken with CLSM (tangential surface); Right-hand, 8-bit image after applying a threshold .....	35

Figure 2-16 Image conversion for counting adhesive-filled Lumens .....	36
Figure 2-17 pH of PF/PVAc resin blends at 25 °C .....	37
Figure 2-18 Viscosity of PF:PVAc=3:1, mix for different time periods under 1000rpm, tested under 50rpm at 25 °C .....	39
Figure 2-19 Viscosities of resin blends with increased PVAc percent, blend for 15 minutes under 1000rpm, tested at 25 °C .....	40
Figure 2-20 Morphology of Neat PF (left) and PVAc (right).....	41
Figure 2-21 Dispersion of resin blends, a, PF:PVAc =75%:25%; b, PF:PVAc =50%:50%; c, PF:PVAc =25%:75% .....	42
Figure 2-22 Dispersion of PF: PVAc=50%: 50% under 1000rpm for; a, 5 minutes; b 10 minutes; c, 15 minutes; d, 20 minutes.....	42
Figure 2-23 Bond performance of assembly joints with wood on tangential surface .....	48
Figure 2-24 Shear stress/strain curve of neat PF, neat PVAc and hybrid adhesive .....	48
Figure 2-25 Adhesive penetration of assembly joints with wood on tangential surface ..	49
Figure 2-26 Comparison of adhesive penetration into sugar maple on tangential surface	50
Figure 2-27 Bond performance of assembly joints with wood on radial surface .....	51
Figure 2-28 Adhesive penetration of assembly joints with wood on radial surface .....	51
Figure 3-1 Pressing schedule for hot-pressing test panels .....	70
Figure 3-2 Resinated strands distributed through forming box .....	71
Figure 3-3 Loose mat and hot pressing .....	71
Figure 3-4 Specimen cutting pattern for test panels. ....	72
Figure 3-5 Severe relative humidity treatment to cycle the specimens through equilibrium moisture contents of 12%, 24%, 5% and back to 12% .....	73

Figure 3-6 Static bending test (Left) and internal bond test (Right).....	74
Figure 3-7 Water submersion (Left) and five-spots thickness measurement (Right).....	75
Figure 3-8 Density Profiles.....	76
Figure 3-9 Model graphs of MOE1 and MOE2.....	86
Figure 3-10 Model graphs of MOE1 and MOE2.....	86
Figure 3-11 Model graphs of I B1and IB2.....	87
Figure 3-12 Model graphs of 2hrs and 24hrs WA .....	87
Figure 3-13 Model graphs of 2hrs and 24hrs TS .....	88
Figure 3-14 Effect of application sequence on MOR1 and MOR2 .....	88
Figure 3-15 Interaction of application sequences of MOR2 at 4%PF, 5%PF and 6%PF, respectively .....	89
Figure 3-16 Effect of application sequence on IB1 and IB2 .....	89
Figure 3-17 Interaction of application sequences of IB1 at 4%PF, 5%PF and 6%PF, respectively .....	90
Figure 3-18 Effect of application sequence on 2hrs WA and 24hrs WA .....	90
Figure 3-19 Interaction of application sequences of 24hrs WA at 4%PF, 5%PF and 6%PF, respectively .....	91
Figure 3-20 Effect of application sequence on 2hrs TS and 24hrs TS .....	91
Figure 3-21 Speculated mechanism of applying PF first and applying PVAc first, respectively .....	92

## LIST OF TABLES

Table 2-1 Summary of parameters in fluorescence microscopy and stain techniques .....	22
Table 2-2 Ratio points of PF/PVAc and corresponding specimen replicates .....	26
Table 2-3 Parameters of PF and PVAc resin .....	26
Table 2-4 Shear block strength of neat sugar maple on both tangential and radial surfaces .....	43
Table 3-1 A total of 32 runs or design points implemented based on D-optimal response surface design by State-Ease.....	68
Table 3-2 Sampling scheme for each panel .....	73
Table 3-3 Statistics of Fitted Models for each Response.....	84
Table 3-4 Percentage differences of hybrid adhesive with 6% PF and varying percent of PVAc relative to control test panels bonded with only 6%PF (All values in cells are percents) .....	85
Table 3-5 Optimization criteria for wood strand panel properties.....	94
Table 3-6 Four optimized solutions for wood strand panels performance .....	94
Table 3-7 Comparison of Optimized solution with control of 6%PF .....	95
Table A-1 Hot press schedule .....	104
Table B-1 P-values of ANOVA & ANCOVA considering density as covariate on tangential surface .....	105
Table B-2 P-values of ANOVA & ANCOVA considering density as covariate on radial surface .....	105
Table B-3 Bond performances of assembly joints with wood on tangential surfaces based on SAS output .....	106

Table B-4 Bond performances of assembly joints with wood on radial grain surfaces based on SAS output.....	106
Table C-1 Statistics of fitted models for each response.....	107
Table C-2 Summery of properties of wood strand composites.....	108

## **CHAPTER 1 INTRODUCTION**

Wood-strand composites are playing an increasingly important role in the wood industry, due to their efficient utilization of raw materials. In terms of optimizing the performance of wood composites, several factors have been found to be most influential. These include resin content, additives, flake geometry, flake alignment, and processing parameters such as temperature and moisture content. A promising approach to improving the structural properties of wood composites panels is to develop a more efficient geometry, for example, in the corrugated shape of strand mats, which is already a mature development in plastic and sheet metal industries (Pang et al. 2007).

An efficient solution to process profiled wood composite panel is for strand mat to go through a thermoforming process such as pultrusion to manufacture products with a net-shape design. These processes that are continuous in nature require both the integrity of the wood strand mat and durable bonding between adhesive and wood strands in the optimization of product quality. Having a multi-functional adhesive, which can offer both enough initial adhesion to avoid unwanted shifting of strand elements during handling and a strong adhesive bond at the end of the curing process, will facilitate development of continuous manufacturing systems for net-shape composite production.

Wang et al. (2010) have proposed an effective multi-functional adhesive system that can potentially be used in thermoforming of wood-strand composites. A combination of thermosetting resin, phenol formaldehyde (PF), and thermoplastic resin, polyvinyl acetate emulsion (PVAc), was suggested and cure kinetics of the resin blend was investigated. The initial adhesion between strands with such an adhesive system can be achieved for mat handling

with PVAc in the first stage, and durable bond strength can be obtained with PF under complete curing in second stage.

## **Previous research regarding hybrid adhesives**

Hybrid adhesives, a combination of two or more adhesives, have the potential to provide multi-functionality in wood composites, as they take advantage of the strengths of several adhesives. Several studies have been conducted on resin blends during the last few years. For instance, a combination-PF Resole and Polymeric Diphenylmethane Diisocyanate (pMDI) hybrid adhesive was studied for its rheological and viscometric properties, penetration and curing behaviors, as well as its chemistry and morphology (Zheng 2002). The study showed that good bond line performance could be accomplished with good resin penetration, a fast cure rate and a certain degree of co-reaction.

When the morphologies of PF/pMDI were studied, it was concluded that the liquid emulsion morphology was preserved in the resulting solid, although there was some inter-diffusion between phases during curing (Riedlinger and Frazier 2008). This PF/pMDI hybrid adhesive was also applied to oriented strand lumber, and properties including the modulus of rupture, modulus of elasticity and internal bond strength proved to be qualified for the CSA O 437.1-93 standards. The OSL with pure PF and hybrid adhesives also passed thickness, swelling and bond durability tests, although the pure pMDI failed to pass (Preechatiwong et al. 2007).

Another hybrid adhesive composed of melamine-formaldehyde and polyvinyl acetate was investigated in a series of papers (Kim and Kim 2005, 2006a, b; Kim et al. 2007), and it was concluded that adding more PVAc not only reduced formaldehyde emissions, but curing temperature as well. Furthermore, the studies found that the thermal stability of the MF/PVAc



increases as PVAc content increases, and initial tackiness can be achieved when the blend is applied on decorative veneer and plywood surfaces. A study on the microcrystallinity and colloidal peculiarities of urea-formaldehyde resin and polymeric diphenylmethane diisocyanates (pMDI) blend was also conducted (Wieland et al. 2007). A resin blend of polyvinyl acetate and a novolac type phenolic resin was studied and the blend seemed miscible in the amorphous phase, with strong inter-association hydrogen bonds between the hydroxyl group of phenolic and the carbonyl group of PVAc (Huang et al. 2002). Another study on the application of a polyvinyl acetate emulsion (PVAc) fortified with urea-formaldehyde (UF) on laminated bamboo found no significant difference between PVAc fortified UF and neat UF in terms of modulus of elasticity and modulus of rupture (Talabgaew and Laemlaksakul 2007). Phenol formaldehyde resole has also been added into PVAc- $\text{AlCl}_3$  catalyzed latex to improve its durability by Lopez-Suevos and Frazier (2006).

## **Objective of the thesis**

The cure kinetics of this PF/PVAc hybrid adhesive has been previously studied (Wang et al. 2010) and results showed that the curing process of PF slowed as PVAc increased. With a PF/PVAc ratio of less than 1:1, cure kinetics did not differ significantly from that of neat PF. In order to evaluate the properties of the binary adhesive-wood bond, studies must explore the interaction between adhesives and adherends, since this influences the bond formation, bond strength, and durability of the bonded assembly. To obtain a comprehensive and persuasive understanding of the binary adhesive-wood surface interaction, performance must also be evaluated using different spatial scales (Frihart 2005). This thesis explores these factors, as well as the processing parameters that influence manufacturing of a wood-strand composite. The main

goal of this thesis is to understand the interaction between the individual resins in the PF/PVAc binary adhesive system and the wood substrate at different levels of scales, and to evaluate the efficacy of applying such a binary adhesive in hot-pressing of wood-strand composite and the effects of resin ratios and their application sequence on composite performance.

The specific objectives of this thesis are to:

- Study the physical properties of the resin blend, and understand its influence on adhesive-wood interaction and bond performance
- Study the interaction between PF/PVAc resins of different blend ratios and wood substrate, and determine the effect of adhesive ratios on bond performance and adhesive gross penetration
- Evaluate the physical and mechanical properties of hot-pressed wood-strand composite as they are affected by the ratio and application sequence of the two individual resins in the hybrid adhesive system

## Organization of the thesis

The structure of the thesis is organized as shown in Figure 1-1.

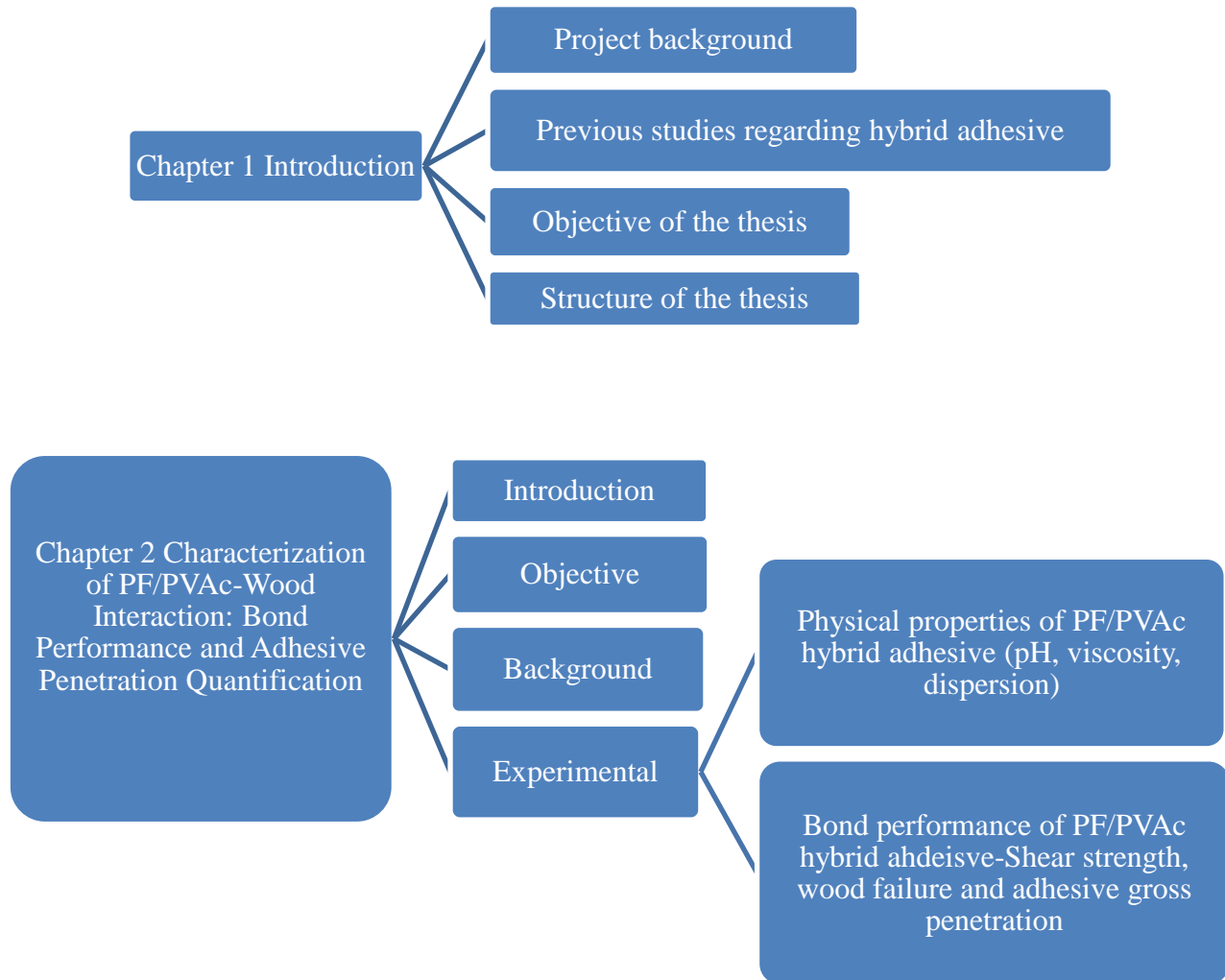


**Figure 1-1 Structure of the thesis**

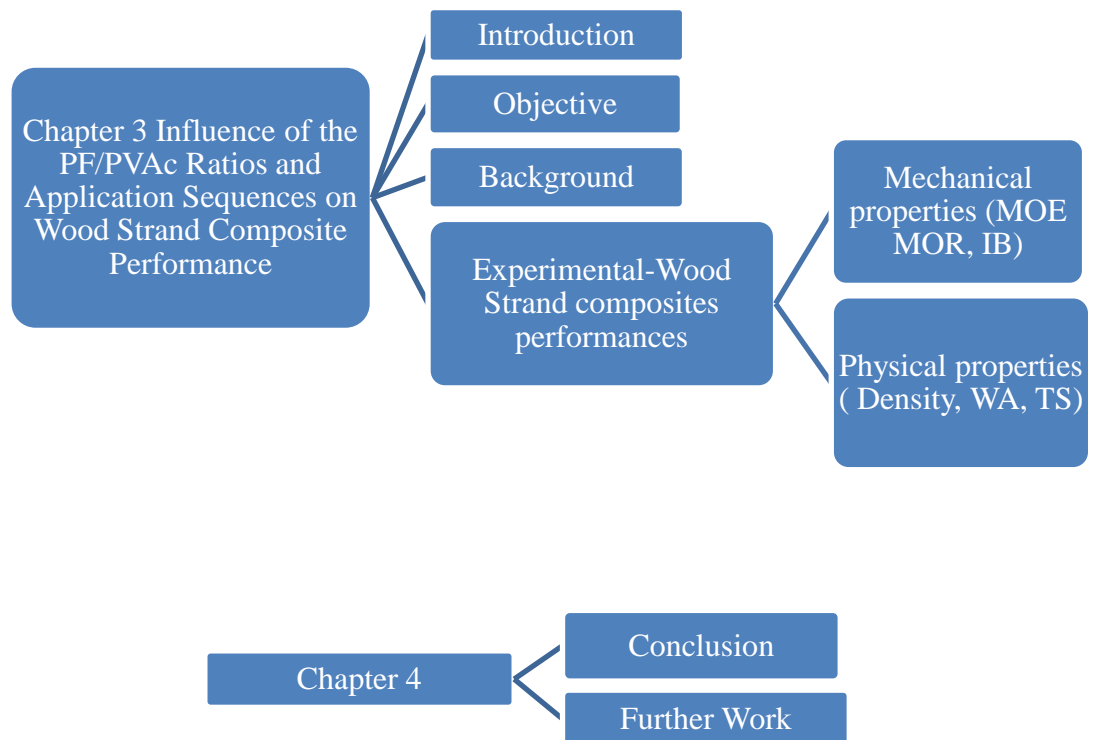


**Figure 1-2 Structure of the thesis**

## References

- Frihart, C. R. (2005). "9 Wood Adhesion and Adhesives." *Handbook of wood chemistry and wood composites*, 215.
- Huang, M. W., Kuo, S. W., Wu, H. D., Chang, F. C., and Fang, S. Y. (2002). "Miscibility and hydrogen bonding in blends of poly (vinyl acetate) with phenolic resin." *Polymer*, 43(8), 2479–2487.
- Kim, S., and Kim, H. J. (2005). "Effect of addition of polyvinyl acetate to melamine-formaldehyde resin on the adhesion and formaldehyde emission in engineered flooring." *International Journal of Adhesion and Adhesives*, 25(5), 456–461.
- Kim, S., and Kim, H. J. (2006a). "Initial tack and viscoelastic properties of MF/PVAc hybrid resins used as adhesives for composite flooring materials." *Journal of Adhesion Science and Technology*, 20(7), 705–722.
- Kim, S., and Kim, H. J. (2006b). "Thermal stability and viscoelastic properties of MF/PVAc hybrid resins on the adhesion for engineered flooring in under heating system; ONDOL." *Thermochimica Acta*, 444(2), 134–140.
- Kim, S., Kim, J. A., An, J. Y., Kim, H. J., Do Kim, S., and Park, J. C. (2007). "TVOC and formaldehyde emission behaviors from flooring materials bonded with environmental-friendly MF/PVAc hybrid resins." *Indoor air*, 17(5), 404–415.
- Lopez-Suevos, F., and Frazier, C. (2006). "Fracture cleavage analysis of PVAc latex adhesives: Influence of phenolic additives." *Holzforschung*, 60(3), 313–317.
- Pang, W., Sandberg, L., Laks, P., and Forsman, J. (2007). "Corrugated strandboard structural panels." *Forest Products Journal*, 57(3), 48–53.
- Preechatiwong, W., Yingprasert, W., and Kyokong, B. (2007). "Effects of phenol-formaldehyde/isocyanate hybrid adhesives on properties of oriented strand lumber (OSL) from rubberwood waste." *Songklanakarin Journal of Science and Technology*, 29(5), 1367–1375.
- Riedlinger, D. A., and Frazier, C. E. (2008). "Morphological analysis of PF/pMDI hybrid wood adhesives." *Journal of Adhesion Science and Technology*, 22(12), 1197–1208.
- Talabgaew, S., and Laemlaksakul, V. (2007). "Experimental Studies on the Mechanical Property of Laminated Bamboo in Thailand." *International Journal of Mathematical, Physical and Engineering Sciences*, 1, 4.
- Wang, Y., Yadama, V., Marie, P. L., and Debes, B. (2010). "Cure Kinetics of PF/PVAc hybrid adhesive for Manufacturing Profiled Wood-Strand Composites." *Holzforschung In press*.
- Wieland, S., Pizzi, A., Grigsby, W., Warnes, J., and Pichelin, F. (2007). "Microcrystallinity and colloidal peculiarities of UF/isocyanate hybrid resins." *Journal of Applied Polymer Science*, 104(4), 2633–2636.
- Zheng, J. (2002). "Studies of PF resole/isocyanate hybrid adhesives." Ph.D Dissertation, Virginia Polytechnic Institute and State University, Blacksburg, Virginia.

# **CHAPTER 2 CHARACTERIZATION OF PF/PVAC-WOOD INTERACTION: BOND PERFORMANCE AND ADHESIVE PENETRATION QUANTIFICATION**

## **Introduction**

Profiled wood-strand composites offer a potentially effective solution for manufacturers to produce specialty composites, such as light-weight laminates, while reducing the consumption of wood fiber and adhesives. Thermoforming, such as roll forming and matched die forming, are potential manufacturing methods when producing profiled veneer composites. Continuous forming of strand-based composites, however, poses some difficulties during the fabrication process due to discontinuous nature of the strand mat. There is a high potential for strands to break apart during the mat handling process. A multi-functional adhesive that provides initial bonding for mat integrity followed by the required bond strength after the manufacturing process is a potential solution pursued in an overall project that this study is part of. A multi-functional, hybrid adhesive, composed of Phenol-formaldehyde (PF) and Polyvinyl acetate emulsion (PVAc), is proposed to provide this dual functionality.

PF is a commonly used adhesive in structural wood composites. It offers good bond strength and durability by forming a 3-D network of molecular structures during the high-temperature curing process. PVAc is a ductile adhesive that offers high initial tackiness under room temperature (Ebnesajjad 2008), and is commonly used for manufacturing furniture. However, both PF and PVAc have weaknesses. PF is a brittle thermosetting resin that does not provide the required adhesion in a strand mat for profile forming, especially at room temperature. PVAc is a thermoplastic adhesive that lacks water-resistance and durability. In order to

effectively use a blend of these two resins, it is critical to understand the interaction between PF and PVAc, as well as the interaction between PF/PVAc and wood materials. Studies on the cure kinetics of PF/PVAc offer insight into the interaction between PF and PVAc and the required temperature for complete curing (Wang et al. 2010), this study will explore the interaction between PF/PVAc and the wood substrate.

## **Objective**

The goal of this study is to characterize the effect of varying proportions of PVAc in PF resin on the physical properties of the hybrid resin blend, and examine the interaction between hybrid adhesive and the wood substrate in terms of bond development and performance.

Objectives to achieve this goal are to:

- Determine physical properties of hybrid adhesive, including pH, viscosity and dispersion and understand their effects on adhesive bond performance
- Evaluate the binary adhesive bond strength and wood failure, and understand the effect of varying proportions of PVAc on bond performance
- Investigate the bond performance difference between tangential and radial glued surfaces
- Quantify the gross penetration of PF/PVAc binary adhesive into sugar maple and study the effects of varying proportions of PVAc in PF on the gross penetration
- Analyze the relationship between adhesive interaction and bond performance

## **Background**

### **Phenol Formaldehyde (PF) and Polyvinyl Acetate (PVAc) Resin**

PF is a common adhesive applied for wood composites which can offer permanently strong bond once it forms a three dimensional network after completely curing. PVAc, on the other hand, builds bond strength as the solvent evaporates.

Phenol formaldehyde (PF) is one of the most common adhesives in the wood industry due to its excellent durability (Frihart 2005a). Normally, there are two types of pre-polymers of PF which can be classified according to formaldehyde/phenol ratios. Novolac, with a formaldehyde/phenol ratio of less than 1, is normally produced under acidic conditions. Resole has a formaldehyde/phenol ratio larger than 1, and is generally formed under base conditions. Resole resin is commonly applied to wood products, since it is a soluble adhesive with good wood-wetting properties. The fact that it can only be cured under heat treatment allows extra product assembly time. A typical chemical reaction is shown in Figure 2-1.

Polyvinyl acetate (PVAc), commonly known as “white glue” is widely used for paper, cloth, plastics, leather and metal foil (Ebnesajjad 2008). PVAc is commonly used for furniture construction and possesses the advantages of low cost, low toxicity, low flammability, and simple application (Pizzi 1989). For processing, the monomers are dissolved in water as an emulsion accompanied with polyvinyl alcohol. The monomers in the emulsion droplets are polymerized, forming a dispersed organic polymer in water. Small droplet sizes are required to maintain product stability (Frihart, 2005). The chemical formula is shown in Figure 2-2.



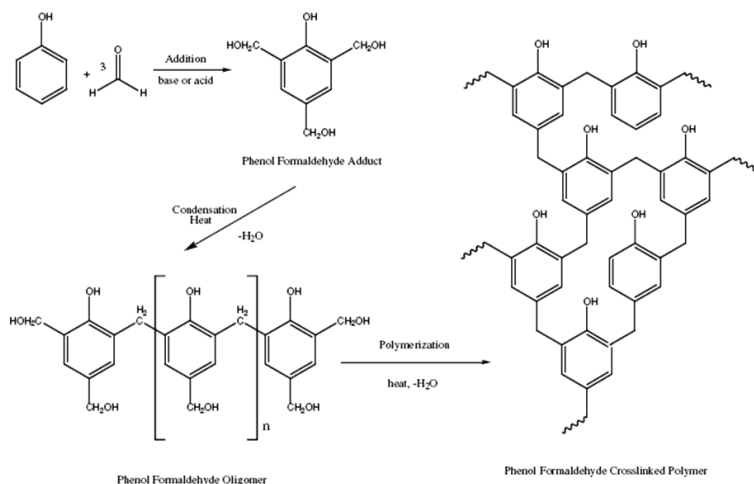


**Figure 2-1 Chemical reaction of phenol formaldehyde (Frihart 2005a)**

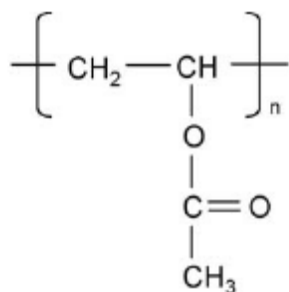


**Figure 2-2 Chemical formula of PVAc (Kim and Kim 2006)**

## Characteristics of wood

Understanding wood structure is essential as it influences adhesive movement and bond performance (Marra 1992). Wood is an orthotropic material with three mutually perpendicular axes: longitudinal, radial, and tangential (Figure 2-3). In most cases, glued wood surfaces are neither completely radial nor tangential surfaces, but in between. Wood is mainly composed of

elongated cells aligned in the longitudinal direction of the stem. Lumens are passageways in the elongated cells, and openings or pits connect these longitudinally and radially-oriented (ray) cells. When liquid resin is applied to wood, it flows and penetrates through lumens, rays, and pits among the wood cells. The variations of the lumens and pits have an important effect on adhesive penetration (Marra 1992). There are typically two kinds of elongated cells: fibers and vessels. Fibers, usually called fiber tracheids, mainly exist in softwood, and offer both strength and conductivity. Vessels exist only in hardwood and serve as conductive tissue; fibers in hardwood provide strength. Hardwood fibers are normally with thicker walls and less interconnecting pits, making it harder for resin to penetrate than in softwood. Hence, hardwood vessels play a dominant role in adhesive penetration. Wood species differ in the sizes, amounts, distribution and porosity of their vessels and fibers. The differences between typical hardwood and softwood are shown in Figure 2-4.

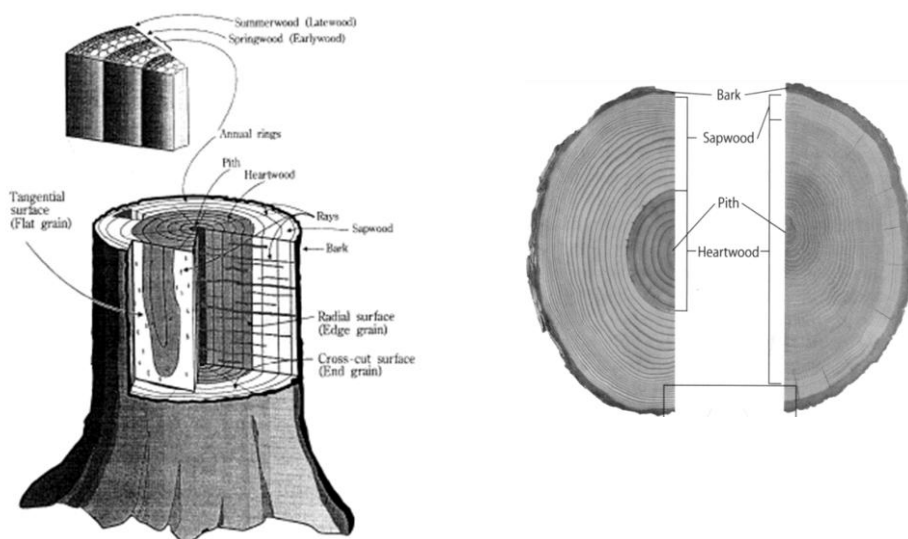


**Figure 2-3 Macroscopy of wood structure (Marra, 1992)**

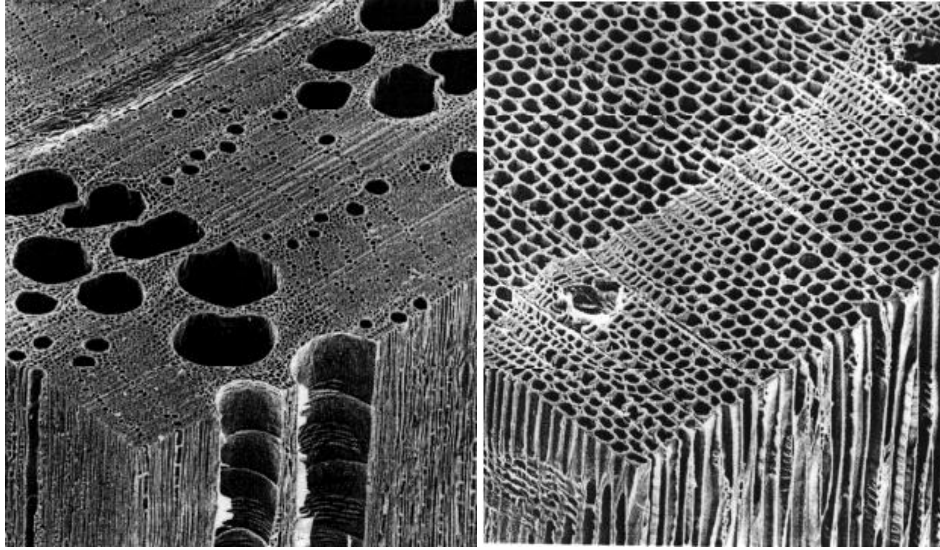


**Figure 2-4 Micrograph of hardwood Red Oak, X100; Softwood, Eastern white pine, X150 (Hoadley 1990)**

## **Adhesive bonding**

### **Adhesive motions for bond formation**

In general, five steps are involved in adhesive motion: resin flow, transfer, penetration, wetting and consolidation (Marra, 1992). Flow occurs when there is enough mobile adhesive and proper contact pressure with the opposite surface. Transfer, affects the opposite surface and can occur with or after flow. Transfer is not necessary when adhesive is applied to both surfaces. Penetration repairs the ruptures created in processing and interlocks the adhesive and wood, which in turn strengthens the interphase. Adhesive penetration will be discussed in detail later in this chapter.

Wetting, a molecular action, follows or occurs with penetration, and plays an important role in adhesion since most wood adhesives are water-borne. Water-borne adhesives are able to wet wood because wood has a relatively polar surface. Wetting can be hindered with the

presence of non-polar substances such as extractives on the wood surface (Hse and Kuo 1988).

Consolidation is the final motion of an adhesive, which hardens the adhesive. There are three types of adhesive consolidation (Marra 1992; Frihart 2005a):

- Loss of solvents: polymers are dissolved in a liquid, commonly water. The loss of the solvent converts these liquids to solids, such as PVAc.
- Polymerization: small molecules polymerize to form the adhesive, such as in PF.
- Solidification by cooling: adhesive is melted and then cooled down to form a solid, such as a hot-melt.

Marra (1992) proposed a chain-link analogy regarding the mechanism of adhesion with wood (Figure 2-5). Based on this theory, bond strength is determined by the weakest link in the chain, and pure wood in link 8 and 9 should be that weakest link (Kamke and Lee 2007) when there is ideal adhesion.

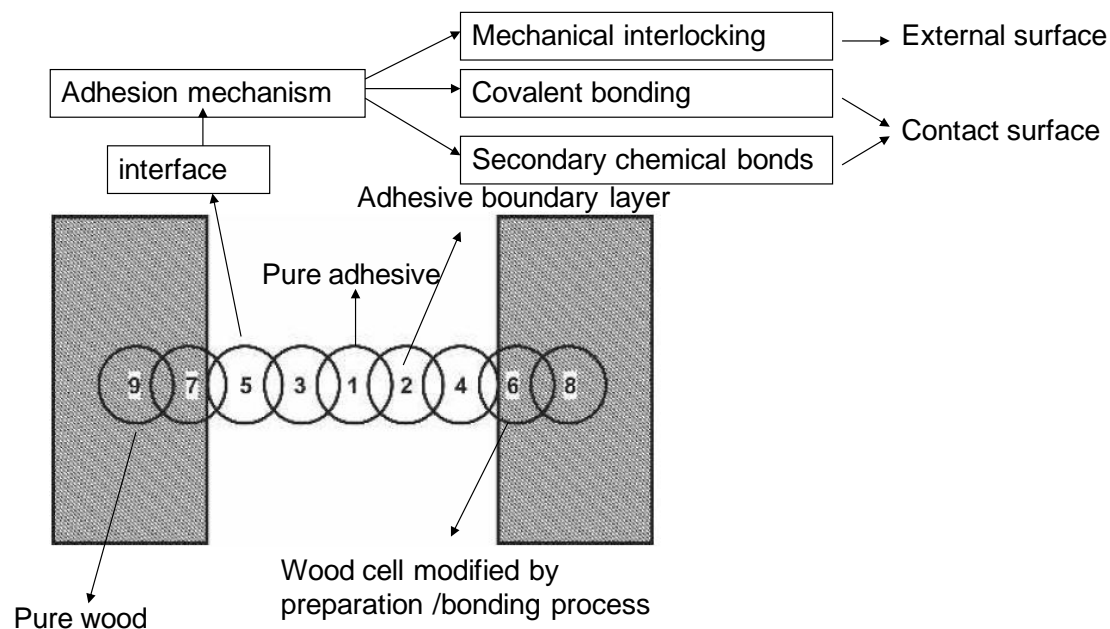


**Figure 2-5 Chain-link analogy for adhesion in wood (Marra 1992)**

### **Wood's effect on adhesive bond performance**

Two physical properties of wood, density and moisture content, have subtle roles on bond performance. Moisture content has a direct influence on the sorption characteristics and dimensional stability of wood, which affects bond formation and bond performance. A water-borne adhesive, such as PVAc, penetrates into wood with the help of solvent and consolidates as the solvent evaporate.

Stress is induced across bond lines when there is a dimensional change due to changes in moisture content. Density is believed to be related to strength, although they separately affect bond performance. Strength is thought to be related to link 8 and 9 (Figure 2-5) and establishes the maximum load carrying capacity, whereas density is related to link 6 and 7 as well as penetration behaviors (Marra 1992). Cell wall of wood, irrespective of species, has a specific gravity of approximately 1.5. Density differs among different species because of differences in the volume of voids. Since adhesive penetration mainly occurs in voids and pits, wood with lower-density allows easier adhesive penetration because of better porosity (Marra 1992). Furthermore, denser wood tends to produce more stress in bond lines when moisture content changes since thicker cell walls tend to shrink and swell more.

### **Adhesive bond performance - shear stress test**

Shear tests are commonly used to evaluate adhesive bond performance. It is often assumed that load is distributed evenly across the whole bond area, but this is not necessarily true. When a load is applied to wood, it is transmitted to the bond, but is not likely to be distributed evenly due to the elastoplastic and anisotropic properties of wood (Marra 1992). The load tends to move mostly to the edges of the bond, usually at end-grain edges. The edges tend to fail first under the maximum load, followed by the rest of the bond. A good estimation of bond

strength comes from dividing maximum load by the total bond area. Bond strength in ductile adhesive tends to be higher than in brittle adhesive, because thermoplastic adhesive efficiently transmits stress to the entire bond area. In thermoplastic resin, the adhesive starved areas are bypassed by the applied load with deformability. In brittle resin, the load is still applied for the unbounded area, causing it to fail from the weak point (Marra 1992). A finite element analysis study (Serrano 2004) of brittle and ductile adhesives also concluded that more brittle an adhesive is, lower the observed local bond strength it tends to have because of the non-uniform stress distribution.

Wood failure percentage is normally obtained from the fractured surface after testing. Deep wood failure reflects good adhesive penetration to some degree. A zero percent wood failure shows weaker adhesive bond strength than wood, whereas a hundred percent wood failure indicates stronger adhesive bond strength than wood (Marra 1992).

### **Adhesive penetration**

Contribution of adhesive penetration to bond strength has been studied by many investigators, but a clear link between the two has not been confirmed (Kamke and Lee 2007). Adhesive penetration in wood substrate occurs on two levels: gross penetration and cell wall penetration. Gross penetration is a mechanical interlock that provides additional mechanical strength, while penetration into the cell walls changes mechanical strength and reaction to moisture.

In the first level, resin flows from the external surface into the capillary structure of wood. Adhesive penetration into this level can repair voids induced by machine damage during processing. Gross penetration mainly happens in cell lumens, due to hydrodynamic flow and

capillary action (Kamke and Lee 2007). Hydrodynamic flow is induced by external compression force, which mates the wood surfaces that are to be bonded. Hydrodynamic flow occurs most easily in a longitudinal direction; penetrate through lumens of slender and long tracheids of softwoods, or the vessels of hardwood. Typically, adhesive penetration in hardwoods occurs through vessels as they are connected end-to-end with perforation plates without pit membranes.

Many factors influence lumen penetration. Some are wood-related, such as lumen size and exposure of the wood surface; others are adhesive-related, such as adhesive viscosity and surface energy; still others are process-related, such as assembly time, pressure, and temperature (Frihart 2005a). Permeability and surface energy play important roles in wood penetration. Wood species and grain direction also affect permeability. It was concluded that permeability in the longitudinal direction can be approximately  $10^4$  greater than in the transverse direction (Siau 1995). Penetration also varies between earlywood and latewood and sapwood and heartwood. Moreover, penetration varies with the slope of grain of the bonded wood. Interestingly, penetration is enhanced when an oblique angle intersects between the cell lumens and external surface (Kamke and Lee 2007).

Adhesive penetration is also affected by the moisture content of wood. UF resin penetration into beech was found to reach its maximum with moisture content of 9%. A study by Sernek (2002) indicated that PF adhesive penetrate more in aspen with 15% moisture content than with 4% moisture content, and penetration was not influenced by heat treatment.

Varieties of methods were used to study cell wall penetration. Thus far, phenol-formaldehyde, urea-formaldehyde, and melamine-formaldehyde have all been shown to penetrate at cell wall level (Bolton et al. 1988; Gindl et al. 2004; Laborie 2002). Cell wall level

penetration is usually related to the molecular size of adhesive components and the water or solvent swelling of the wall structure. Only in one case (Nearn 1965) adhesive components in the cell wall have been claimed to improve bond strength. Frihart (2005a) proposed four models for the cell wall penetration effect on bond strength:

- Oligomers and monomers dissolve in the cell walls without a reaction, which reduces stress because of lower dimensional change
- Adhesive reacts with cell wall components and forms crosslink structures, which increases the strength of the surface wood cells
- Adhesives polymerize and form a mechanical interlock in a finger-type at nano-scale level
- Adhesives form an interpenetrating polymer network with the cell wall's polymeric components

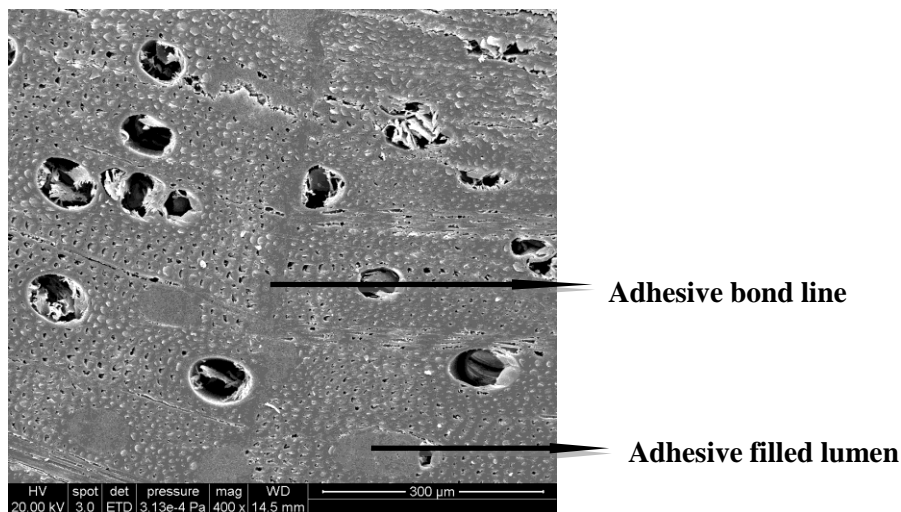
These models were all built on the idea that dimensional change in the surface cells will be reduced, which will improve the bond strength by decreasing the stress gradient between the adhesive and the wood.

In general, an optimal penetration can repair machining damage and enable better stress transfer between laminates. Too much penetration can lead to a starved bond line resulting in a weak bridge between the wood surfaces, whereas too little penetration can limit the formation of wood-adhesive interaction (Frihart 2005b) . Hence, it is important to understand adhesive penetration and its influence on bond performance.



## **Penetration observation methods**

Adhesive penetration studies have been conducted using transmission electron microscopy (TEM), transmitted and reflected light microscopy, scanning electron microscopy (SEM), and fluorescence microscopy. Electron microscopy methods, such as SEM and TEM offer higher magnification, but the grey-scale image makes differentiation between adhesive and wood phases hard to achieve (Figure 2-6). However, quantification of adhesive penetration can be studied in combination with energy dispersive X-ray analysis (EDXA) or electron energy loss spectroscopy (ELLS). Kamke and Lee (2007) have reviewed literature regarding adhesive penetration and described these methods in details.



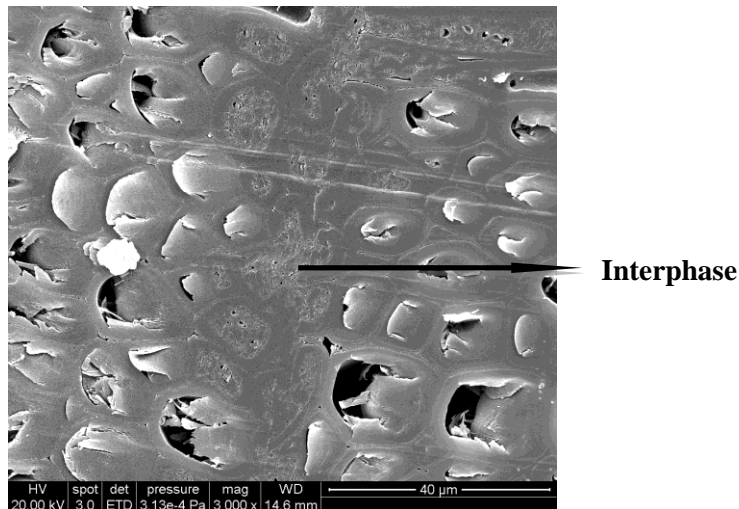


**Figure 2-6 PF-Sugar maple adhesion interphase taken by FEI 200F SEM**

### **Penetration quantification via fluorescence microscopy and stain technique**

Fluorescent microscopy, which can offer good color contrast, has shown much promise for differentiating the adhesive from neat wood in the adhesive-wood interphase (Kamke and Lee 2007). Some adhesives are auto-fluorescent, whereas others are only fluorescent when treated with dyes or pigments (Chandler et al. 2007). The basic principle for fluorescence is that certain material emits visible fluorescence when it is irradiated by light of a specific wavelength; it involves three steps as shown in Figure -2-7.

- Energy is absorbed by the atom, which becomes excited. The atom absorbs the energy when it is excited by light of a specific wavelength.
- The electron jumps to a higher energy level.
- The electron falls back to the ground state, releases some energy, and then emits a fluorescence photon.

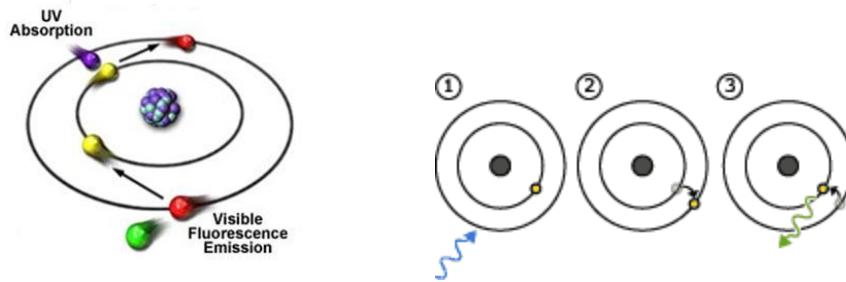


**Figure -2-7 Principles of fluorescence atoms (“Nobel Web, The Fluorescence Microscope” 2010)**

The stain technique is usually used along with fluorescence microscopy to increase color contrast. In terms of adhesive penetration quantification, a manual method was conducted by Brady and Kamke (1988). They used film photography to create photomicrographs of bond lines and projected them onto a calibrated grid. To quantify adhesive penetration, they counted the appropriate grid squares. As digital image processing and analysis technique developed rapidly in 1990s, adhesive penetration could be quantified in a much faster way (Johnson and Kamke 1992). Penetration of PF with different molecular weight distributions in flakes have been studied using a combination of fluorescence microscopy, stain technique and digital image analysis (Johnson and Kamke 1992; Johnson and Kamke 1994). Table 2-1 summarizes the parameters in fluorescence microscopy and stain techniques based on a series of studies on penetration (Kamke and Lee 2007).

**Table 2-1 Summary of parameters in fluorescence microscopy and stain techniques**

<b>Species</b>	<b>Resin</b>	<b>Excitation/Emission (nm)</b>	<b>Stain Dye</b>	<b>Reference</b>
<b>Douglas-fir, Aspen</b>	<b>PF</b>	<b>410/510</b>	<b>0.2% acridine red</b>	<b>Brady and Kamke (1988)</b>
<b>Yellow poplar</b>	<b>PF</b>	<b>365/420</b>	<b>0.5% toluidine blue O</b>	<b>Johnson and Kamke (1992)</b>
<b>Beech</b>	<b>UF</b>	<b>365/420</b>	<b>0.5% brilliant sulphaflavine +0.5% safranin O</b>	<b>Sernek et al. (1999)</b>
<b>Yellow poplar , Loblolly pine</b>	<b>MDI</b>	<b>365/420</b>	<b>0.5% safranin O</b>	<b>Kamke (2004)</b>
<b>Beech</b>	<b>UF</b>	<b>450/515</b>	<b>0.5% safranin O</b>	<b>Gavrilović-Grmuša et al. (2008)</b>
<b>Yellow poplar</b>	<b>PF</b>	<b>360/400/420</b>	<b>0.5% toluidine blue O</b>	<b>Zheng (2002)</b>
<b>Yellow poplar</b>	<b>MDI</b>	<b>360/400/420</b>	<b>0.5% toluidine blue O</b>	<b>Zheng (2002)</b>
<b>Southern red oak</b>	<b>Epoxy</b>	<b>360/400/420</b>	<b>0.5% safranin O</b>	<b>Kamke (2004)</b>
<b>Southern red oak</b>	<b>polyvinyl acetate</b>	<b>470/500/515</b>	<b>0.5% safranin O</b>	<b>Kamke (2004)</b>

A study by Chandler et al. (2007) examined penetration of four commercial adhesives in acetylated and unmodified wood and concluded that adhesive penetration does not always relate to bond strength and wood failure. Zheng et al. (2004) observed in a study of penetration of PF/pMDI hybrid resin that the penetration among different hybrid resin ratios did not follow a logical pattern. They found the effective penetration of pMDI was not better than that of PF

although the viscosity of pMDI is lower than that of PF. The pMDI was assumed to be underestimated with this method as it penetrated to the molecular level (Zheng et al. 2004).

### **More advanced technique-confocal microscopy application on adhesive penetration**

Confocal laser scanning microscopy (CLSM) uses a light microscope, a scanning mechanism, and a motorized focus and laser source. CLSM is more advanced than conventional fluorescence microscopy (White et al. 1987). It has several key advantages, such as a controllable depth of field, the elimination of out-of-focus noise, and detectability for thick and opaque specimens with optical sections. CLSM uses spatial filtering to eliminate out-of-focus light or flare in specimens thicker than the plane of focus.

In this study, CLSM was used rather than fluorescence microscopy because it yields a better image contrast. Image contrast, a difference between the maximum and minimum intensity of two points in the image, is a crucial factor in differentiating spots of interest from background noise (Confocal tutorial 2010). With a conventional microscope, the specimen is lit laterally and vertically at the same time, with ordinary extended light as light source. Image quality is affected by all the lit spots from the whole illuminated field. This can create a weak image contrast, since the illuminated dots interfere with each other laterally and produce stray lights.

In confocal microscopy, a plate with a small hole called a pinhole is placed in front of the image detecting device (shown in Figure 2-8). In this case, noise light from both the under-focal-plane and the above-focal-plane are focused at a plane either behind or in front of the pinhole, which is blocked by the pinhole. Only the light from focal plane, which is focused at the pinhole, can reach the image detector. CLSM was found to be effective and has been widely used for adhesive distribution analysis (Cyr et al. 2007; Grigsby et al. 2005; Loxton et al. 2003) .

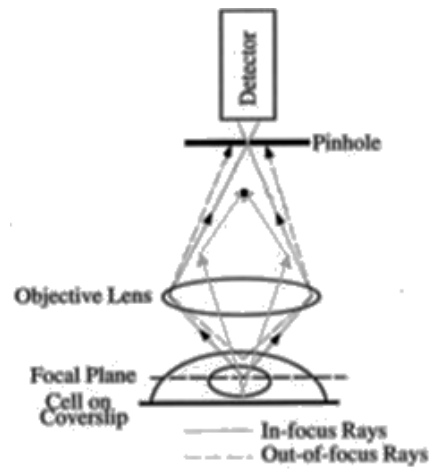


**Figure 2-8 Key point for confocal microscopy-pinhole (Confocal tutorial 2010)**

## **Materials and Methods**

### **Experimental Design**

To efficiently investigate the effect of PF/PVAc ratio on hybrid adhesive-wood interaction, design points were determined based on Combined D-optimal design with components PF and PVAc as mixture components and grain surface (tangential, radial) as a categorical factor (shown in Table 2-2). Information from this analysis can be used to optimize the settings of a process (such as PF/PVAc ratio) to give a maximum or minimum response (such as penetration or bond strength) while also taking into consideration influence of other factors (such as radial or tangential surface). D-optimal design was chosen to minimize the error of the model coefficients (Stat-Ease 2005), and to minimize the number of runs while gaining sufficient information regarding influence of independent variables on the response. The runs were augmented with additional runs to provide estimates of lack of fit and pure error. In this Chapter, the total resin for each blend ratio applied on wood surface was constant based on solid content.

### **Materials**

Sugar maple (*Acer saccharum*) lumber (1.5m long by 25.4mm thick by 76 -152 mm wide) was utilized in preparing all specimens for penetration and bond performance characterization. Specimens were prepared such that adhesive-wood interaction can be studied on both tangential (plain-sawn) and radial surfaces (quarter-sawn). Adhesives used in this study are commercially produced phenol formaldehyde (PF) for face layer of OSB from Hexion in Oregon, and polyvinyl acetate homopolymer emulsion (Assembly 161™) from Franklin International. Adhesive properties given by the companies are shown in Table 2-3.

**Table 2-2 Ratio points of PF/PVAc and corresponding specimen replicates**

<b>Component PF %</b>	<b>Component PVAc %</b>	<b>Grain direction</b>	<b>Shear Blocks</b>	<b>Penetration Specimens</b>
<b>100</b>	<b>0</b>	<b>Tangential</b>	<b>20</b>	<b>5</b>
<b>80</b>	<b>20</b>	<b>Tangential</b>	<b>16</b>	<b>4</b>
<b>75</b>	<b>25</b>	<b>Tangential</b>	<b>20</b>	<b>4</b>
<b>67</b>	<b>33</b>	<b>Tangential</b>	<b>16</b>	<b>4</b>
<b>50</b>	<b>50</b>	<b>Tangential</b>	<b>20</b>	<b>4</b>
<b>25</b>	<b>75</b>	<b>Tangential</b>	<b>24</b>	<b>4</b>
<b>0</b>	<b>100</b>	<b>Tangential</b>	<b>16</b>	<b>3</b>
<b>100</b>	<b>0</b>	<b>Radial</b>	<b>16</b>	<b>3</b>
<b>75</b>	<b>25</b>	<b>Radial</b>	<b>12</b>	<b>3</b>
<b>50</b>	<b>50</b>	<b>Radial</b>	<b>12</b>	<b>3</b>
<b>25</b>	<b>75</b>	<b>Radial</b>	<b>12</b>	<b>3</b>
<b>0</b>	<b>100</b>	<b>Radial</b>	<b>12</b>	<b>3</b>

**Table 2-3 Parameters of PF and PVAc resin**

<b>Resin</b>	<b>PH (@25 °C)</b>	<b>Viscosity (@25 °C, cps)</b>	<b>Solid Content (%)</b>	<b>Mw (g/mol)</b>
<b>PF</b>	<b>10-11.5</b>	<b>230-330</b>	<b>55.7</b>	<b>Based on a typical commercial face PF for OSB</b>
<b>PVAc</b>	<b>4.2-4.6</b>	<b>150-240</b>	<b>42-45</b>	<b>266,000</b>



## **pH Testing**

Since PF was a strong alkaline and PVAc was acid, a potential reaction could occur once they are blended together. To determine if pH plays a role in hybrid adhesive behavior as blend ratios change, pH of resin blends with different ratios were measured prior to manufacturing the specimens. The total weight for each resin blend was the same. The calculated amount of PF was slowly poured into the beaker to mix with PVAc, which was weighted ahead of time. Then resins were mixed with a one-inch diameter mixer (Arrow 850) for 15 minutes at 1000rpm, and pH was immediately tested by OAKTON Acorn pH 5 meter at 25 °C afterwards.

## **Viscosity and Morphology of PF/PVAc Resin Blends**

A polymer is a very complex chemical component, and behaves in an even more complex manner when two or more polymers are blended together. Since viscosity determines the flow characteristics of the adhesive which influences the penetration into wood, viscosity of the resin blends was measured with a Brookfield viscometer with a set-up temperature at 25°C based on ASTM Standard D-1084-97 (2004). To understand the influence of mixing time on blend quality of the two resins in terms of dispersion of one in the other, blends of resin mixed at 1000rpm to different time periods (5 minutes, 10 minutes, 15 minutes, and 20 minutes) was studied. The total weight for each resin blend was the same. Viscosity was measured using the Brookfield viscometer at 25 °C while spinning it at 50 rpm. A drop of resin blend was placed on a glass slide after mixing and dispersion of PVAc in PF resin was observed under fluorescence microscopy.

## Shear Strength

### Neat Sugar Maple

Shear strength of solid maple was determined to compare with shear strength of adhesive assembly joints. Since the properties of different wood resources vary, we processed wood from the same batch of assembly joints with 25.4mm thickness for preparing wood shear block specimens. Material was conditioned for over two weeks at a temperature of 20 °C and a RH of 65%. Three 305 mm long and 63.5mm wide pieces with varied thicknesses were glued using PF and then cut to target dimensions (63.5 x 50.8 x 50.8 mm) for shear block test based on guidelines specified in ASTM D 143 (ASTM Standard 2006b). The thicknesses of three pieces varied as it ensured the specimens having solid wood in the shear area (Figure 2-9).



**Figure 2-9 Glued wood specimen for neat wood shear block test**

### **Adhesive Assembly joints**

To test the shear strength of the adhesive bond line, conditioned sugar maple lumber was planned to 19.05mm thickness and then cut to length and width of 304.8mm and 63.5mm. Resins with different blend ratios (based on solid content) were mixed at 1000rpm for a period of 15 minutes. The total weight for each resin blend was approximately 40 grams. Blended resin was then brushed on each surface of the maple block at a spread rate of 55g/cm<sup>3</sup>.

After applying the resin, blocks were clamped at a pressure of 1MPa. Pressure was applied by 4 clamps (Figure 2-10). Torque exerted by each clamp was determined based on a simplified formula (Bickford and Nassar 1998) in Equation 2-1.

$$T = 0.2 FD$$

**Equation 2-1**

Where, T is torque, 0.2 is the nut factor, F is the clamp force (preload), and D is the nominal diameter. The actual pressure was applied slightly higher to account for their expansion when heated. Assembled joints were placed in a preheated oven to cure at 150 °C for 3.5 hours and the torque was double checked 20 minutes after the assembly joints were placed in the oven. PVAc shear block specimens were prepared in a similar manner; however, they were not placed in a pre-heated oven but in a conditioning room with a relative humidity of 50% and a temperature of 20°C for 48 hours. All assembled joints were conditioned at this humidity and temperature for over 10 days after curing until their weights stabilized and remained constant.

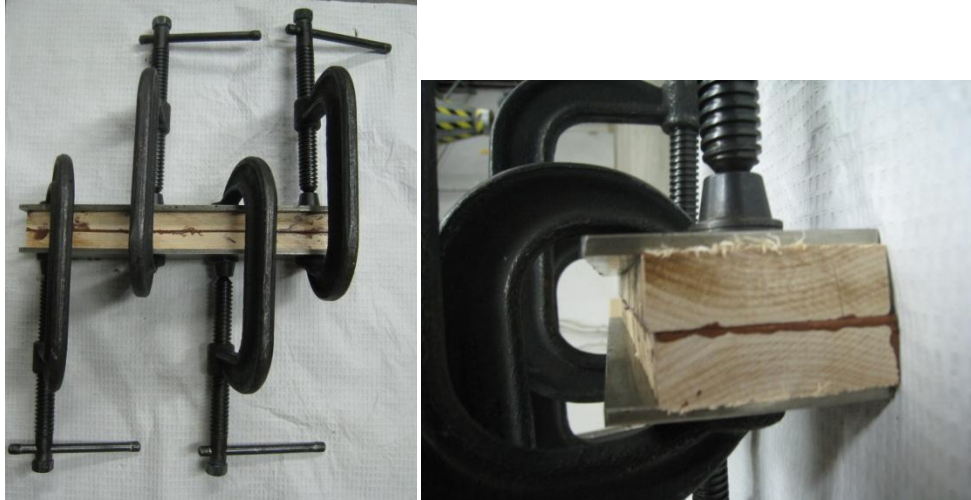
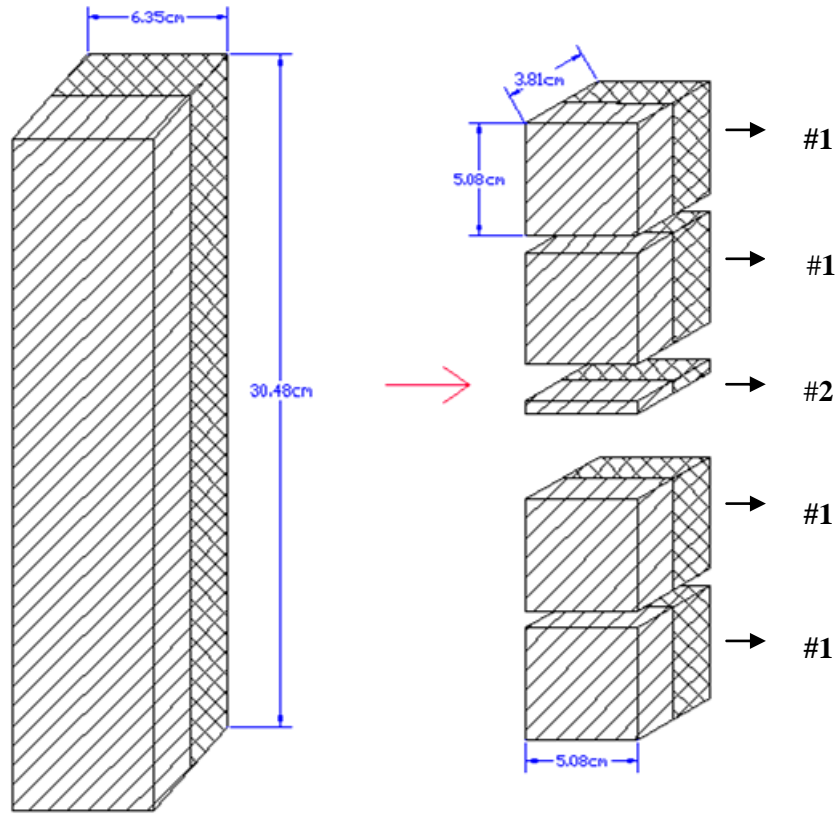


**Figure 2-10 Clamp procedure for shear bonding, tangential to tangential surface**

At least four assembly joints were processed for each of the seven PF/PVAc resin blend ratios on tangential surface and three assembly joints for each of the five PF/PVAc resin blend ratios on radial surface. From each assembly joints, four shear block specimens and one thin specimen were obtained for shear test and adhesive penetration analysis (Figure 2-11). The total shear block specimens and penetration specimens are shown in Table 2-2 .



**#1 Block shear specimen, #2 Adhesive penetration specimen**

**Figure 2-11 Specimens cutting from assembly joint**

Based on a preliminary study, wood failure was difficult to calculate since resin blend with higher PVAc content is lighter in color and difficult to distinguish from wood. Fast green fluorescent dye with a concentration of 0.02% was added into the PVAc prior to resin blending to differentiate from maple, and obtain better image contrast for adhesive penetration as well.

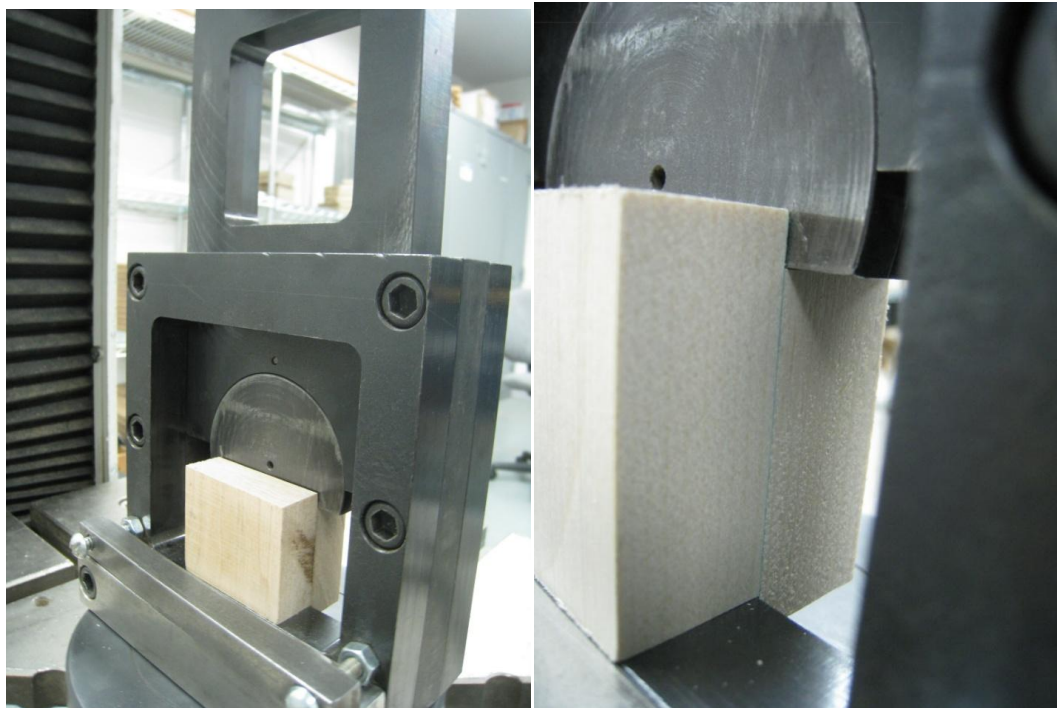


**Figure 2-12 Shear block test conducted with Instron 4400R**

Shear test was conducted according to ASTM D 905-03 (ASTM Standard 2004) with an Instron 4400 R series universal testing machine (Figure 2-12). Loading speed was 5mm/min. The peak value of the load at breakage was recorded. Bonding area of each shear block was measured afterwards. Each fracture surface was photographed and analyzed using Image J software to calculate wood failure. Threshold was adjusted based on a modified image algorithm (Yang et al. 2008). All the threshold images were double checked and compared with the original colored images for accuracy.

## **Penetration Quantification**

### **Fluorescence of Resin**

In the preliminary studies, it was observed that PF is naturally fluorescent, whereas PVAc is not. However, when PVAc was bond to wood with heat, PVAc bond line became fluorescent

(Figure 2-13). Different fluorescence dyes were tried on PVAc to differentiate from PF.

However, the fluorescence spectra of PVAc were always the same as those of PF and wood after it was cured at 150 °C. The fluorescence of PF and wood was because of aromatic structures.

During heating, some components of wood could have reacted with PVAc. This implies that either they form a fluorescent component strong enough to cover the fluorescence of the added dye in PVAc, or they form an aromatic-like structure which leads to a similar fluorescence pattern as that of PF and wood. We could not confirm this for certain. In this study, collective penetration of PF and PVAc was quantified and not individual adhesive penetration.

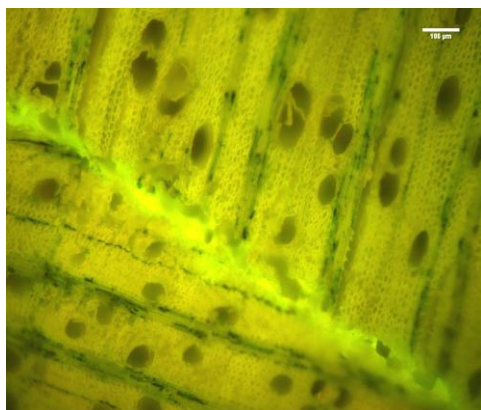


**Figure 2-13 Bond line of neat PVAc without dye after heating at 150 °C, Tangential surface of sugar maple glued with radial surface, taken by Leica Fluorescence Microscopy**

In this study, both toluidine blue solution and safranin O solution were used to stain wood. A clear image of both wood and adhesive can be obtained with safranin O solution, whereas a good contrast between wood and adhesives can be acquired with toluidine blue. In order to quantify adhesive penetration, toluidine blue was used because of good contrast.

### **Sample Preparation for Penetration Image**

From each assembly joint, a block with dimensions of 6.35 mm by 38 mm by 50.8 mm from the middle was obtained for adhesive penetration. The penetration through the assembly joint was assumed to be the same. Block was trimmed, smoothed and sectioned into 80  $\mu\text{m}$  thick along the entire bond line by sliding microtome (Figure 2-14). Although thicker specimens can be observed well with CLSM, thin section was obtained for easier and quicker staining in this study. Section was stained with 1% toluidine blue aqueous solution for 15 minutes to suppress the autofluorescence of the maple. Then the section was rinsed with distilled water and dried. Penetration image was taken with confocal laser scanning microscopy, Zeiss LSM 510 META. The equipment condition was set to a Diode laser of 405nm, a beam of splitter (HFT) of 405/488, and a long pass filter (LP) of 475nm for all the specimens, and the detection wavelength was narrowed to between 475 nm and 600 nm. Uniform magnification was applied to all the images, and the sight area of each image is 1800  $\mu\text{m}$   $\times$  1800  $\mu\text{m}$ . Around 15 images were taken along the bond line of each section. The same procedures were followed for all assembly joints.

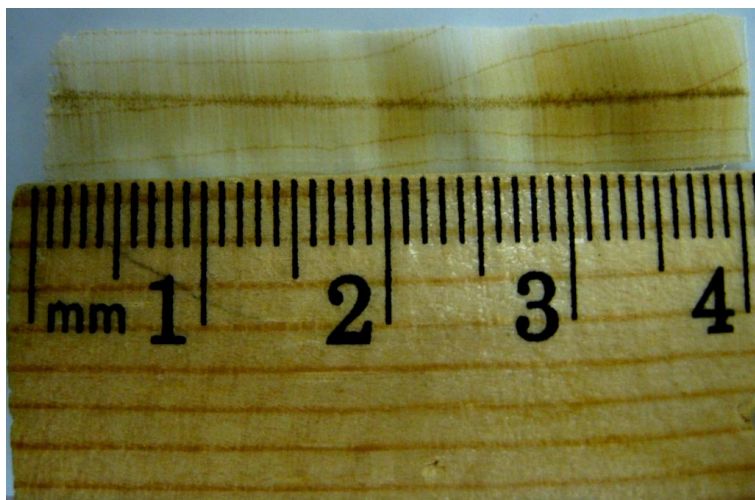


**Figure 2-14 A 80  $\mu\text{m}$  Section Cut from Sliding Microtome**



## **Penetration Quantification Methods**

Penetration images were converted to 8 bits and the threshold was adjusted afterwards (Figure 2-15). For each bond line section, the quantified penetration value was based on 15 images across the bond line. To comprehensively understand adhesive penetration, three different quantification methods were conducted.

1. Effective penetration, using from previous studies (Sernek et al, 1999; Zheng et al, 2004), was calculated based on Equation 2-2.

$$\text{Effective Penetration (EP)} = \frac{\text{Total area of penetrated adhesive particles in the field of view}}{\text{Bonding Length in the field of view}} \quad \text{Equation 2-2}$$

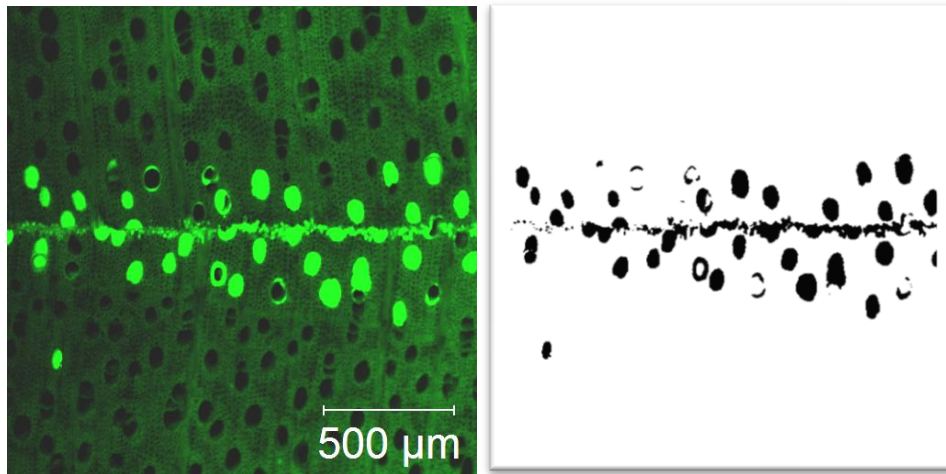


**Figure 2-15 Images of adhesive penetration Left-hand, binary adhesive bond line taken with CLSM (tangential surface); Right-hand, 8-bit image after applying a threshold**

## 2. Maximum penetration depth

A straight distance from the bond line to the furthest penetrated lumen in each image was averaged based on 15 images across the bond line to characterize the best penetration ability of each hybrid adhesive blend ratio.

## 3. Numbers of penetrated lumens

The numbers of penetrated lumens in each image ( $1800\text{ }\mu\text{m}\times 1800\text{ }\mu\text{m}$ ) were counted with a confined size area to exclude the lumens that filled less than half a percentage, and circularity was restricted to exclude the bond line area (Figure 2-16). Overlapped penetrated lumens were manually counted and added to the total number. Numbers of penetrated lumens were averaged and this is based on the sight area of  $1800\text{ }\mu\text{m}\times 1800\text{ }\mu\text{m}$ .

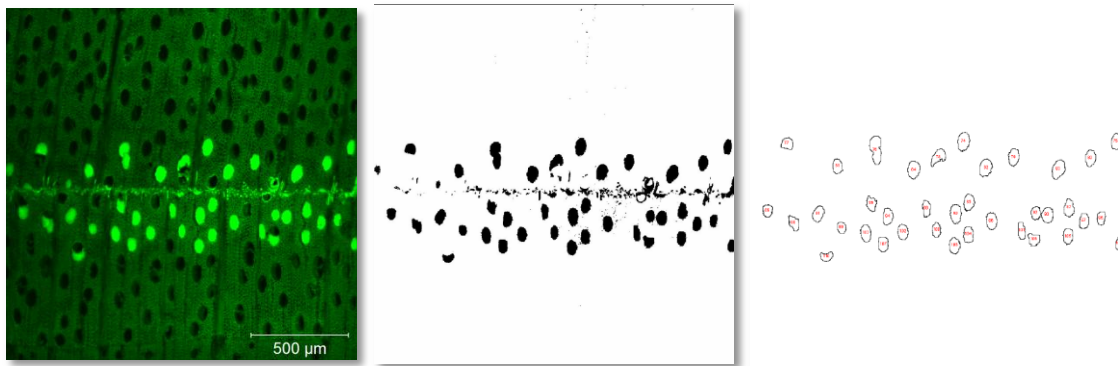


**Figure 2-16 Image conversion for counting adhesive-filled Lumens**

## Results and Discussion

### pH Value

The pH of neat PF was approximately  $11.08 \pm 0.1$  and the pH of PVAc was  $4.03 \pm 0.23$ . When PF and PVAc were blended, their pH values were very close to that of the neat PF (Figure 2-17). It's not surprising since sodium hydroxide in PF is a strong alkaline, whereas polyvinyl acetate in PVAc is a weak acid (Kotz and Purcell 1991). Since there is no change in pH of hybrid adhesive compared to neat PF, the conditions in regards to pH for PF polymerization in the resin blend would not be altered significantly.

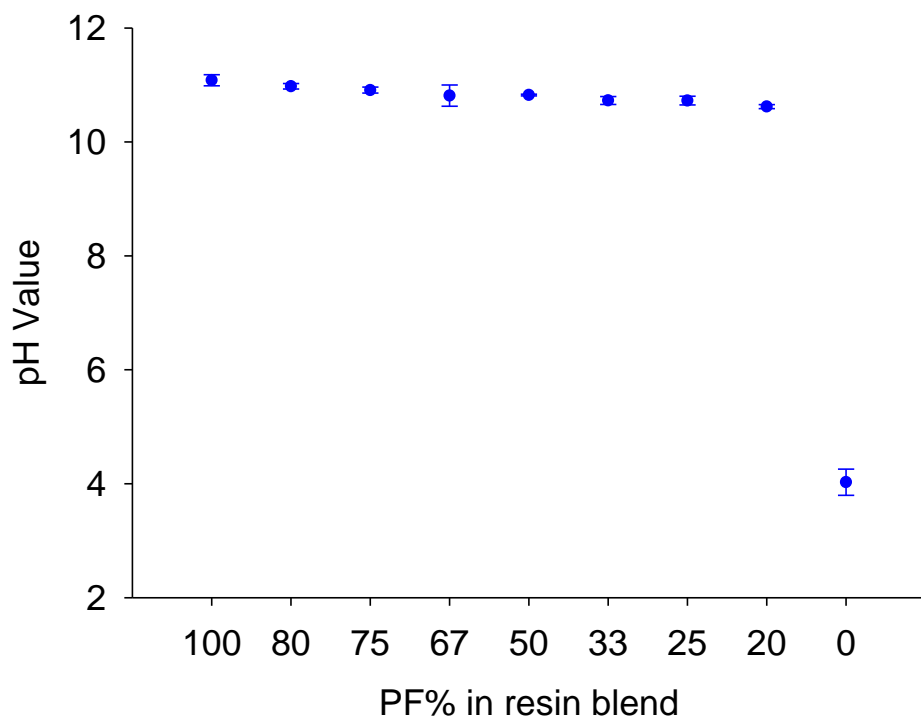
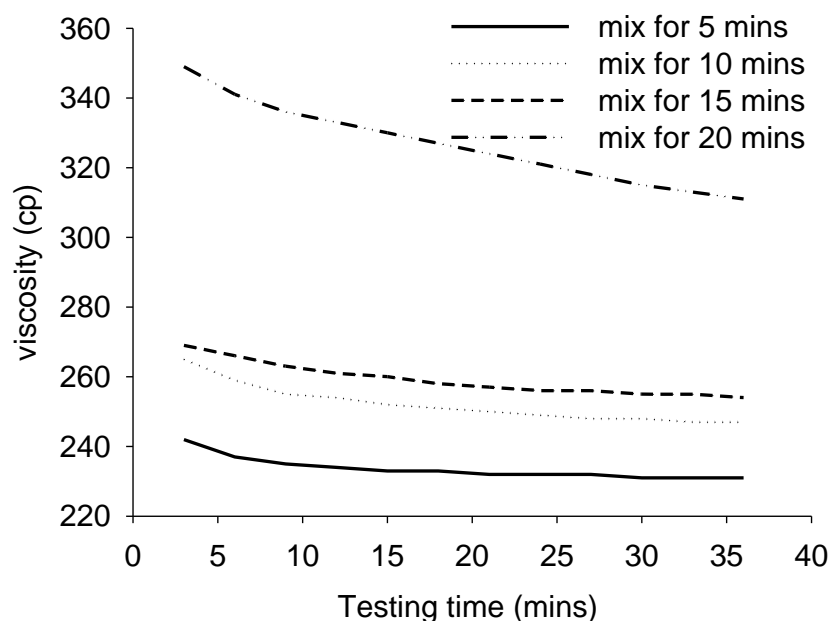


Figure 2-17 pH of PF/PVAc resin blends at 25 °C

## Viscosity and Dispersion of Resin Blends

When PF was mixed into PVAc, the viscosity of the blends first increased and then decreased dramatically, until it reached a relatively constant value. Blending periods of 5 minutes, 10 minutes, 15 minutes and 20 minutes were tested for the different blend ratios. The viscosities of the PF:PVAc blend at a 3:1 ratio under different blending periods are shown in Figure 2-18. The viscosity with a blending period of 20 minutes was significantly higher than the other blending periods, indicating potential changes in polymer physical behavior. It is possible that high rate of shear mixing at longer mixing periods during resin blending may have increased the temperature of the blend thus initiating PF polymerization and an increase in blend viscosity. Based on characterization of viscosity (Figure 2-18), a mixing period of 15 minutes was chosen for the following study because lower viscosity is desired for sufficient adhesive penetration and easy application. Moreover, based on our preliminary study, the bond performance of hybrid adhesives with a mixing time of 15 minutes was generally better than that with 10 minutes.



**Figure 2-18 Viscosity of PF:PVAc=3:1, mix for different time periods under 1000rpm, tested under 50rpm at 25 °C**

The same type of PF and PVAc were used for both the bond performance study (Chapter 2) and wood strand panels manufacturing (Chapter 3) although they were from different batches. Batch 1 resins were used for experiments in this chapter, and batch 2 resins were used for the wood strand panels manufacturing in Chapter 3. The viscosities from both batches were tested, and the results are shown in Figure 2-19. All of the adhesive blends were mixed for 15 minutes. The viscosity dropped immediately after a small amount of PVAc was added, and then increased as more PVAc was added. Neat PVAc was stirred under 1000rpm with a period of 5 mins, 10mins, and 15 mins, respectively to examine shear mixing rate effect on PVAc. No significant increase in viscosity of neat PVAc was observed which indicates the stability of PVAc particles under 1000rpm.

The viscosity change of PF/PVAc blend is suspected to be related with change in pH and the PF/ PVAc ratios in resin blend. Generally, to stabilize the PVAc dispersions, sufficient electrostatic and/or steric repulsion are needed to resist particle aggregation (Lovell and El-Aasser 1997). Surfactants functions as stabilizer through adsorption at the polymer-water interface. It is known that emulsion system is sensitive to pH and that influences its stability (Erbil 2000). Surfactants can be readily destroyed by changing in pH, which helps with demulsification treatment. The change in pH splits the surfactants and affects the interfacial properties of emulsion droplets, which influences the emulsion stability (Chen et al. 2000). When PVAc is dominant in the blend, the surfactant becomes instable due to the change in pH and the PVAc particles may start to agglomerate resulting in increased viscosity. However, when PF is dominant in the blend, the PF solution may dilute the agglomerated PVAc particles, which in turn decreases the viscosity.

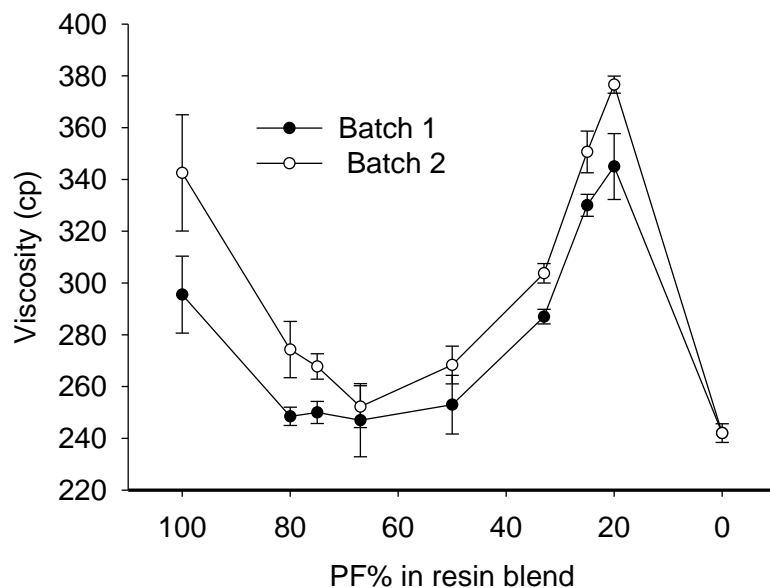


**Figure 2-19 Viscosities of resin blends with increased PVAc percent, blend for 15 minutes under 1000rpm, tested at 25 °C**

Dispersions were studied to better understand the viscosity change of resin blends. Dispersions of all blends and neat resins were observed right after blending. Pure PF was in a uniform status; whereas PVAc was in an emulsion status with small droplets dispersed inside water (Figure 2-20). Huang et al (2002) studied the miscibility of novolac PF resin and polyvinyl acetate blend and found that the blend was miscible in the amorphous phase because of the hydrogen bonding between hydroxyl groups of phenolic resin and carbonyl groups of PVAc. In our study, the resole type PF and PVAc were not miscible when PF dominated the blend as per the dispersion image. The blends separated into two phases once they were mixed together. However, the blend seemed to be more uniform when the PVAc content was higher than 50% (Figure 2-21). The immiscibility of the PF/PVAc blend could be advantageous for our study as it could enable PF and PVAc to function separately, forming both strong bonds and good initial adhesion. The dispersion of the resin in the blend improved with longer blending times, possibly leading to higher viscosity (Figure 2-22).

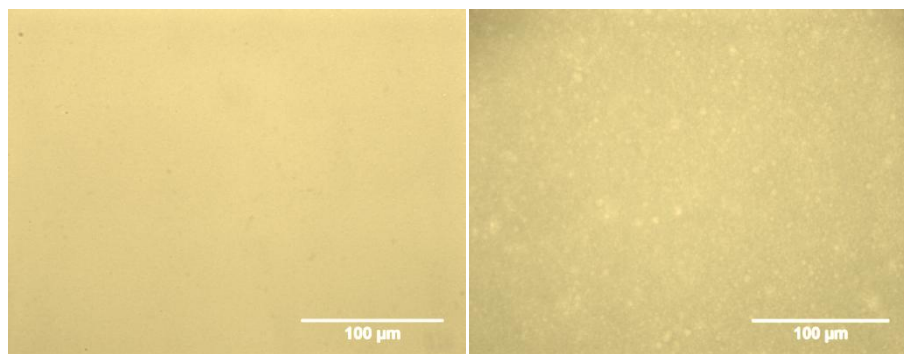


**Figure 2-20 Morphology of Neat PF (left) and PVAc (right)**

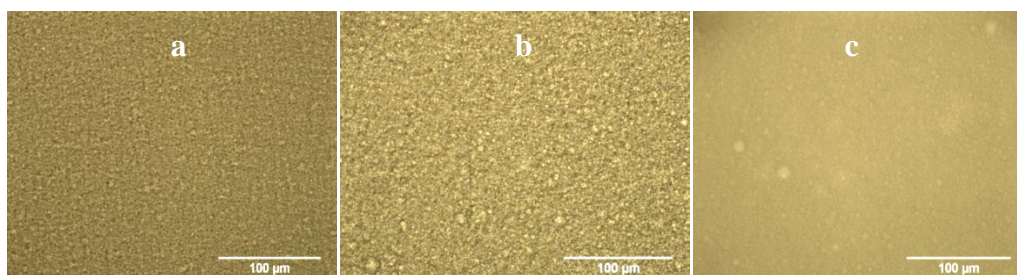


**Figure 2-21 Dispersion of resin blends, a, PF:PVAc =75%:25%; b, PF:PVAc =50%:50%; c, PF:PVAc =25%:75%**

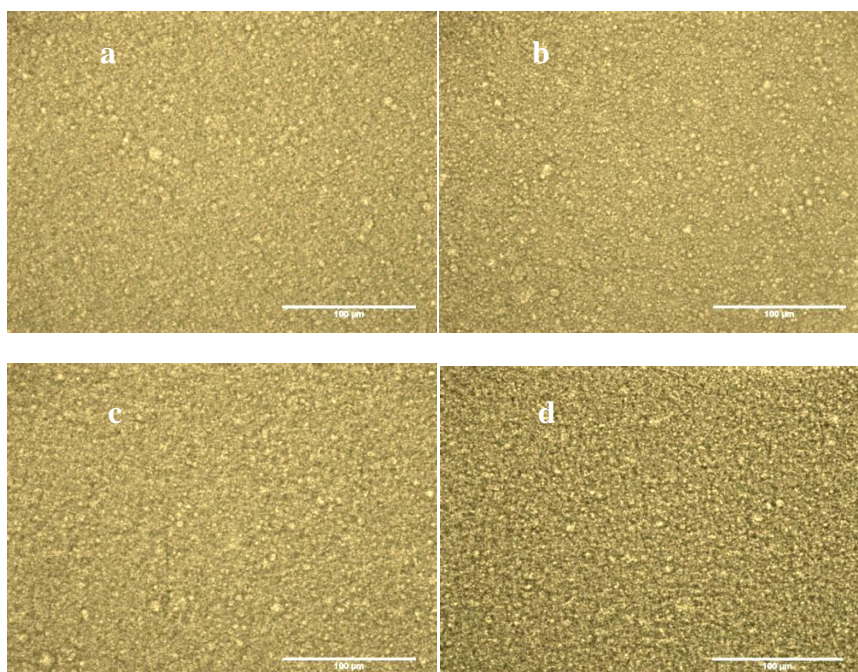


**Figure 2-22 Dispersion of PF: PVAc=50%: 50% under 1000rpm for; a, 5 minutes; b 10 minutes; c, 15 minutes; d, 20 minutes**

### **Shear Block Strength of Neat Sugar Maple**

The results of shear strength tests of sugar maple are shown in Table 2-4. The densities of all the wood blocks were calculated based on wood weights with a moisture content of 8%.



COVs of shear strength variation are 8% and 11% for tangential and radial surfaces, respectively.

A simple analysis of covariance (ANCOVA) was conducted to examine grain surface and density effects on bond performance. Based on SAS output, density is not a significant covariate for the shear strength of sugar maple, however, contribution of different grain surfaces to bond shear strength is significant. The bond shear strength of the tangential surface is significantly higher than that of the radial surface. Grain orientation effect on shear strength of maple parallel to the grain has been studied by Okkonen and River (1989) and they found the shear strength on tangential shear plane was significantly higher than that of radial shear plane. The difference on tangential and radial shear plane may due to the large ray volumes of maple which help to resist shearing in tangential plane, whereas in radial plane they readily shear (Okkonen and River 1989).

**Table 2-4 Shear block strength of neat sugar maple on both tangential and radial surfaces**

Bonded Surface	Density(g/cm <sup>3</sup> )	Shear Strength (MPa)	COV
Tangential	0.69 ±0.01	22.31 ±1.85	8%
Radial	0.70 ±0.03	18.21 ±1.92	11%

### **Bond Performance and Adhesive Penetration of binary adhesives**

The densities of wood with adhesive bond on tangential (plain-sawn) and radial (quarter-sawn) surfaces were 0.71 ±0.03g/cm<sup>3</sup> and 0.69 ±0.03g/cm<sup>3</sup> based on 8% MC, respectively. Since density varied greatly and theoretically affects bond performance, ANCOVA was conducted to examine effect of density as a suspected covariate. Test results of tangential and radial bonded

surfaces were examined separately, since the percentage levels for these two grain surfaces are different (7 ratios for tangential and 5 ratios for radial).

As mentioned earlier, four shear block specimens and around 15 penetration images for each assembly joint were obtained. The average values of shear strength, wood failure, effective penetration, maximum penetration depth, and the number of penetrated lumens for each individual assembly joint were calculated and used to perform analysis of covariance (ANCOVA) using SAS. The interaction between density (covariate) and percentage (factor) was examined and then removed, since no significant interactions were found.

Neither shear strength nor wood failure was found to be significantly affected by density, which agrees with shear test results for neat sugar maple. Hence, shear strength and wood failure percentage were calculated without density adjustments. All responses related to penetration quantification were significantly influenced by density, and were adjusted by ANCOVA without interaction terms. Overall bond performance was found to be better on tangential surfaces than radial surfaces, while there were no obvious differences in terms of adhesive penetration.

For joints bonded on tangential surface, the PF/PVAc ratio has a significant influence on both bond performance and adhesive penetration at 0.05 level ( $\alpha=0.05$ ). The shear strength of a hybrid adhesive with less than 50% PVAc is comparable with that of neat PF (Figure 2-23). Neat PVAc also has a relatively high shear strength which could be attributed to its ductility. The shear stress/strain curve also demonstrates that PVAc is more deformable than both hybrid adhesive and neat PF (Figure 2-24). As mentioned earlier, ductile adhesive tends to have higher observed local bond strength because the stress can be effectively transmitted through the entire bond area (Marra 1992; Serrano 2004). However, the high shear strength of PF and PVAc does

not lead to higher or equal strength of the hybrid adhesive. This indicates that the ductility advantage of PVAc does not effectively transfer to the hybrid adhesive, which could be due to the immiscibility of the two resins in the blend.

As shown in Figure 2-23, wood failure decreases slightly as PVAc is added, and this becomes obvious as PVAc content increases above 50%. Obviously, neat PVAc has the weakest interaction with wood, as compared to hybrid adhesive and neat PF. Addition of PVAc in the blend certainly leads to a decrease in adhesive-wood interaction, especially when PVAc content dominates.

In terms of adhesive penetration, no obvious decreases occur for hybrid adhesive with PVAc content below 50%. As shown in Figure 2-26, hybrid adhesive penetration with 75% PF is similar to neat PF; however, it tends to decrease as PVAc content increases to more than 50%. A noticeable decrease in adhesive penetration occurs with 50%PVAc and further decrease is observed with 75%PVAc.

Based on penetration graph (Figure 2-25), the number of penetrated lumens of 80%PF blend is slightly higher than that of neat PF; however, 75% PF and 67%PF blends did not seem to differ significantly from neat PF. In theory, lower viscosity of resin leads to easier penetration, but it is not that simple because penetration is related to more than just one factor. Penetration was confirmed to decrease with higher weight average molecular weight of resin (Johnson and Kamke 1992). Generally, the molecular weight ( $M_w$ ) of PF resole ranged from a couple hundred to 30,000 g/mol (Ani et al. 2004). Wang (2007) have studied the cure kinetics of two commercial PF resole used in face and core layers for OSB manufacturing and the measured  $M_w$  are 621 g/mol for face PF and 6576 g/mol for core PF, respectively. The PF resole used in this study is a

typical face PF for OSB with relatively low molecular weight, whereas the Mw of PVAc in this study is approximately 266,000 g/mol. Hence, the Mw of hybrid adhesive should be greater than PF resole and smaller than PVAc. Although the viscosity of PVAc is slightly lower than PF, penetration is more difficult, since PVAc molecules are much bigger than PF molecules.

We speculate that on one hand with PVAc content less than 50%, viscosity of hybrid adhesive is lower than PF which would facilitate deeper penetration; but, on the other hand, the molecular weight of hybrid adhesive is larger than PF and could play an opposite role on adhesive penetration. These conflicting effects could partially explain the slight and insignificant difference of penetration between hybrid adhesive with less than 50%PVAc and neat PF. As PVAc content increased beyond 50%, both the viscosity and molecular weight of hybrid adhesive could be higher than PF, which could have lead to significant decrease in penetration. However, this speculation has to be confirmed in future studies.

Maximum penetration depth continually decreases as PVAc content increases in the resin blend. The continuous decrease in maximum penetration depth indicates that the penetration ability of hybrid adhesive is hindered by addition of PVAc. Neat PVAc had the lowest maximum penetration depth among all the formulations. A study by Mendoza et al. (2010) concluded that PVAc most likely stays in the bond line with only few vessels filling with adhesive, and they propose that the penetration limitation of PVAc relates to the hardening process.

Effective penetration followed a similar decreasing trend, except for a relatively lower value at 67%PF. Note that the concept of effective penetration only considers overall penetration area, without taking lumen size into account. The average size of the penetrated lumen of the specimens with 67% PF is  $3150\mu\text{m}^2$ , whereas it is  $3779\mu\text{m}^2$  for specimens with 50% PF content.

Overall smaller lumen sizes result in a lower calculated effective penetration, which shows a lower effective penetration of 67% PF than of the 50% PF. Therefore, effective penetration method could not accurately demonstrate the penetration situation since it is interfered by variance of lumen sizes. Instead, the actual penetration is better indicated by counting the number of resin-filled lumens.

As for bond performance on the radial surface, shear strength did not differ significantly among specimens with a PF content of 50% or more. Only the formulation with 25% PF content was significantly lower than the others (Figure 2-27). Wood failures for all the formulations cannot be concluded to be significantly different due to large variation (Figure 2-28); but it is noteworthy that the mean values of wood failure for both 25% PF and neat PVAc are lower, which could indicate weaker adhesive-wood interactions.

Overall penetration on a radial surface of 75% PF was lower than that of 50% PF, and these differed from penetration on a tangential surface (Figure 2-28). However, analysis indicates a decreasing trend of penetration as PVAc percent increases.

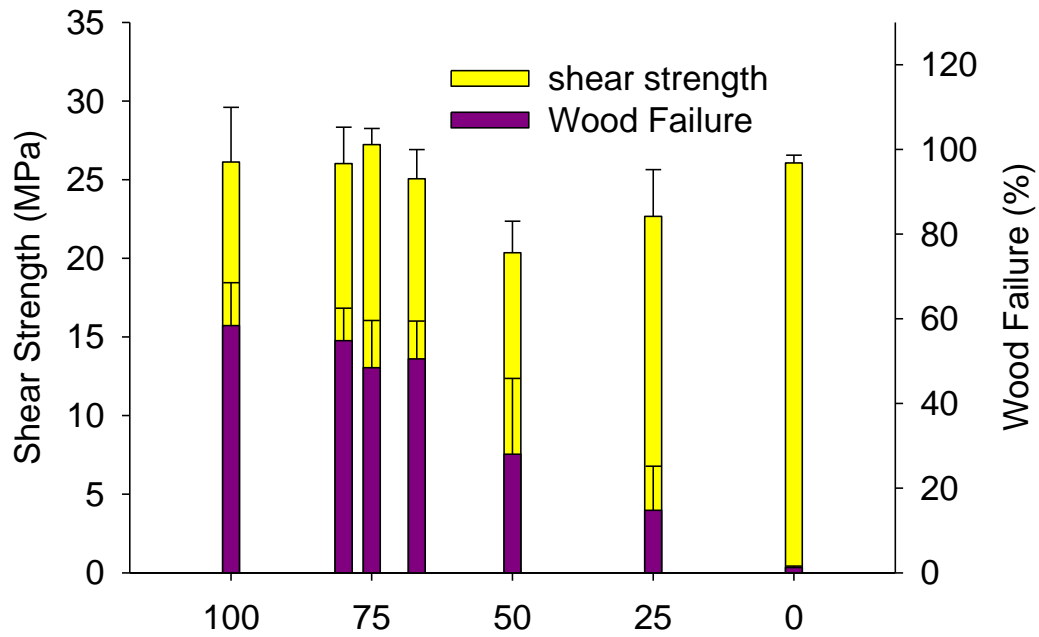


Figure 2-23 Bond performance of assembly joints with wood on tangential surface

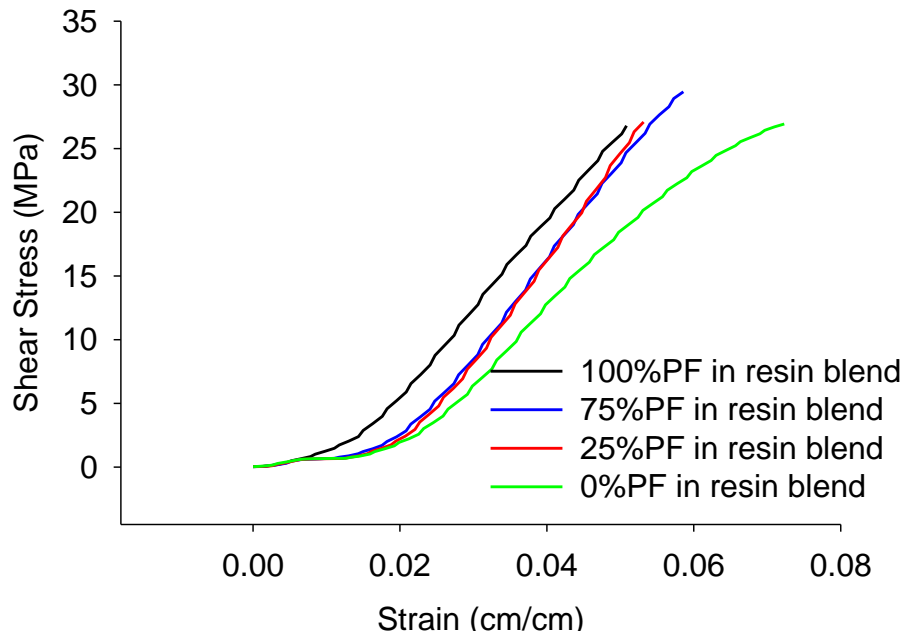
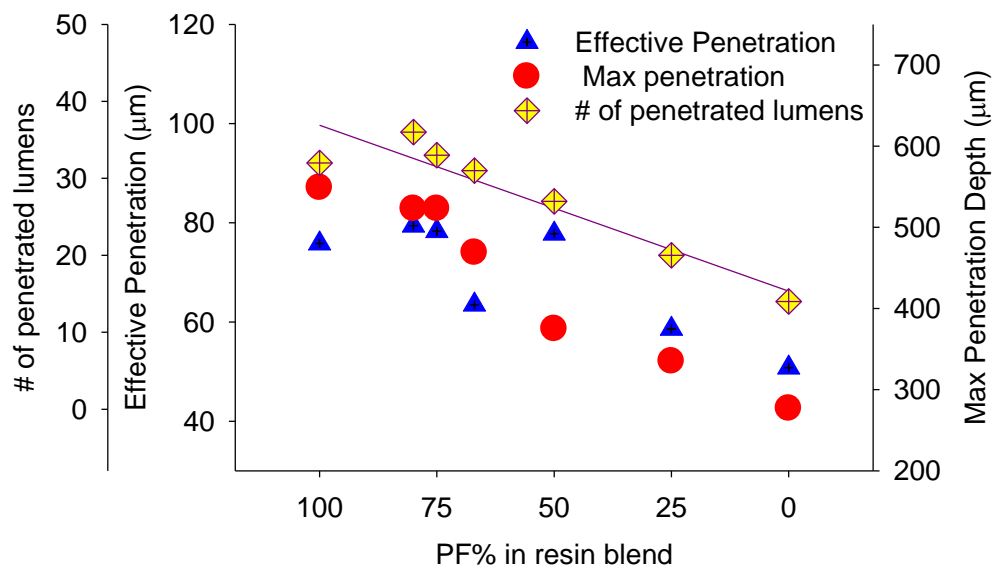
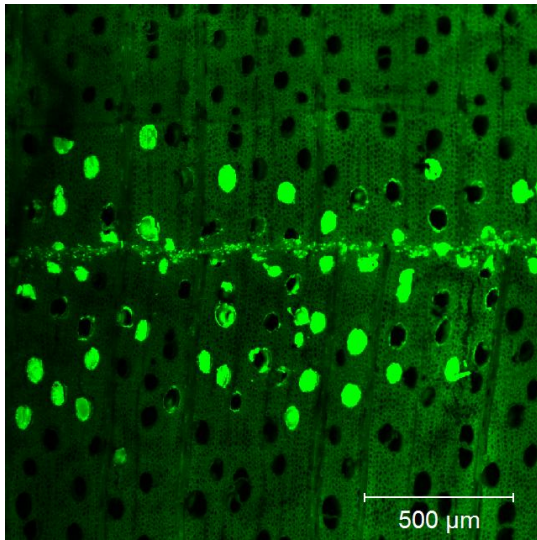


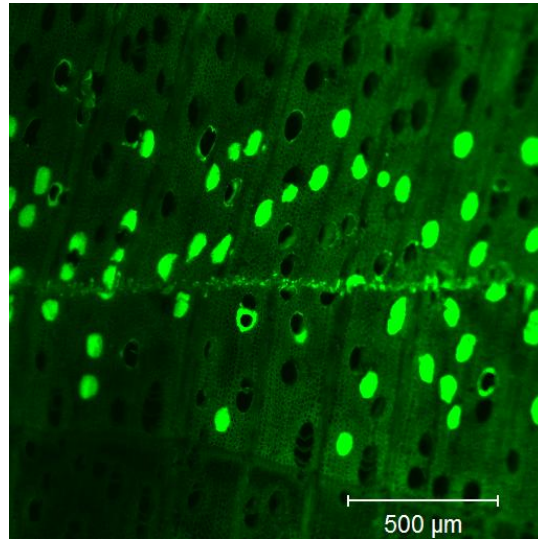
Figure 2-24 Shear stress/strain curve of neat PF, neat PVAc and hybrid adhesive



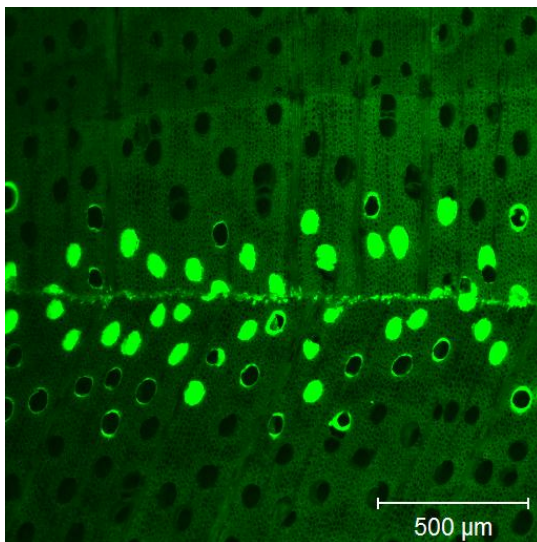
**Figure 2-25 Adhesive penetration of assembly joints with wood on tangential surface**



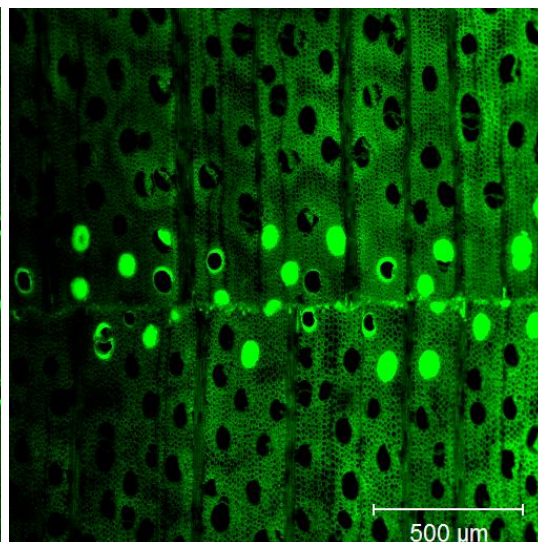
**PF:PVAc=100%:0%**



**PF:PVAc=75%:25%**



**PF:PVAc=50%:50%**



**PF:PVAc=25%:75%**

**Figure 2-26 Comparison of adhesive penetration into sugar maple on tangential surface**



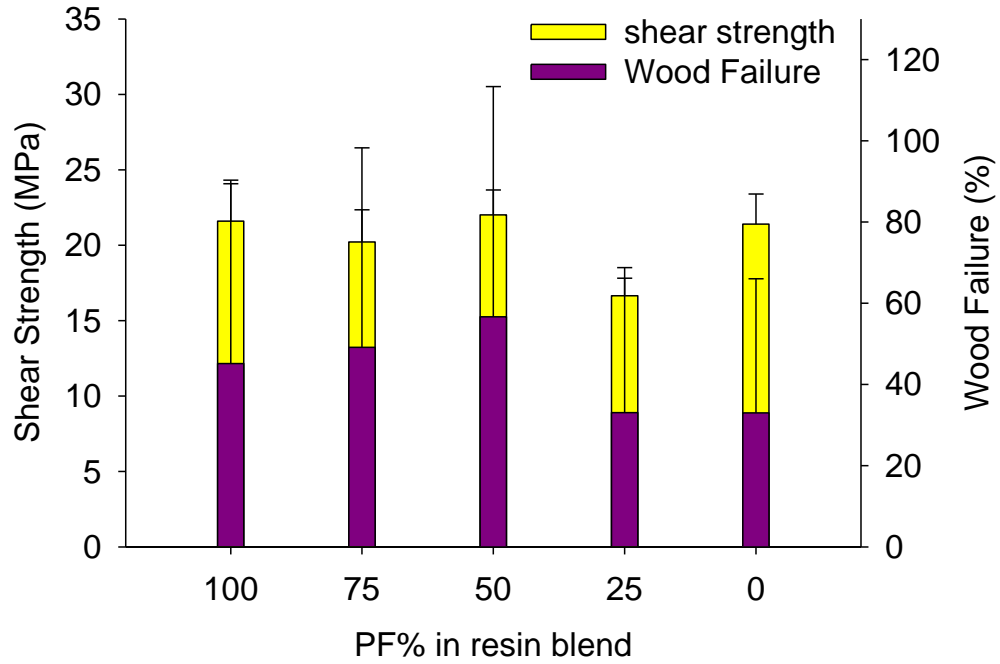


**Figure 2-27 Bond performance of assembly joints with wood on radial surface**

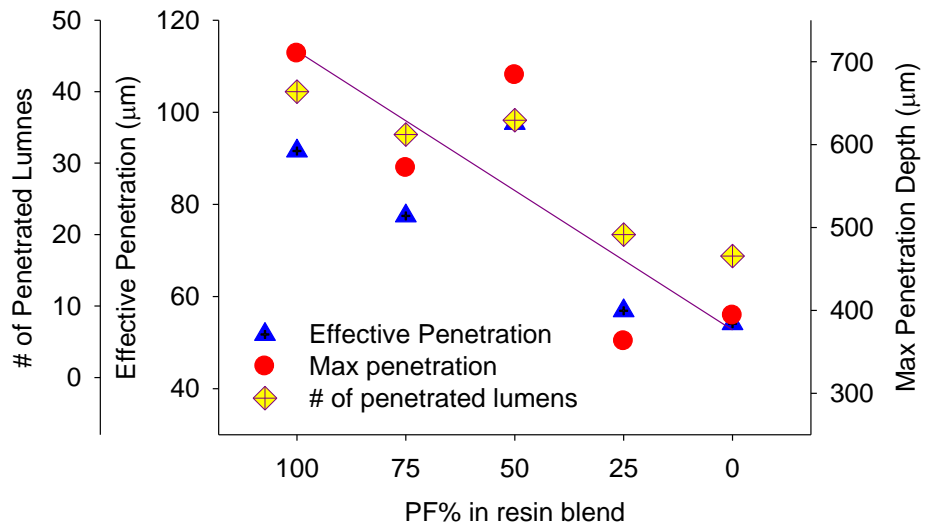


**Figure 2-28 Adhesive penetration of assembly joints with wood on radial surface**

## Summery and Conclusions

PF/PVAc hybrid adhesive was first studied in terms of their physical properties which included pH, viscosity, and dispersion, all of which critically influence hybrid adhesive performance. The interaction between hybrid adhesive and wood substrate was also investigated, specifically in terms of adhesive bond performance and adhesive penetration. Performance on both tangential and radial bonded wood surfaces was evaluated as well. Conclusions include:

- The pH of PF/PVAc resin blend is dominated by the pH of PF, resulting in a strong alkaline like neat PF.
- The viscosity of resin blends is directly related to the mixing time and blend ratio. Viscosity decreases initially with small additions of PVAc, but then increases to an even higher value than that of neat PF as PVAc content rises beyond 50%, despite the fact that the viscosity of PVAc is slightly lower than that of PF.
- Based on visual inspection of micrographs, the PF/PVAc blend is immiscible when PF dominates, but seems to be more uniform when PVAc dominates in the blend ratio.
- The shear strength of the bond with the binary adhesive on tangential surfaces was generally greater than that on radial surfaces; however, there was no significant difference in adhesive penetration.
- The bond performance of the PF/PVAc hybrid adhesive is comparable with neat PF when the proportion of PF is more than 50% in the blend.
- The interaction between wood and hybrid adhesive deteriorates with increasing PVAc content in the blend, as reflected by decreased wood failure percentages and decreased adhesive penetration.

- Adhesive penetration was significantly influenced by density. The overall adhesive penetration does not significantly decrease when PVAc content was less than 50%, but dramatically decreased when PVAc dominated in the blend.
- Among the three quantification methods, effective penetration method ran into limitations when lumen size varied widely. In this case, counting penetrated lumens seemed better to characterize penetration.

## References

- Ani, F. N., Wong, C. C., and Nor, H. M. (2004). "Properties of oil-palm-shell-based phenol wood adhesives compared with petroleum-based phenol wood adhesives." *Journal of Oil Palm Research*, 16(1), 54–65.
- ASTM Standard. (2004). *ASTM D905-03 Standard Test Method for Strength Properties of Adhesive Bonds in Shear by Compression Loading*.
- ASTM Standard. (2006a). *ASTM D1084-97 Standard Test Methods for Viscosity of Adhesives*.
- ASTM Standard. (2006b). *ASTM D143-94 Standard Test Methods for Small Clear Specimens of Timber*.
- Bickford, J. H., and Nassar, S. (1998). *Handbook of bolts and bolted joints*. CRC Press.
- Bolton, A. J., Dinwoodie, J. M., and Davies, D. A. (1988). "The validity of the use of SEM/EDAX as a tool for the detection of UF resin penetration into wood cell walls in particleboard." *Wood Science and Technology*, 22(4), 345–356.
- Brady, D. E., and Kamke, F. A. (1988). "Effects of hot-pressing parameters on resin penetration." *Forest products journal*, 38(11-12), 63–68.
- Chandler, J. G., Brandon, R. L., and Frihart, C. R. (2007). "Examination of adhesive penetration in modified wood using fluorescence microscopy." *Forest Products Journal*, 57(5), 1–10.
- Chen, C., Lu, C., Chang, C., Yang, Y., and Maa, J. (2000). "Influence of pH on the stability of oil-in-water emulsions stabilized by a splittable surfactant." *Colloids and Surfaces A: Physicochemical and Engineering Aspects*, 170(2-3), 173-179.
- Confocal tutorial. (2010). "Confocal tutorial: Priniples: How confocal differs AMU Dept Pathol Univ Hel." <[http://www.hi.helsinki.fi/Amu/AMU%20Cf\\_tut/Cf\\_tut\\_part1-3.htm](http://www.hi.helsinki.fi/Amu/AMU%20Cf_tut/Cf_tut_part1-3.htm)> (Jul. 8, 2010).
- Cyr, P., Riedl, B., and Wang, X. (2007). "Investigation of Urea-Melamine-Formaldehyde (UMF) resin penetration in Medium-Density Fiberboard (MDF) by High Resolution Confocal Laser Scanning Microscopy." *Holz als Roh- und Werkstoff*, 66(2), 129-134.
- Ebnesajjad, S. (2008). *Adhesives Technology Handbook*. William Andrew.
- Erbil, H. Y. (2000). *Vinyl acetate emulsion polymerization and copolymerization with acrylic monomers*. CRC Press.
- Frihart, C. R. (2005a). "9 Wood Adhesion and Adhesives." *Handbook of wood chemistry and wood composites*, 215.
- Frihart, C. R. (2005b). "Adhesive bonding and performance testing of bonded wood products." *Advances in adhesives, adhesion science, and testing*, 2(7), 1-12.
- Gavrilović-Grmuša, I., Miljković, J., Djiporović-Momčilović, M., and Radošević, G. (2008.). "Penetration of urea-formaldehyde adhesives in wood tissue, part I: Radial penetration of UF adhesives into beech." *Bulletin of the Faculty of Forestry*, 98, 39–48.
- Gindl, W., Schöberl, T., and Jeronimidis, G. (2004). "The interphase in phenol-formaldehyde and polymeric methylene di-phenyl-di-isocyanate glue lines in wood." *International Journal of Adhesion and Adhesives*, 24(4), 279–286.
- Grigsby, W. J., Thumm, A., and Kamke, F. A. (2005). "Determination of resin distribution and coverage in MDF by fiber staining." *Wood and Fiber Science*, 37(2), 258–269.
- Hoadley, R. B. (1990). *Identifying wood: accurate results with simple tools*. Taunton Press.
- Hse, C. Y., and Kuo, M. L. (1988). "Influence of extractives on wood gluing and finishing-a review." *Forest Products Journal*, 38(1), 52-56.

- Johnson, S. E., and Kamke, F. A. (1992). "Quantitative analysis of gross adhesive penetration in wood using fluorescence microscopy." *The Journal of Adhesion*, 40(1), 47–61.
- Johnson, S. E., and Kamke, F. A. (1994). "Characteristics of phenol-formaldehyde adhesive bonds in steam injection pressed flakeboard." *Wood and fiber science: journal of the Society of Wood Science and Technology (USA)*, 26(2), 259-269.
- Kamke, F. A., and Lee, J. N. (2007). "Adhesive penetration in wood-A review." *Wood and Fiber Science*, 39(2), 205–220.
- Kim, S., and Kim, H. J. (2006). "Thermal stability and viscoelastic properties of MF/PVAc hybrid resins on the adhesion for engineered flooring in under heating system; ONDOL." *Thermochimica Acta*, 444(2), 134–140.
- Kotz, J. C., and Purcell, K. F. (1991). *Chemistry and chemical reactivity*. Saunders College Pub.
- Laborie, M. P. (2002). "Investigation of the wood/phenol-formaldehyde adhesive interphase morphology." Ph.D Dissertation, Washington State University, Pullman, WA.
- Lovell, P. A., and El-Aasser, M. S. (1997). *Emulsion polymerization and emulsion polymers*. J. Wiley.
- Loxton, C., Thumm, A., Grigsby, W. J., Adams, T. A., and Ede, R. M. (2003). "Resin distribution in medium density fiberboard. Quantification of UF resin distribution on blowline-and dry-blended MDF fiber and panels." *Wood and Fiber Science*, 35(3), 370–380.
- Marra, A. A. (1992). *Technology of wood bonding*. Van Nostrand Reinhold.
- Mendoza, M., Hass, P., Wittel, F. K., Niemz, N., and Herrmann, H. J. (2010). "Adhesive Penetration in Beech Wood Part 2: Penetration Model. - Google Search." <<http://www.google.com/search?q=Adhesive+Penetration+in+Beech+Wood+Part+2%3A+Penetration+Model.&ie=utf-8&oe=utf-8&aq=t&rls=org.mozilla:en-US:official&client=firefox-a>> (Jul. 8, 2010).
- "Nobel Web, The Fluorescence Microscope." (2010). <<http://www.google.com/search?q=Nobel+Web%2C+The+Fluorescence+Microscope&ie=utf-8&oe=utf-8&aq=t&rls=org.mozilla:en-US:official&client=firefox-a>> (Jul. 8, 2010).
- Okkonen, E. A., and River, B. H. (1989). "Factors affecting the strength of block-shear specimens." *Forest products journal*, 39(1), 43–50.
- Pizzi, A. (1989). *Wood adhesives*. CRC Press.
- Sernek, M., Resnik, J., and Kamke, F. (1999). "Penetration of liquid urea-formaldehyde adhesive into beech wood." *Wood and Fiber Science*, 31(1), 41-48.
- Sernek, M. (2002). "Comparative analysis of inactivated wood surfaces." Ph.D Dissertation, Virginia Polytechnic Institute and State University, Blacksburg, Virginia.
- Serrano, E. (2004). "A numerical study of the shear-strength-predicting capabilities of test specimens for wood-adhesive bonds." *International Journal of Adhesion and Adhesives*, 24(1), 23–35.
- Siau, J. F. (1995). *Wood: Influence of moisture on physical properties*. Dept. of Wood Science and Forest Products, Virginia Polytechnic Institute and State University.
- Stat-ease (2005). Helps in Stat-ease software.
- Wang, J. (2007). "Cure kinetics of wood phenol-formaldehyde systems." Ph.D Dissertation, Washington State University, Pullman, WA.
- Wang, Y., Yadama, V., Marie, P. L., and Debes, B. (2010). "Cure Kinetics of PF/PVAc hybrid adhesive for Manufacturing Profiled Wood-Strand Composites." *Holzforschung In press*.
- White, J. G., Amos, W. B., and Fordham, M. (1987). "An evaluation of confocal versus

- conventional imaging of biological structures by fluorescence light microscopy.” *Journal of Cell Biology*, 105(1), 41-48.
- Yang, Y., Gong, M., and Chui, Y. H. (2008). “A new image analysis algorithm for calculating percentage wood failure.” *Holzforschung*, 62(2), 248–251.
- Zheng, J. (2002). “Studies of PF resole/isocyanate hybrid adhesives.” Ph.D Dissertation, Virginia Polytechnic Institute and State University, Blacksburg, Virginia.
- Zheng, J., Fox, S. C., and Frazier, C. E. (2004). “Rheological, wood penetration, and fracture performance studies of PF/pMDI hybrid resins.” *Forest Products Journal*, 54(10), 74–81.

# **CHAPTER 3 INFLUENCE OF THE PF/PVAC RATIO AND ADHESIVE APPLICATION SEQUENCE ON WOOD STRAND COMPOSITE PERFORMANCE**

## **Introduction**

Wood strand panels, such as oriented strand board, are commonly used in structural panels for wood-framed buildings in the U.S., and is gaining market share outside the U.S. as well (Hansen 2006; Spelter et al. 2006). Wood strand composite is a panel product made by hot-pressing a network of wood strands in a mat. Strands are flaked from small diameter logs potentially resulting in high conversion rates. A value-added product based on wood strand composite, such as lightweight sandwich panels (Voth 2009) , can be manufactured with reduced wood fiber and resin requirements

Corrugated wood composites, as one of those value-added wood composites, have been investigated since 1970s and have shown the feasibility of processing. However, the method could not be commercially applied because of the complicated design and high cost (Pang et al. 2007). Easier manufacturing method, such as conventional mat forming and pressing methods have shown adaptability for shallow corrugated composites, but more work is required before further application, including panel geometry, adhesive type and level (Pang et al. 2007).

To make the three dimensional wood composite products, commercially adaptable and simpler fabrication method needs to be developed using thermoforming techniques. However, in processes involving continuous thermoforming it is critical to handle a mat of discontinuous

elements with little disturbance to maintain mat integrity and produce a quality end product.

This project is part of a larger study where the goal is to develop a continuous method of manufacturing profiled wood-strand composite products. A hybrid adhesive system, which combines the excellent bonding capabilities of PF with the superior tackiness and toughness of PVAc, is being explored. The goal is to achieve good initial adhesion using PVAc for easier mat handling and develop a durable bond using PF during the curing process under heat and pressure. This study examines the performance of hybrid adhesives in wood-strand composite panels made of hybrid poplar. Before applying binary PF/PVAc adhesive system to manufacturing profiled wood strand composites, it is critical to understand the interaction between PF and PVAc resins during bond formation and its influence on wood strand composite's performance in terms of its physical and mechanical properties. This will contribute significantly to the body of research on the use of hybrid adhesives in manufacturing of strand-based composites.

To achieve desired initial adhesion, bond strength of PF could potentially be compromised by adding PVAc due to interference with direct interaction with wood (spreading, wetting, and penetration). It is hypothesized that use of PVAc with PF may interfere with spreading and penetration of PF into wood strands, and thus reduce bond quality among the strands in a wood-strand composite. This interference is speculated to be influenced by the proportion of PVAc in the resin blend and the sequence of resin application onto the strands during the blending process.

## **Objective**

The objective of this study was to understand the influence of adhesive blend ratio and the sequence of adhesive application on the bond strength and performance of wood-strand



composite. To meet or surpass the required performance in a cost-efficient manner, PF/PVAc ratio and adhesive application method must be optimized. To meet the objective, laboratory-based wood strand composites were evaluated by performing the following tasks:

- Investigate the influence of PF/PVAc blend ratios on mechanical and physical properties of manufactured wood-strand composite, including its modulus of elasticity, modulus of rupture, internal bond strength, density profile, thickness swelling, and water absorption capacity
- Study the impact of sequence of adhesive application on wood strand composite performance
- Analyze the effect of hybrid adhesive composition and application sequence on composite performance when exposed to varying environmental conditions allowing it to shrink and swell
- Optimize PF/PVAc blend ratios for acceptable performance in terms of mechanical and physical behavior

## **Background**

### **Adhesive Blend for Wood Composite**

#### **Value-added Wood Composites**

Three dimensional composites, such as corrugated fiberboard and metal plates, have been successfully applied for many years (LeBlanc et al. 1971; Sivachenko 1978). This idea has been applied to wood composites in 1970s; and different manufacturing methods, such as molds, have been tried (Bach 1989; Caughey et al. 1981; Geimer and Lehmann 1977). Shallow small

corrugated panels have been made by Price and Kesler (1974) in early 1970s but resulted in under-desired properties due to bad flow properties of the mat. Others studies have successfully manufactured deep corrugated panels b. However, those methods could not be commercially applied because of the complicated fabrication process which leads to high cost. Pang et al. (2007) manufactured shallow corrugated panel with conventional mat forming and pressing methods and stated that the resin type and level need to be further investigated.

### **Application of Resin Blend**

In wood composites industry, there are several kinds of commonly used resins, phenol-formaldehyde (PF), urea formaldehyde (UF), melamine formaldehyde (MF), melamine-urea-phenol formaldehyde (MUPF), polymeric diphenyl methylene di isocyanate (pMDI) and polyvinyl acetate (PVAc) (Sellers 2000). Phenol-formaldehyde (PF) is widely used in almost all kinds of wood composites, such as plywood, laminated veneer lumber (LVL), oriented strand boards and hardboard. Polyvinyl acetate emulsion is mainly used as assembly glues for decorative plywood and glued hardwood lumber (Sellers 2000).

Combination of different resins has been applied to wood composites for a long time for different reasons, such as lower cost and better composite properties. Resins that are applied at a high load (more than 5% resin solids on dry wood) account for up to 34% of the manufacturing cost, which is higher than wood materials (Adams and Broline 2006). Hence, manufacturers attempt to minimize the cost by partially replacing with a cheaper resin while achieving acceptable strength.

Different types of resins have been applied to manufacturing the same panel. In OSB, for example, slow curing and pre-cure-resistant PF has been applied to the surface layer, as it

directly contacts the heated press platen and has better cure conditions. Faster-curing PF, with a higher molecular weight and lower cure condition, is applied to the core layer (Phillips 2000). This strategy helps to shorten press time and increase OSB properties.

Phenol-formaldehyde (PF) and polymeric isocyanate (pMDI) are sometimes applied in combination in manufacturing OSB. PF is relatively cheap and does not adhere to the platens, thus suitable for face layers. Whereas, PMDI is exclusively used as a core adhesive (Phillips 2000) since it performs well in the core, and tends to stick to the hot platen when applied to face layers. For example, Wang et al. (2007) studied indoor-use particleboard with low formaldehyde emissions made from recycled wood-waste particles, using pMDI for core layer and PF for face and back layers. They found that MOR, IB, and TS were superior to the conventionally fabricated particleboard. Another study (Preechatiwong et al. 2007) directly applied the PF/pMDI blend to oriented strand lumber, and found that the ratio of 75/25 performed the best, while a 50/50 ratio performed the worst due to phase separation in both adhesives. A combination of thermosetting and thermoplastic resin, Polyvinyl acetate emulsion (PVAc) fortified with urea-formaldehyde (UF), on laminated bamboo has been studied, where the results showed that there was no significant difference between PVAc fortified UF and neat UF in terms of modulus of elasticity and modulus of rupture (Talabgaew and Laemlaksakul 2007).

## **Characteristics of Wood Composites Performance**

### **Density Profile**

Wood density is a critical quality factor of wood composite products in terms of both economy and efficiency (Hsu 1997). At the same panel density, raw wood materials with lower density can be highly compacted, leading to a higher contact surface area between wood

furnishings. Uniformity can also be achieved with lower density wood materials (Hsu 1997), which results in better mechanical properties and lower variability.

Density distribution is classified in the horizontal and vertical directions. Horizontal density distribution (HDD) describes density variations through the plane of panel, while vertical density distribution (VDD) represents density variation through panel thickness. HDD is influenced by particle geometry and forming (Linville 2000). Variation occurs when different overlapped particle layers are pressed to the same thickness within a mat. For HDD, it is assumed that larger particles have larger variations (Linville 2000). According to Suchsland (1973), horizontal density variation should be avoided, since it causes differential thickness and swelling, which in turn leading to damaging stresses in the panels (Linville 2000).

A typical vertical density profile of panels through the thickness includes high-density face layers, a low-density core and a nearly symmetrical pattern from the panel midpoint (Winistorfer et al. 1996). A vertical density profile is affected by varied furnish moisture content and the press closure rate. The tails of the vertical density distribution are also related to the press closure rate (Winistorfer et al. 1996). A vertical density profile is an important panel characteristic, since it influences panel's properties (Wang and Winistorfer 2000; Winistorfer et al. 1996). These include panel surface quality, fastener performance, bending properties and internal bond strength.

### **Modulus of Elasticity and Modulus of Rupture**

The modulus of elasticity (MOE) and the modulus of rupture (MOR) characterize wood composite mechanical performance. A laminate theory for a composite MOE model confirmed that the MOE of the board is likely to increase with a high surface density (Xu 1999). MOR also

showed an increasing trend as density increased (Kelly 1977). Other studies show that the MOR and MOE of Douglas fir flake-particle mixture board increased dramatically as resin content increased from 2% to 4%, and reached optimum levels with resin contents of 4% to 8% (Lehmann 1970). Normally, the strength and stiffness of wood tends to decrease as moisture content (MC) increases, when the MC is still below the fiber saturation point (Simpson and TenWolde 1999). For wood composites, the same trend occurs (Wu and Suchsland 1997). It was concluded that density and moisture content have significant effects on MOE and MOR (Kelly 1977; Shi et al. 2005).

### **Internal bond**

Internal bond (IB) refers to the tensile strength perpendicular to the panel plane, and is an important mechanical property. IB has been found to increase as the specific gravity of a board increases, although at a decreasing rate (Kelly 1977). Panel density has a positive influence on IB properties (Hse et al. 1975; Vital et al. 1974). Assuming that IB is correlated with density, IB specimens are more likely to break in the plane with the lowest density. In this case, failure tends to occur in the core layer when a panel has a density profile with a high density surface and a low density core. Also, IB tends to be higher for a specimen with a more uniform density profile, since it has relatively uniform strength through panel thickness (Linville 2000). Moreover, higher IB strength can be achieved with higher resin content (Lehmann 1970). However, Strickler (1959) and Geimer (1975) claim that there is no significant correlation between core density and internal bonds, due to moisture and press cycle effects (Kelly 1977). A laboratory-based study by Maloney (1975) suggests that IB actually decreases with the specific gravities of boards above 0.75 at a phenol formaldehyde resin of 6% (based on oven-dried wood).

## **Dimensional Stability**

Since wood composite is commonly used for structural purposes, it is more likely to serve as an exterior material and may be exposed to severe conditions including high humidity or temperature. Hence, it is important to understand the adhesive durability of wood composites under severe weather conditions.

Among different composite directions, the most significant change occurs across the thickness direction (Wu and Lee 2002). Concluded by Kollman et al (1975), swelling in the thickness direction increases with moisture content at an increasing rate (Kelly 1977). Two mechanisms are proposed for thickness swelling: recoverable thickness swelling, originates in the wood itself, and non-recoverable swelling, generated by the relief of residual compression (commonly called spring-back) (Wang and Winistorfer 2003).

Vital et al. (1974) concluded that panel density had an inverse effect on water absorption and thickness swelling. This could be due to the fact that boards with higher density have fewer voids, slowing water penetration speed (Kelly 1977). Thickness stability can also be enhanced with higher resin content. This probably occurs because spring-back and differential shrinkage stresses are enhanced with more resin (Hann et al. 1962; Lehmann 1970). Better interparticle bonding may also form when more resin is added, but cannot be further improved when resin content rises certain percentage (Kelly 1977).

Wu and Piao (1999) studied the relationship between thickness swelling and internal bond loss with four types of commercial OSB. Although IB strength did not noticeably decrease when moisture content changed from oven-dried up to 8%, it decreased significantly when the MC increased above 12%. A linear relationship formed between thickness swelling and water

absorption during a short-term soaking test, and the swelling rate varied based on specimen density.

### **Effect of Resin Content**

The influence of resin on wood composite performance has been investigated in several studies (Lehmann 1970; Wu and Lee 2002). Extended press time is necessary to eliminate the moisture content of boards that will be treated with resin, since cured resin can be weakened by high moisture content (Geimer and Christiansen 1996). Some studies have evaluated the correlation between MOE, MOR and overall resin content, and found no obvious increase on the strength of flake boards when the amount of urea-formaldehyde adhesive increased (Post 1958). Lehmann (1970) also ran studies with urea-formaldehyde at contents of 2%, 4% and 8%, and found only slight increases in MOE and MOR, whereas a continued increase of IB in the resin range. Shuler (1973) studied the particleboard manufactured with chipping residues at 7 levels of urea-formaldehyde (from 2% to 12%), and found no obvious increase in both MOR and MOE when adhesive resin was increased by more than 5%. Furthermore, when board properties were compared between adhesive content of 10% and 12%, MOE and MOR were lower at resin content of 12% than resin content of 10%. In addition, thickness swelling after 2-hour and 24-hour water soaking showed more swelling at resin content of 12% than at 10%. Studies by Clad W (1967) also conclude that board quality does not improve when adhesive content goes beyond 12% (Kelly 1977). Particleboards made with two isocyanate resins, pMDI and EMDI, showed significant higher values of MOE, MOR when resin content increased from 2% to 4%, and MOE and MOR's did not increase significantly when resin content increased from 4% to 6%. On the other hand, IB in particleboard increased as resin content increased from 2% to 4% to 6% (Papadopoulos et al. 2002). Another study regarding the fine particle content of OSB with PF

resin also concluded that resin content had no significant influence on MOE or MOR (Lee and Tahir 2003).

## **Materials and Methods**

### **Experimental Design**

There are two main objectives in this Chapter. One is to study the effects of increasing PVAc content on PF's ability to bond with wood strands during hot-pressing. The other is to investigate the influence of sequence of resin application (i.e., apply PF first then PVAc, apply PVAc first and then PF, or apply a blend of PF/PVAc) on the bond formation and performance. A response surface model was implemented with two numerical factors (PF and PVAc content) and one categorical factor (adhesive application sequence) for understanding and modeling the effects.

Response surface methodology (RSM) has been used for optimization of wood composites performance as it achieves the same results with minimum effort of process comparing with traditional methods of experimentation (Park et al. 1999; Wang and Lam 1999). RSM helps determine how a response is affected by a set of quantitative variables or factors over a specified region. The highly accurate models from this design (Wang and Lam 1999) can then be used to optimize the settings of a process (such as PF/PVAc ratio and application methods) to give a maximum or minimum response (MOE, MOR, IB, WA, or TS, in this case). D-optimal design was chosen to determine the test runs in the design space to minimize the number of runs and error (Adams 2006). Additional runs were added to provide estimates of lack of fit and pure error. A quadratic response model was chosen to determine the number of runs. Since the amount of PF used in manufacturing OSB is generally between 4 to 6 percent, PF resin content was



confined to between 4 and 6 percent. PVAc was confined to between 1 and 6 percent based on a previously conducted study on cure kinetics of PF/PVAc hybrid adhesive by Wang et al. (2010). The adhesive application sequence had three levels: apply blend, apply PF first, and apply PVAc first. The DesignExpert® DOE software generated 23 runs based on the input factors and their ranges. Based on geometric candidate set of fixed coordinates, design points included vertices, edge and axial points, centroid, and intermediate points. Two more runs of 6% PF were added as controls, and seven additional runs were included to minimize experimental error. All the formulations are shown in Table 3-1.

## **Materials**

Hybrid poplar, an appropriate raw material for wood composite panels because of its high productivity (Zhou 1990), low density, and uniform cell structure, was chosen as the raw material for wood strand panel fabrication.

The strands were produced using a disc strander at the Composite Materials and Engineering Center (CMEC) at Washington State University from hybrid poplar (*Populus deltoides*) logs. The target dimension of the produced strands was 150 mm long by 12 mm wide by 0.5 mm thick. Strands were conditioned to a MC of approximately 10% after processing (Wang et al. 2010). Commercially produced PF and PVAc resins described in Chapter 2 were used in fabricating the test panels.

**Table 3-1 A total of 32 runs or design points implemented based on D-optimal response surface design by State-Ease**

<b>PF (%)</b>	<b>PVAc (%)</b>	<b>Sequences</b>	<b>PF(%)</b>	<b>PVAc(%)</b>	<b>Sequences</b>
<b>6</b>	<b>6</b>	<b>Blend</b>	<b>4</b>	<b>1</b>	<b>PVAcFirst</b>
<b>6</b>	<b>6</b>	<b>PFFirst</b>	<b>4</b>	<b>1</b>	<b>PFFirst</b>
<b>6</b>	<b>6</b>	<b>PFFirst</b>	<b>4</b>	<b>1</b>	<b>Blend</b>
<b>6</b>	<b>6</b>	<b>PVAcFirst</b>	<b>5</b>	<b>1</b>	<b>Blend</b>
<b>6</b>	<b>6</b>	<b>Blend</b>	<b>5</b>	<b>2.25</b>	<b>PFFirst</b>
<b>6</b>	<b>6</b>	<b>PVAcFirst</b>	<b>5</b>	<b>1</b>	<b>PVAcFirst</b>
<b>4</b>	<b>6</b>	<b>PFFirst</b>	<b>6</b>	<b>1</b>	<b>PVAcFirst</b>
<b>5.5</b>	<b>3.5</b>	<b>PVAcFirst</b>	<b>6</b>	<b>0</b>	<b>NA</b>
<b>4</b>	<b>6</b>	<b>PFFirst</b>	<b>6</b>	<b>0</b>	<b>NA</b>
<b>4</b>	<b>6</b>	<b>Blend</b>	<b>6</b>	<b>2</b>	<b>Blend</b>
<b>4</b>	<b>3.5</b>	<b>PVAcFirst</b>	<b>6</b>	<b>2</b>	<b>PVAcFirst</b>
<b>6</b>	<b>1</b>	<b>Blend</b>	<b>6</b>	<b>2</b>	<b>PFFirst</b>
<b>6</b>	<b>1</b>	<b>PVAcFirst</b>	<b>5</b>	<b>2.25</b>	<b>PFFirst</b>
<b>6</b>	<b>1</b>	<b>PFFirst</b>	<b>5.5</b>	<b>3.5</b>	<b>PVAcFirst</b>
<b>5</b>	<b>3.5</b>	<b>Blend</b>	<b>6</b>	<b>1</b>	<b>Blend</b>
<b>4</b>	<b>6</b>	<b>Blend</b>	<b>4</b>	<b>2</b>	<b>Blend</b>

## **Wood Composite Manufacturing**

Strands were dried to a MC of approximately 3% and screened to remove fines. Based on the runs in Table 3-1, desired PF and/or PVAc adhesive was distributed onto the strands in a drum blender as per the application sequence. A study on cure kinetics of PF/PVAc hybrid adhesive by Wang et al. (2010) showed that the curing process of the PF/PVAc hybrid adhesive system takes longer than that of neat PF. A second curing peak was observed with the addition of PVAc, which moved towards higher temperatures as PVAc content increased. The first curing temperature peak occurred at around 145°C, and the second peak was around 157°C. Since the curing process slows down with increasing amount of PVAc, trial runs were conducted with maximum PVAc and PF contents included in experiment design (see Table 3-1) to determine the hot-pressing schedule. Resins were applied to strands with an air atomized sprayer in a rotating drum with three sequences: PF first, PVAc first or a predetermined blend. To prepare resin blends, desired PF and PVAc resin proportions were mixed for 15 minutes at 1000rpm until it formed a uniform-colored blend.

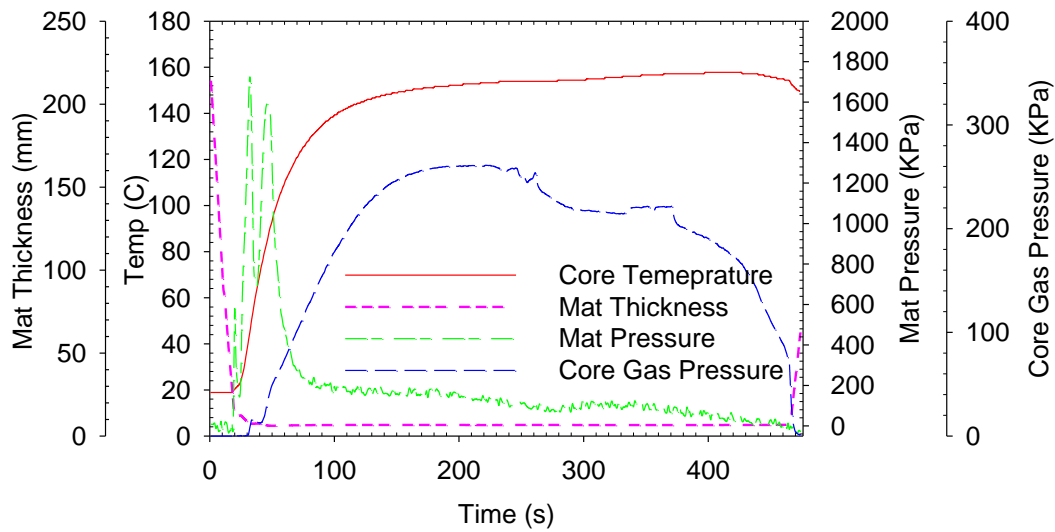


**Figure 3-1 Pressing schedule for hot-pressing test panels**

Adhesive blended strands were hand-distributed through a forming box above an aluminum caul sheet (Figure 3-2). The table under the caul sheet oscillated to help the strands evenly pass through the vanes. All panels were manufactured with a hydraulic 0.914m<sup>2</sup> oil-heated press using a Pressman<sup>TM</sup> control system. Based on the gas pressure and core temperature recorded by temperature and pressure probes inserted into the core of the mat during trial runs, the hot-pressing schedule was determined (Figure 3-1). Loose mat was hot-pressed with a platen temperature of 160°C (Figure 3-3). Finally, pressed boards were trimmed to 0.508m by 0.508m from 0.66m by 0.66m. A total of 32 test panels were manufactured. The target density and the thickness for all panels were 0.59g/cm<sup>3</sup> and 6.35mm respectively.



**Figure 3-2 Resinated strands distributed through forming box**



**Figure 3-3 Loose mat and hot pressing**

## **Testing for Mechanical and Physical Properties**

The specimens from the first run were excluded from the data analysis as its opening time during hot pressing was extended to release excess gas pressure compared to all the other panels. Test specimens for all the 31 panels were cut as per the cutting scheme shown in Figure 3-4. Dimensions of the specimens are given in Table 3-2. Specimens were conditioned at 20<sup>0</sup>C and 65% RH for over two weeks after manufacturing to reach an equilibrium moisture content (EMC) of 12%. Vertical density profiles were scanned for all internal bond specimens using a

nondestructive X-ray vertical density profiler.

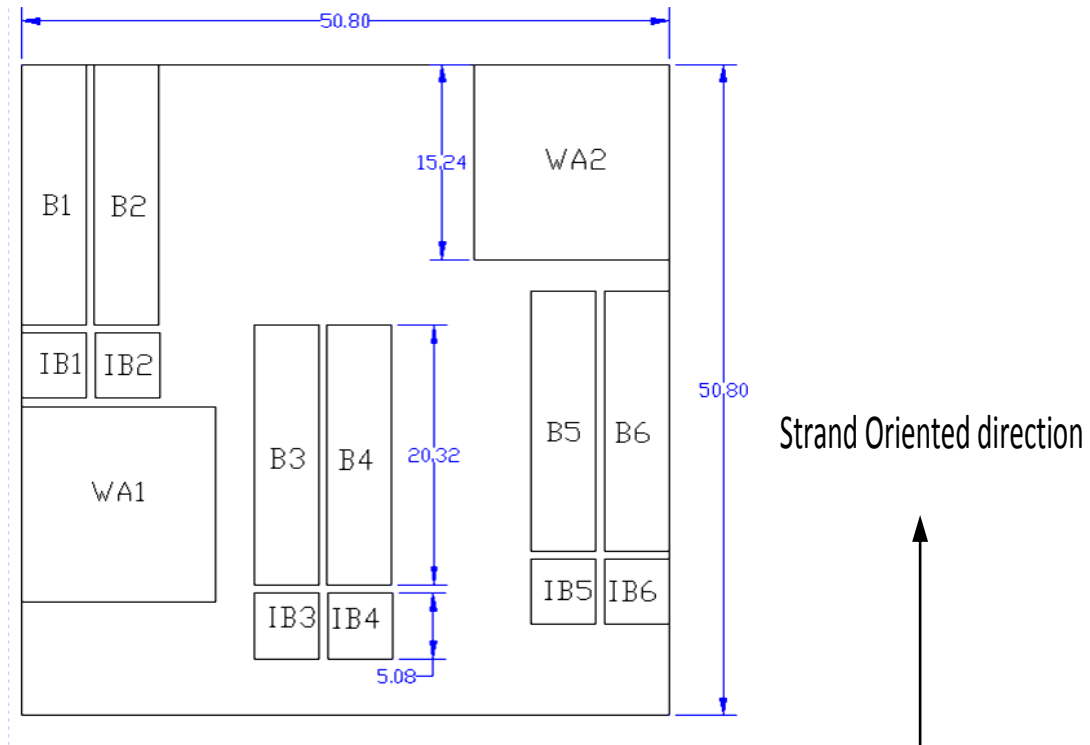


**Figure 3-4 Specimen cutting pattern for test panels.**

**Unit in Figure: cm; B-Bending; IB-Internal Bond; WA-Water absorption and Thickness Swelling;**

**For Bending and IB, #1, 3, 5-Conditioned at 20°C and 65%RH; #2, 4, 6-Severe Condition**

**Treatment**

**Table 3-2 Sampling scheme for each panel**

Test	Target Dimensions (mm)	# of specimens per panel	Total # of specimens
Bending under normal condition	50.8 × 203.2 × 6.35	3	93
Bending with severe condition treatment	50.8 × 203.2 × 6.35	3	93
Vertical density profile	50.8 × 50.8 × 6.35	6	186
IB under normal condition	50.8 × 50.8 × 6.35	3	93
IB with severe condition treatment	50.8 × 50.8 × 6.35	3	93
Water absorption and thickness swelling	152.4 × 152.4 × 6.35	2	62

Half the specimens for bending and IB remained in the same conditioning room, and half were subjected to varying cycles of temperature and relative humidity as shown in Figure 3-5 in a different conditioning chamber. These will be referred to as specimens subjected to severe relative humidity treatment. Specimens were conditioned at each step until they reached their EMC at the set condition.

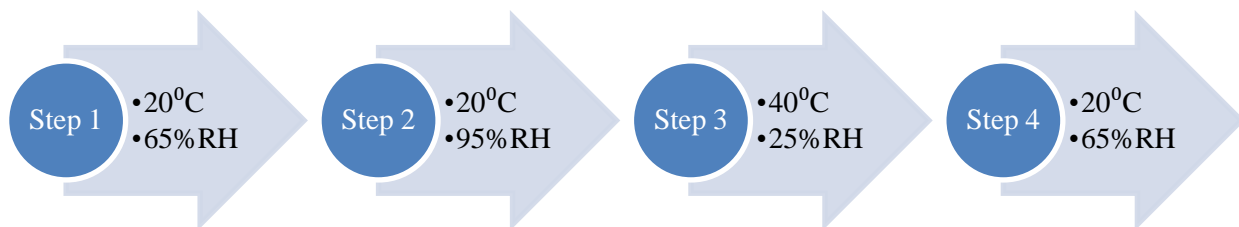


**Figure 3-5 Severe relative humidity treatment to cycle the specimens through equilibrium moisture contents of 12%, 24%, 5% and back to 12%**

Three-point bending and internal bond tests were conducted using an Instron testing machine according to ASTM D1037-99 (ASTM Standard 2006) (Figure 3-6). Density of flexure

specimens and internal bond specimens were obtained based on the weights and dimensions right before testing; moisture content of flexure specimens were obtained based on dried weights after 24 hours of oven drying.

Thickness swell and water absorption were carried out in accordance with ASTM D1037-99. Specimens were weighed, and thicknesses were measured at 5 fixed points for each specimen after 2-hours and 24-hours of water submersion.

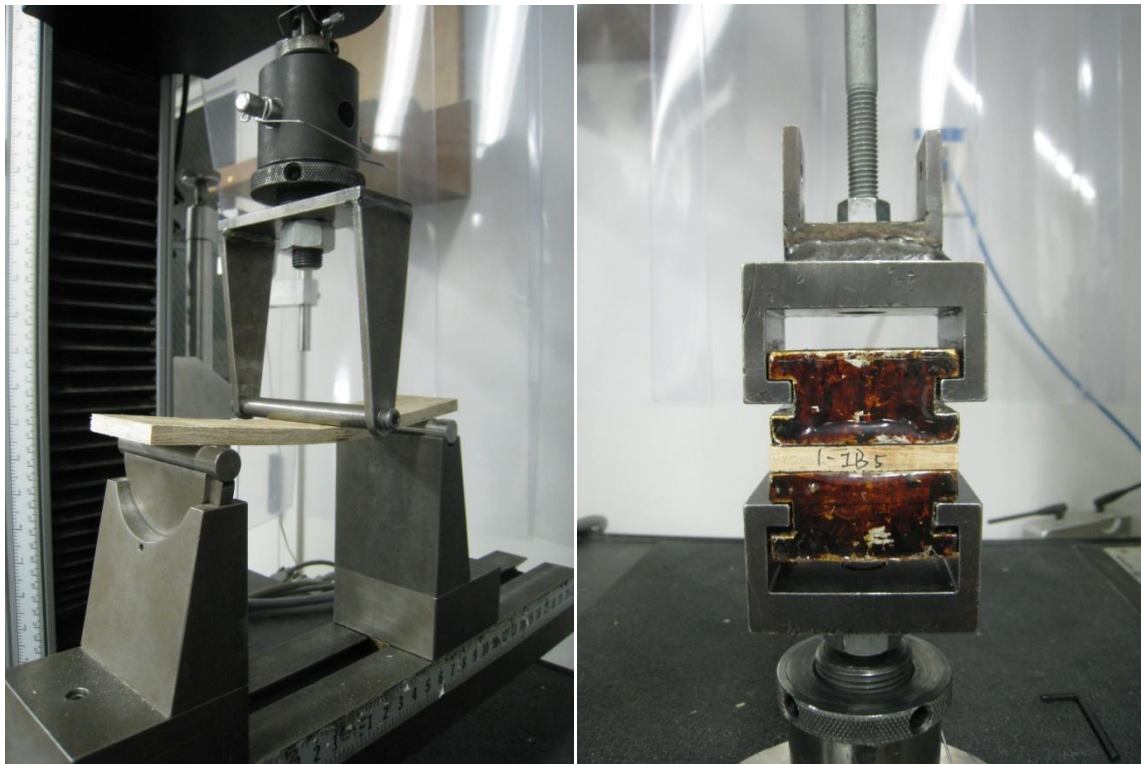


**Figure 3-6 Static bending test (Left) and internal bond test (Right)**





**Figure 3-7 Water submersion (Left) and five-spots thickness measurement (Right)**

## **Results and Discussion**

### **Density Profile**

The average thickness of all the panels immediately after fabrication was  $6.51 \pm 0.36$  mm, which expanded to  $6.87 \pm 0.40$  mm after two weeks of conditioning at 20°C and 65% RH. Panels with more resin content generally have a smaller expand as more resin help to resist spring back and differential shrinkage stresses (Hann et al. 1962). The overall density profile pattern is similar for all panels (Figure 3-8) due to identical pressing schedule. The slight difference among formulations could be due to the different moisture content of raw materials (wood strands and resin blend) of different formulations before hot pressing. The resulting profile, which exhibits high density near the edge and low density in the core, is typical for a hot-pressed wood-strand panel.

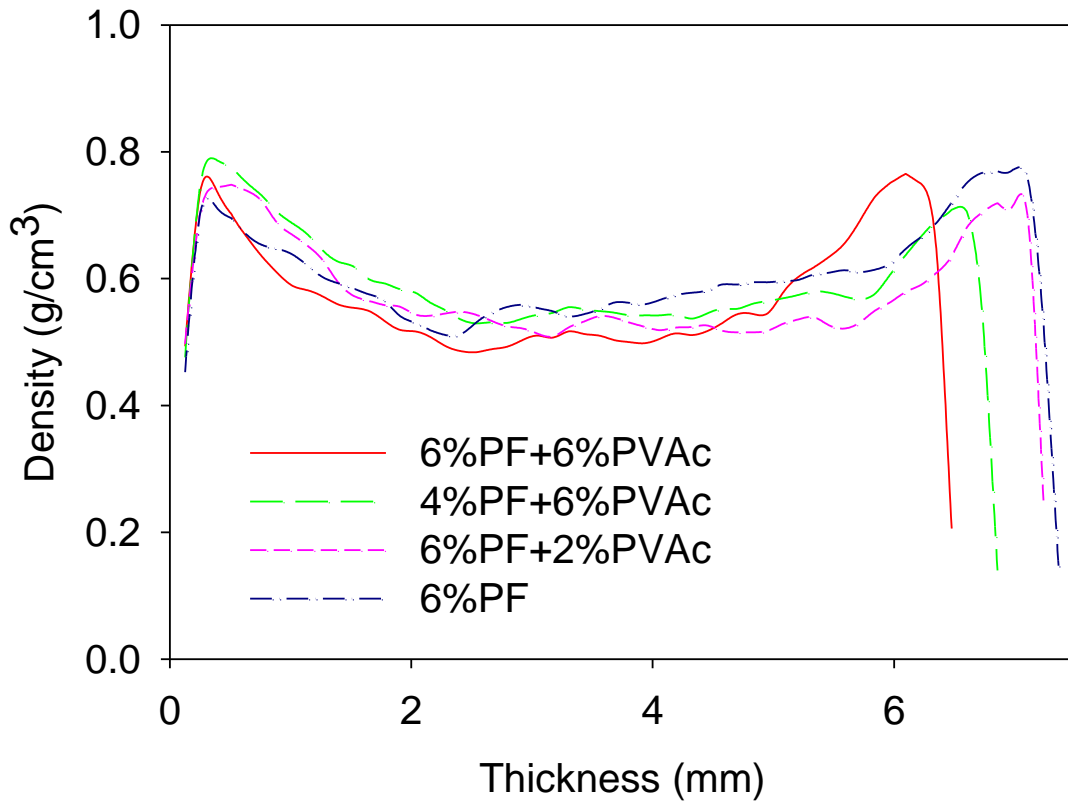


**Figure 3-8 Density Profiles**

### **Density Effect as a Covariate**

As the objective is to examine the influence of resin ratio and application sequence, density effects were analyzed for their significance especially as it influences flexure properties, internal bond strength, and dimensional stability. This study examined the effect of density on all responses using analysis of covariate (ANCOVA) with SAS statistical program. The interaction between covariates and factors was first examined and then removed from ANCOVA, since no significant interaction was found. Each corresponding response was then adjusted based on a homogenous slope model using ANCOVA excluding interaction term. Results show that density

was a significant positive covariate for flexure specimens under both normal and severe RH conditions. For IB specimen, the lowest density point in the core of density profile shows significant influence and its effect is removed by ANCOVA adjustment.

For the water absorption and thickness swelling tests, there is no error term to examine interaction, since there are only two replicates in each run. Normally there are two options under this circumstance, one is to use analysis of variance (ANOVA), ignoring the covariate effect; the other is to apply ANCOVA, omitting the potential interaction term (Silkmitter et al. 1999). In this case, density was analyzed as a covariate, since previous studies have shown that density significantly influences WA and TS properties (Shi et al. 2005; Qinglin Wu and Lee 2002; Zhou 1990). And thus, it was assumed that there was no interaction between density and runs in this study. Density showed a significant negative effect on WA after 2-hours and 24-hours of water submersion, and also on TS after 24-hours of water submersion. TS after 2-hours showed an insignificant density effect, and were calculated using analysis of variance (ANOVA) instead.

After proper adjustments, all response values were input into Design-Expert software. The best fitted models were chosen based on the statistical information from three aspects. Sequential model shows the statistical significance of adding each model terms in the model; the lack of fit test diagnoses if the data fits the chosen models well; and the model  $R^2$  value that estimates how well the model explains the variation of data (Stat-ease 2005). Response surface model gives a statistical trend in responses and offers valid information regarding difference in properties due to the treatment factor (PF and PVAc percent, application sequence) in this experimental design space. Statistics of each fitted model are shown in Appendix C . All specimens conditioned at 20 °C and 65% RH to reach a moisture content of 12% are referred to MOE1, MOR1 and IB1 from henceforth; and specimens exposed to a severe RH treatment are

referred to as MOE2, MOR2 and IB2 henceforth. Water absorption and thickness swelling under 2-hours and 24-hours submersion are referred to as 2hrs WA, 24hrs WA, 2hrs TS and 24hrsTS, respectively.

### **Effects of PF/PVAc ratios**

To evaluate the PF/PVAc ratio effect on mechanical and physical properties, the response surfaces are compared for the three application sequences (apply blend, apply PF first and apply PVAc first). Percentage differences of properties between hybrid PF/PVAc at 6%PF and varying proportions of PVAc and control specimens with 6%PF are shown in Table 3-4.

### **Modulus of Elasticity**

The average MC of flexure specimens under normal condition was  $8.72\% \pm 0.43\%$  before testing. For specimens exposed to severe RH treatment, the MC of the flexure specimens increased to  $18.48\% \pm 1.24\%$  at  $20^{\circ}\text{C}$  and 95%RH, then dropped to  $4.32\% \pm 0.43\%$  at  $40^{\circ}\text{C}$  and 25%RH, and reached an average MC of  $9.60\% \pm 0.65\%$  at the end prior to testing.

Response surface analysis indicated that neither resin content nor application sequence has a significant influence on MOE in reduced models (Table 3-3). As shown in Figure 3-9, addition of PF under 5% has a slightly positive effect on MOE1 but an opposite effect with more than 5% PF. MOE2 under severe RH treatment has a significant decrease compared to those under normal condition. MOE2 showed a continuous but slight increase with increasing PF content up to 6%.

Since the fitted reduced models for MOE is only significant at 0.1 level, conclusions need to be carefully drawn. As shown in Table 3-4, at 6%PF level, increase in PVAc content seems to have a positive followed by a negative effect on MOE, as reflected by the average change of

relative decrease of MOE1 from -4.9% to 10% and to -1.2% and average relative difference of MOE2 ranged from -2.5% to 8.9% to 4.9%. Increasing resin content to certain level was shown to have an insignificant increase in MOE in previous studies, and even a negative effect can be found at resin percent of more than 12% (Post 1958; Lehmann 1970; Kelly 1977; Papadopoulos et al. 2002). In this study, the trend in MOE is speculated to be influenced by application sequences, which will be discussed later.

### **Modulus of Rupture**

As applied load is transferred through shear from element to element in a short fiber composite, the effects of bond formation and performance will be greater on MOR than MOE. As PVAc percent increased from 0% to 6%, the MOR1 under normal condition had a slight increase with addition of either PF or PVAc (Figure 3-10); whereas MOR2 under severe RH treatment shows a turning point as PVAc content goes above 4-5%. It indicates that addition of PVAc above 4-5% could be detrimental to composite strength performance when subjected to severe and changing environmental conditions. We speculate that excess PVAc tends to interfere with PF in terms of spreading and penetration. With increased PVAc content, there is a greater chance for PVAc to be in direct contact with wood and thus interfere with PF bonding with wood. Under high humidity environment, the acetylene groups in PVAc are relatively ready to be partially hydrolyzed and turn into hydroxyl groups (Qiao and Eastal 2001). A comparatively weak interaction is formed with wood by secondary forces leading to water molecules easily penetrating into the interface between PVAc and wood. This leads to adhesive softening that reduced adhesion and cohesion. In this case, PVAc tends to weaken the bond between wood strands under severe RH treatment, and lead to a reduction in strength with repeated shrinking and swelling action of the composite. Bond strength could be potentially further hindered by

increase of PVAc to a higher percent and this interference becomes especially obvious when applying PVAc first, which will be discussed later.

### **Internal Bond Strength**

Internal bond, which characterizes the bond strength between wood strands, affects mat integrity under hot-pressing. IB1 and IB2 followed a similar trend (Figure 3-11), with both showing a linear, increasing trend as overall resin (PF and PVAc) content increased. Furthermore, IB increased faster with the addition of PVAc from 1% to 6% than with the addition of PF from 4% to 6%. Due to its ductile nature, PVAc deforms more easily and can transmit stress more evenly than brittle adhesive such as PF (Marra 1992). This ductility ensures that PVAc distributes stress more efficiently than PF, which in turn tends to increase internal bond strength. Advantage of this ductility of adhesive on bond performance was also manifested in the performance behavior of PVAc in Chapter 2, where shear strength of PVAc was comparable to that of neat PF and showed better deformability in the stress/strain curve.

### **Dimensional Stability**

The overall trend for water absorption (WA) and thickness swelling (TS) under 2 hours and 24 hours periods are very similar. Both WA and TS increased quickly during the first two hours of water submersion, and a large percent of thickness swelling occurred during the first 2 hours of treatment. Both PF and PVAc content had a significant influence on water absorption and thickness swelling in most cases (Table 3-3). As shown in Figure 3-12 and Figure 3-13, more resin appears to increase water resistance and dimensional stability. Four percent PF and one percent PVAc had the most WA and TS, and 6% PF combined with 6% PVAc had the least WA and TS. In addition, PF reduced water absorption and thickness swelling more efficiently, water resistance and dimensional stability improved much more quickly as PF increased from 4%

to 6% than it did when PVAc increased from 1% to 6%. Resin combination of 6% PF and 1% PVAc exhibited lower WA and TS than 4% PF and 6% PVAc.

## **Effects of Resin Application Sequence**

### **Generally Superior Performance when Applying PF First**

Although application sequence effect only shows significant difference in MOR1, IB1 and IB2 (Table 3-3); similar trends in application sequence developed in all of the other responses as shown in response surface model graphs. In terms of overall mechanical performance, applying PF first is better (Figure 3-14 and Figure 3-16) in most cases. Some interactions can be seen in MOR2 and IB1 which will be discussed later.

For WA and TS, applying PF resulted in the lowest values, suggesting better water resistance and dimensional stability in 2hrs WA, 2hrs, and 24hrs TS, although a difference was shown in 24 hrs WA (Figure 3-18 and Figure 3-20). Applying PVAc generally shows similar water resistance and dimensional stability as applying blend.

### **Interaction in Application Sequences**

Analysis of the data indicates an interaction between the application sequence and the amount of PVAc applied. In cases where higher percentage of PVAc is applied first, there seems to be an interference with the PF penetration. We speculate that application of more PVAc first results in greater probability of PVAc sandwiched between the wood strands and PF (Figure 3-21), thus potentially decreasing the spreading, wetting, and penetration capacity of PF. This behavior leads to a bond that weakens with repeated shrinking and swelling of the composite when exposed to changing relative humidity. Drop in properties (MOR2, IB1 and IB2) after undergoing severe RH treatment is an evidence of this behavior.

MOE is also speculated to be affected by application sequence although significance is not shown in fitted model, which could be due to the noises induced by other factors outside the design of experiment. At PF percent of 6% (Table 3-4), MOE2 had a continuous increase as PVAc increased from 1% to 2% to 6% when applying PF first, whereas MOE2 under severe RH condition showed a continuous decrease as PVAc increased from 1% to 2% to 6% when applying PVAc first.

As mentioned earlier, PVAc offers good bond under normal condition, as shown in relatively high shear strength in Chapter 2. When high moisture is induced during severe RH treatment, the bond between resin and wood strands tend to deteriorate; and it could be further deteriorated as PVAc increases. As shown in Figure 3-14, MOR2 dropped as PVAc content increased when PVAc is applied first. We speculate that at lower amounts of PVAc, it contributes through its ductility and helps with the stress transfer among wood strands. However, with application of more PVAc, there is a negative effect as it is not known for its moisture durability. Applying PVAc first shows more severe decrease in MOR2 than applying PF first or applying blend (Figure 3-15).

As for IB strength (Figure 3-16 and Figure 3-17), applying PVAc first leads to an increase in internal bond strength (IB1) at an increasing rate than the other two sequences. At 4%PF level, applying PVAc is better especially at 6% PVAc. As PVAc percent is dominated in the blend and has more direct contact with wood, the ductility of PVAc plays an important role on increase in IB strength. However, after undergoing severe RH treatment, internal bond strength (IB2) lost its advantage with applying PVAc first compared to the other two applications sequences. This is further evidence of interference of PVAc with PF-wood interaction with increasing PVAc content when PVAc is applied to the strands first.



For 24hrs WA, applying blend shows the worst water resistance, however with an improvement with addition of more PVAc. As shown in Figure 3-19, applying blend is even better than the other two application sequences when PVAc is dominant in the blend (6%PVAc and 4%PF). This could be related to the uniform morphology of resin blend with more than 50% of the blend composed of PVAc, further explanation need to be explored.

As more PVAc is added in resin blend, PF penetration is more likely to be hindered. When the adhesive was sprayed onto strands, it covered the strands with uniform small droplets. It is known that PF has better penetration ability than PVAc due to its small molecular structure, which was also confirmed by the penetration quantification results discussed in Chapter 2. When applying PF first, PF penetrates into wood easily and forms a strong interaction with wood (Figure 3-21). Bond between PF/PVAc and wood strand could be further strengthened with addition of more PVAc to some extent. When applying PVAc first, it could not penetrate into wood as easily as PF and PVAc may form thin film quickly on strand surface and hinder the interaction between PF and wood strands and interfere with the penetration of PF, thus leading to less durable bonding among strands under severe condition.

As seen in Chapter 2, PF/PVAc was immiscible when the ratio was above 1. In an immiscible blend, the specimens could debond at the weakest point when the resins in the blend are not evenly distributed due to phase separation. The poor performance with applying blend rather than PF first, indicates that PVAc and PF could interfere with each other and result in neither of them interacting with wood adequately.

**Table 3-3 Statistics of Fitted Models for each Response**

Responses	Model	P-value			
		model	PF	PVAc	Sequences
MOE1 <sup>#</sup>	Reduced Linear	0.0736*	0.1232	NA	NA
MOE2 <sup>#</sup>	Reduced Linear	0.0174*	0.0174*	NA	NA
MOR1 <sup>#</sup>	Linear	0.0423**	0.3024	0.1217	0.0493**
MOR2 <sup>#</sup>	Quadratic	0.0214**	0.0056**	0.0463**	0.3583
IB1 <sup>#</sup>	2FI	<0.0001**	0.0069**	<0.0001**	0.0029**
IB2 <sup>#</sup>	Linear	<0.0001**	0.0385**	<0.0001**	0.0188**
WA <sup>2hrs#</sup>	Linear	0.0075**	0.0011**	0.0865	0.5403
TS <sup>2hrs<sup>^</sup>IS<sup>^</sup></sup>	Linear	0.0001**	<0.0001**	0.0055**	0.5324
WA <sup>24hrs# ^P<sup>^</sup></sup>	2FI	<0.0001**	<0.0001**	<0.0001**	0.1546
TS <sup>24hrs# ^I<sup>^</sup></sup>	Linear	0.0013**	0.0004**	0.0255**	0.3665

1-Specimens under normal condition (20°C, 65%RH); 2-Specimens under severe condition cycle treatment

<sup>#</sup> Response was adjusted by ANCOVA including density as covariate ; <sup>IS<sup>^</sup></sup> Data was under inverse square transformation; <sup>I<sup>^</sup></sup> Data was under inverse transformation; <sup>P<sup>^</sup></sup> Data was under Power transformation with a Lambda of -1.89; \*\*Significant at Alpha=0.05; \*Significant at Alpha=0.1

**Table 3-4 Percentage differences of hybrid adhesive with 6% PF and varying percent of PVAc relative to control test panels bonded with only 6%PF (All values in cells are percents)**

PF 6%												
PVAc	1%				2%				6%			
Sequences	PF	PVAc	Blend	Avg	PF	PVAc	Blend	Avg	PF	PVAc	Blend	Avg
MOE1	-4.5	-3.9	-6.3	-4.9	4.2	8.4	17.3	10.0	12.8	-7.3	-8.9	-1.2
MOE2	-9.2	9.2	-7.4	-2.5	0.4	4.7	21.6	8.9	17.4	2.5	-5.1	4.9
MOR1	-1.3	-13.9	-18.7	-11.3	3.3	-6.9	2.0	-0.5	9.4	-6.0	-11.1	-2.6
MOR2	-12.0	1.6	-15.6	-8.7	3.8	-0.4	5.6	3.0	5.4	-2.3	-6.9	-1.2
IB1	65.5	4.6	-34.5	11.9	56.3	33.3	-8.0	27.2	86.2	101.1	33.3	73.6
IB2	60.0	-17.3	-34.7	2.7	38.7	36.0	9.3	28.0	102.7	88.0	44.0	78.2
2hrs-WA	-16.9	0.0	27.3	3.5	-14.3	-1.3	9.1	-2.2	-7.8	-1.3	-14.3	-7.8
24hrs-WA	2.7	5.4	14.9	7.7	-9.5	-2.7	4.1	-2.7	-8.8	-6.8	-6.8	-7.4
2hrs-TS	4.0	12.0	52.0	22.7	-4.0	-4.0	36.0	9.3	-4.0	-8.0	-4.0	-5.3
24hrs-TS	-14.3	-5.4	0.0	-6.5	-17.9	-7.1	10.7	-4.8	-23.2	-17.9	-7.1	-16.1

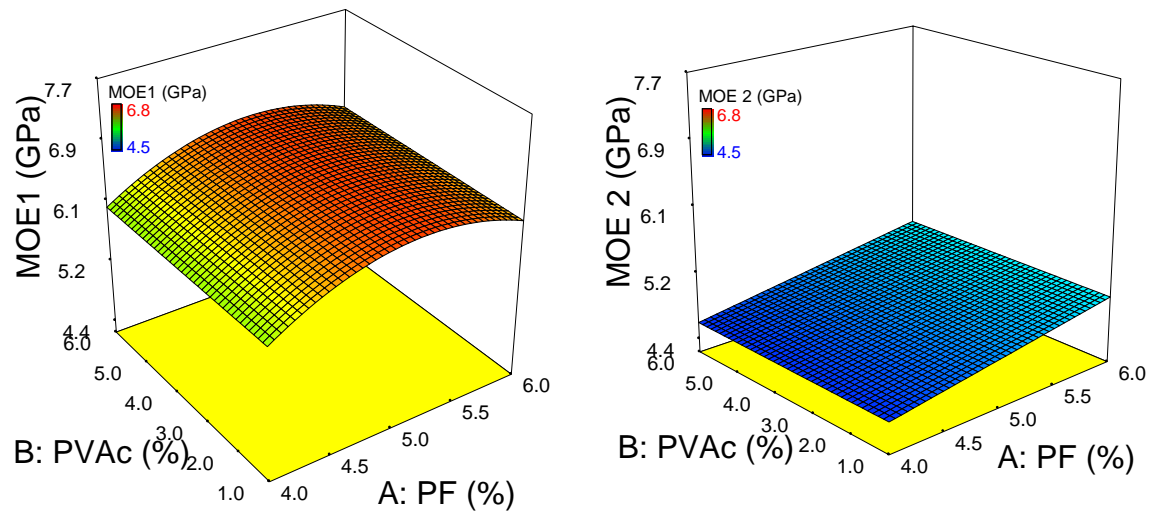


**Figure 3-9 Model graphs of MOE1 and MOE2**

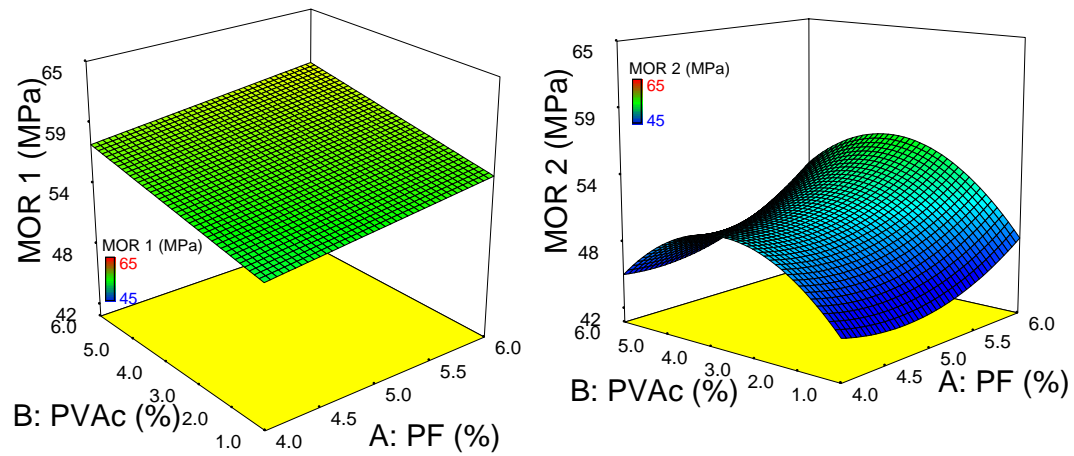


**Figure 3-10 Model graphs of MOR 1 and MOR 2**

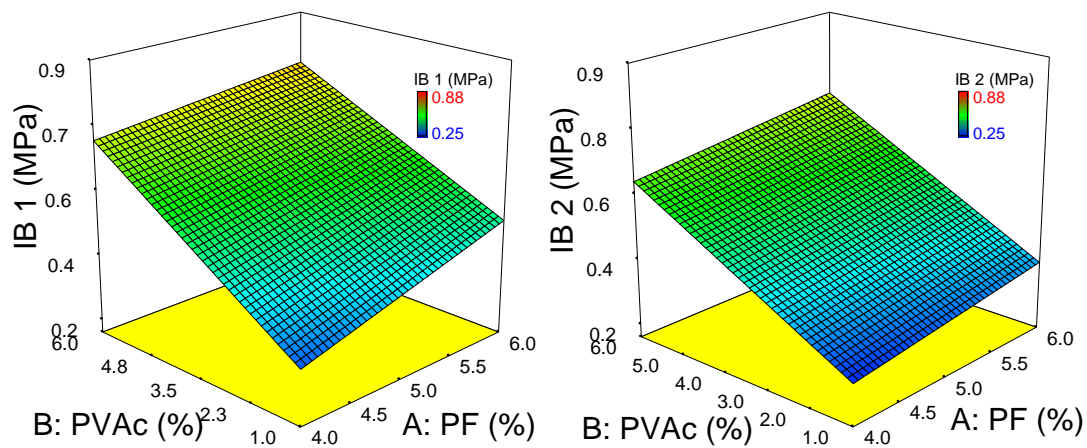


**Figure 3-11 Model graphs of IB 1 and IB 2**

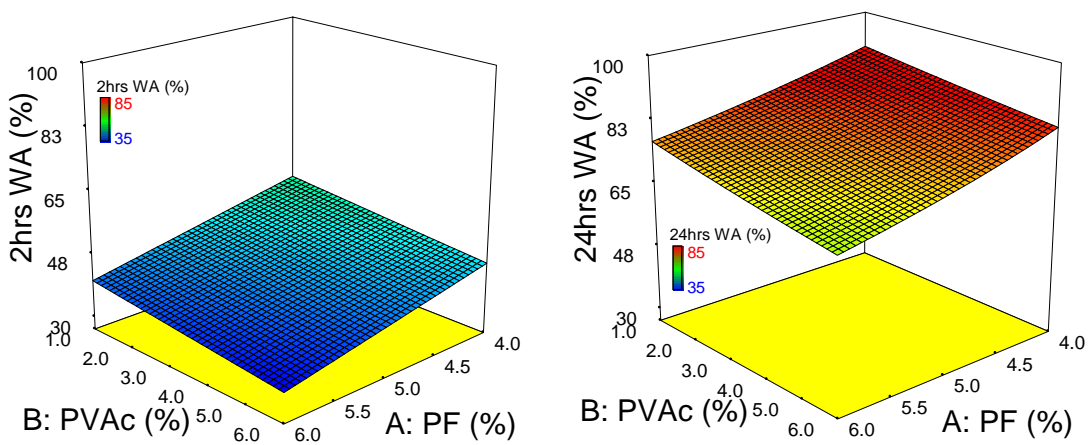


**Figure 3-12 Model graphs of 2hrs and 24hrs WA**

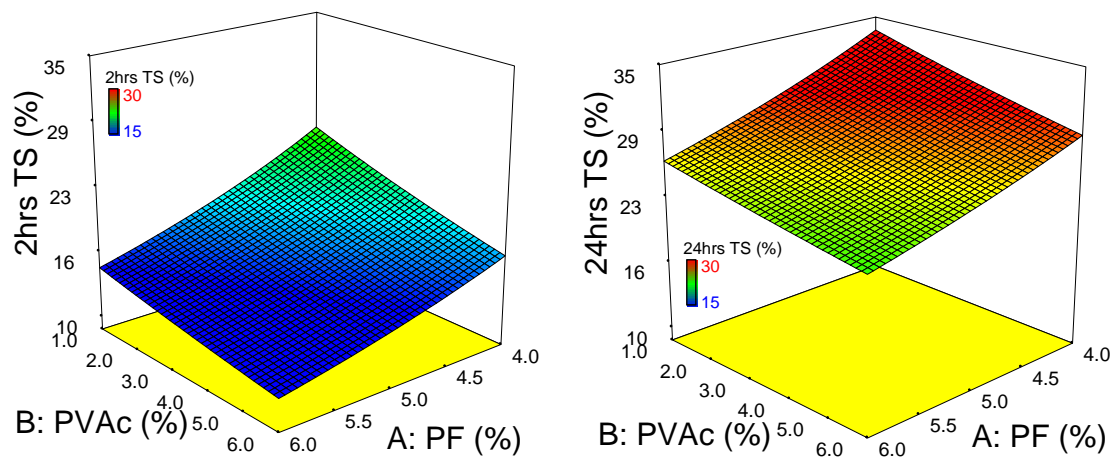


Figure 3-13 Model graphs of 2hrs and 24hrs TS

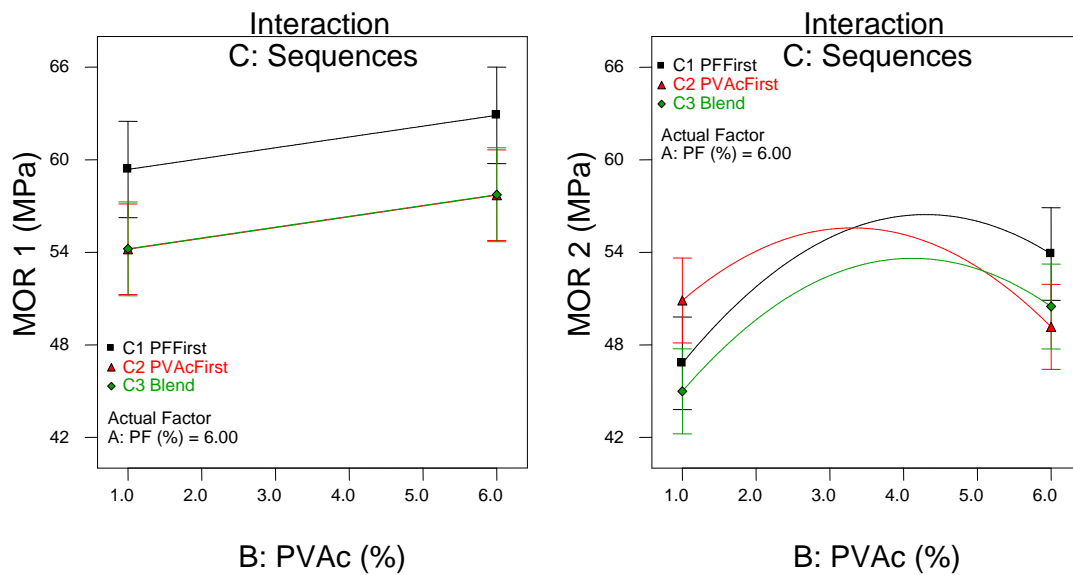
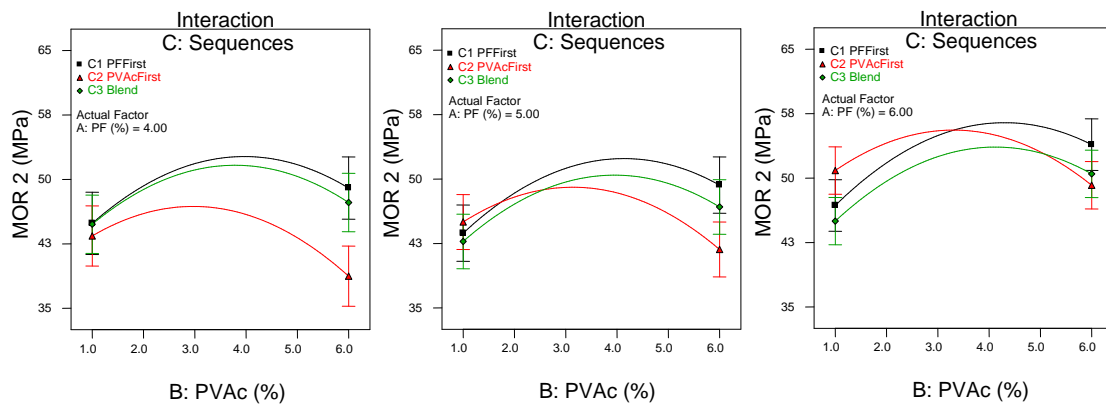
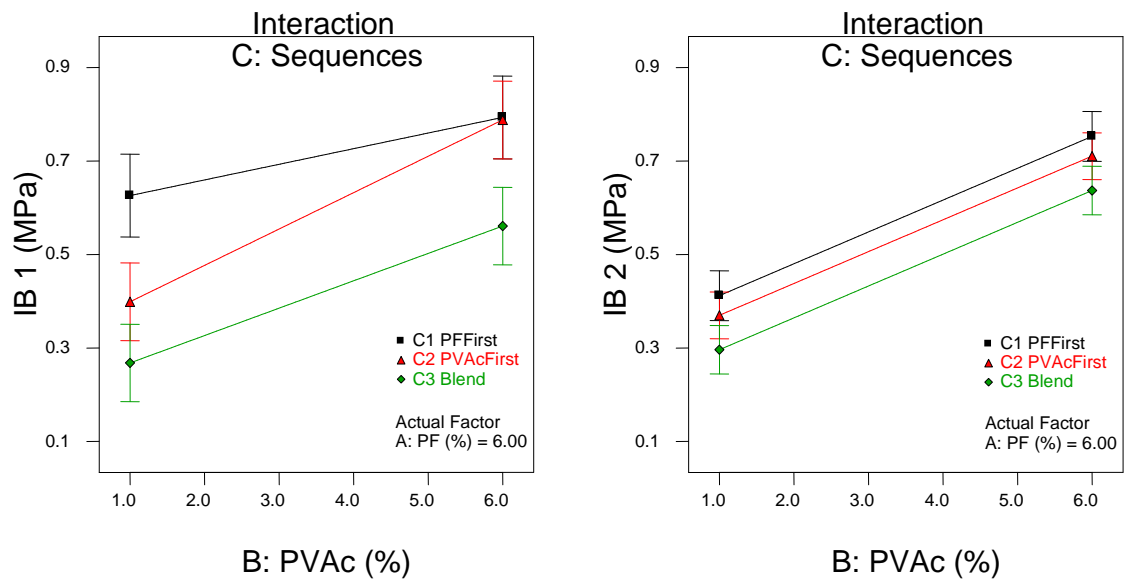


Figure 3-14 Effect of application sequence on MOR1 and MOR2



**Figure 3-15 Interaction of application sequences of MOR2 at 4%PF, 5%PF and 6%PF, respectively**



**Figure 3-16 Effect of application sequence on IB1 and IB2**

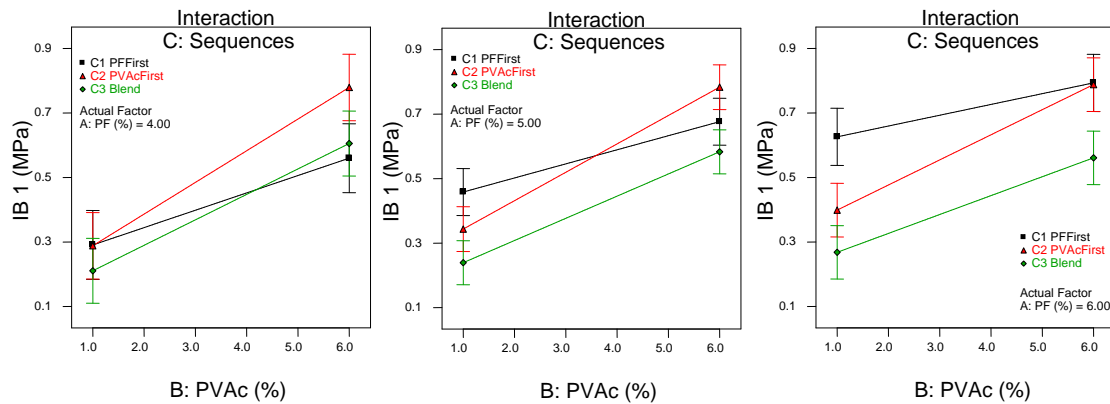


**Figure 3-17 Interaction of application sequences of IB1 at 4%PF, 5%PF and 6%PF, respectively**

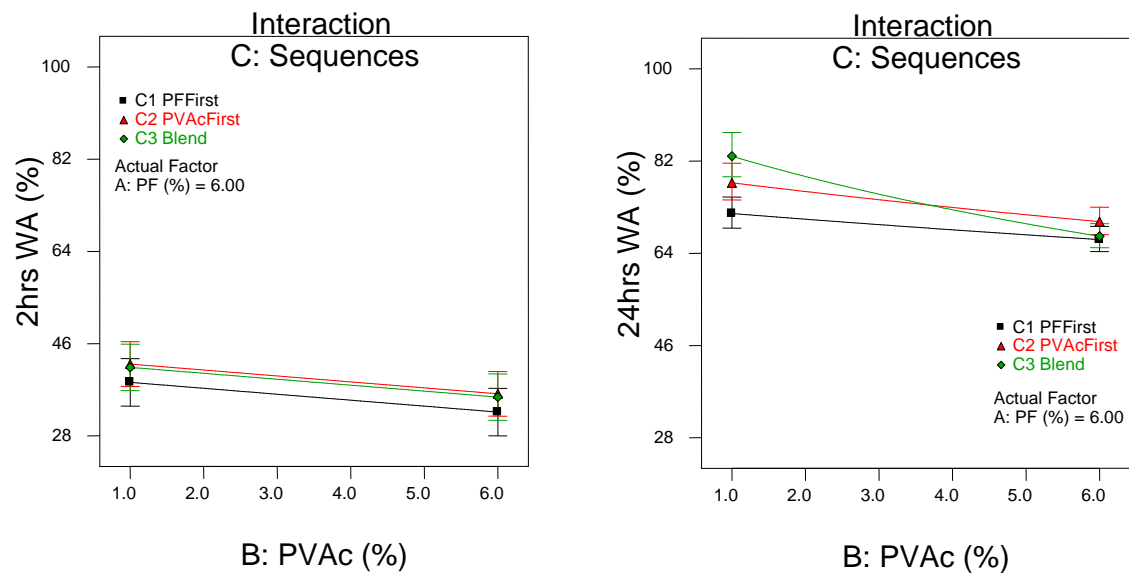


**Figure 3-18 Effect of application sequence on 2hrs WA and 24hrs WA**



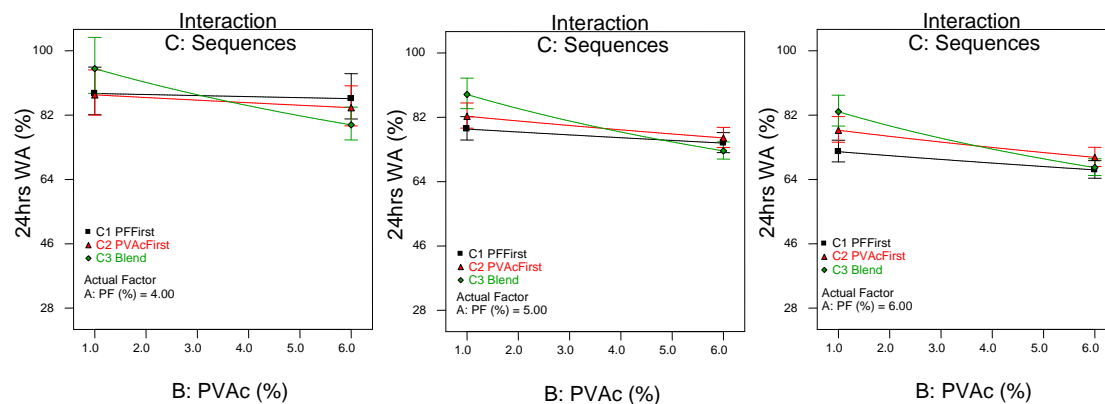


**Figure 3-19 Interaction of application sequences of 24hrs WA at 4%PF, 5%PF and 6%PF, respectively**

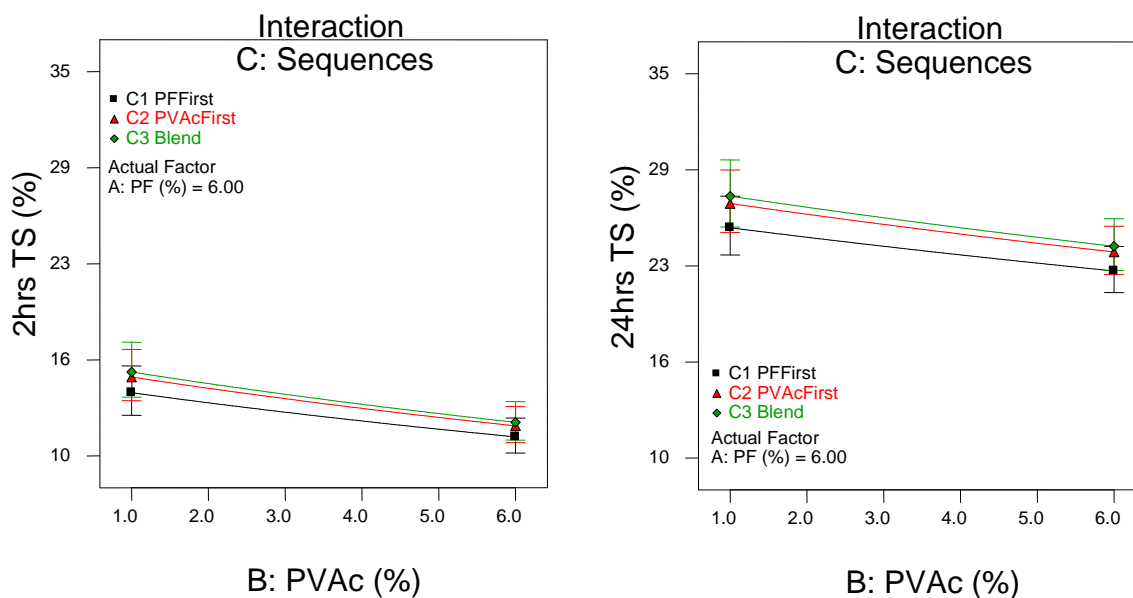


**Figure 3-20 Effect of application sequence on 2hrs TS and 24hrs TS**

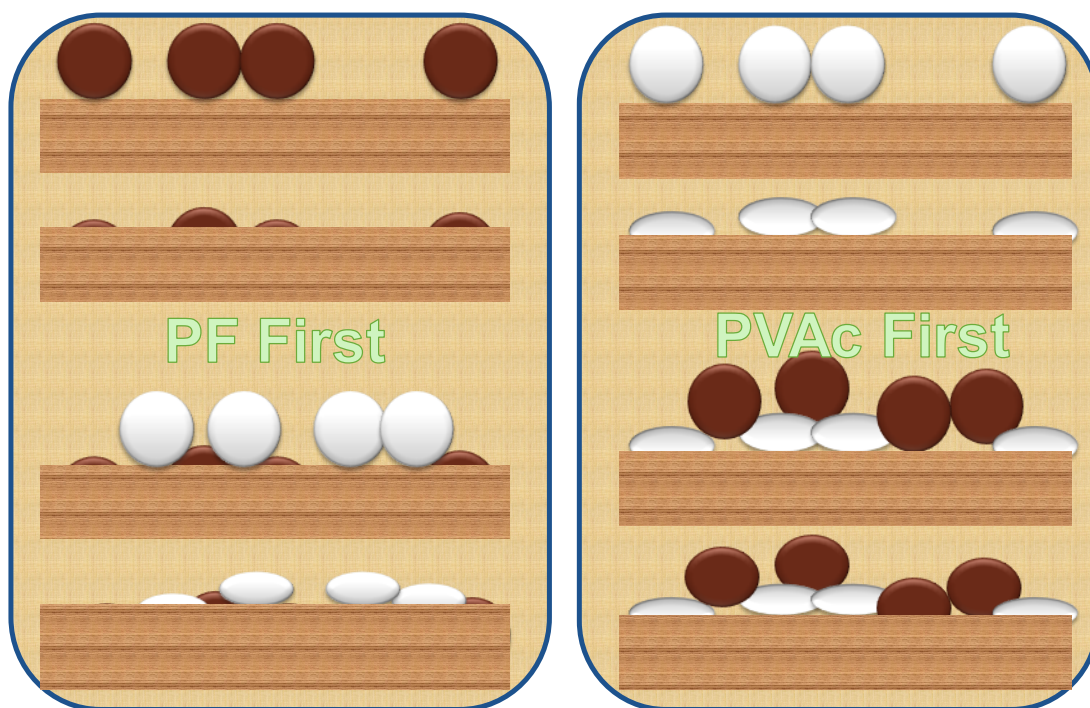


**Figure 3-21 Speculated mechanism of applying PF first and applying PVAc first, respectively**

## Optimization

A numerical optimization was conducted in Design-Expert<sup>®</sup> to determine optimum solutions (PF/PVAc ratios and sequence of application) which simultaneously satisfy the requirements placed on each factor and response. For optimization purposes, the insignificant terms of some responses with relatively low predicted  $R^2$  were removed from the model using backward elimination regression with a significance level of 0.1. This helped to reduce noise and create a model with better prediction capabilities. However, both MOE and MOR had relatively small predicted  $R^2$  for the reduced model, which means there are other factors excluded from this experiment design greatly influences the MOE and MOR. Therefore, MOE and MOR were excluded from the optimization process. All responses were set up according to their level of importance from 1 to 3, with 3 being the highest. IB1 was assigned a range from 0.43 MPa to 0.95 MPa, with 0.43 MPa as the average for control specimens with 6% PF (typical required OSB IB is ~0.35 MPa). IB2 was given a range from 0.38 MPa to 0.75 MPa, with 0.38 MPa as the average for control specimens. All other factors were minimized. PVAc is minimized in the range of 1% to 5% since PVAc with more than 5% shows negative effect on MOR2, which implies a PVAc percent threshold. Four optimized solutions are shown below in Table 3-6. A PF/PVAc ratio ranging from 1:0.6 to 1:0.77 were suggested to produce wood-strand panels with comparable properties when bonded with only 6% PF. These results reinforce findings of Wang et al. (2010) that as long as proportion of PVAc is less than 0.5 in a PF/PVAc resin blend, it does not significantly hinder the bond formation and performance development with PF resin. Based on the first solution with a desirability of 0.506, all responses were predicted as a reference and compared against control 6% PF (Table 3-7). MOE, MOR, WA and TS of the optimal PF/PVAc ratio are all comparable with that of control 6% PF, and IB shows at least 30% better than that of

control 6%PF.

**Table 3-5 Optimization criteria for wood strand panel properties**

<b>Name</b>	<b>Goal</b>	<b>Lower Limit</b>	<b>Upper Limit</b>	<b>Importance</b>
<b>PF (%)</b>	<b>minimize</b>	<b>4</b>	<b>6</b>	<b>3</b>
<b>PVAc (%)</b>	<b>minimize</b>	<b>1</b>	<b>5</b>	<b>1</b>
<b>Sequences</b>	<b>is in range</b>	<b>PFFirst</b>	<b>Blend</b>	<b>3</b>
<b>IB 1 (MPa)</b>	<b>is in range</b>	<b>0.43</b>	<b>0.95</b>	<b>3</b>
<b>IB 2 (MPa)</b>	<b>is in range</b>	<b>0.38</b>	<b>0.75</b>	<b>3</b>
<b>2hrs WA (%)</b>	<b>minimize</b>	<b>28.7</b>	<b>67.0</b>	<b>2</b>
<b>2hrs TS (%)</b>	<b>minimize</b>	<b>9.7</b>	<b>31.6</b>	<b>2</b>
<b>24hrs WA (%)</b>	<b>minimize</b>	<b>64.8</b>	<b>104.6</b>	<b>2</b>
<b>24hrs TS (%)</b>	<b>minimize</b>	<b>18.5</b>	<b>45.5</b>	<b>2</b>

**Table 3-6 Four optimized solutions for wood strand panels performance**

<b>#</b>	<b>PF (%)</b>	<b>PVAc (%)</b>	<b>Sequences</b>	<b>IB 1 (MPa)</b>	<b>IB 2 (MPa)</b>	<b>2hrs WA (%)</b>	<b>2hrs TS (%)</b>	<b>24hrs WA (%)</b>	<b>24hrs TS (%)</b>	<b>Desirability</b>
<b>1</b>	<b>4.99</b>	<b>3.06</b>	<b>PFFirst</b>	<b>0.6</b>	<b>0.5</b>	<b>44</b>	<b>16</b>	<b>77</b>	<b>28</b>	<b>0.506</b>
<b>2</b>	<b>4.84</b>	<b>3.41</b>	<b>PVAcFirst</b>	<b>0.6</b>	<b>0.5</b>	<b>44</b>	<b>17</b>	<b>79</b>	<b>28</b>	<b>0.499</b>
<b>3</b>	<b>4.85</b>	<b>3.72</b>	<b>Blend</b>	<b>0.5</b>	<b>0.4</b>	<b>44</b>	<b>16</b>	<b>80</b>	<b>28</b>	<b>0.493</b>
<b>4</b>	<b>4.84</b>	<b>3.71</b>	<b>Blend</b>	<b>0.5</b>	<b>0.4</b>	<b>44</b>	<b>16</b>	<b>80</b>	<b>28</b>	<b>0.493</b>

**Table 3-7 Comparison of Optimized solution with control of 6%PF**

<b>Response</b>	<b>Prediction</b>	<b>6%PF</b>	<b>Response</b>	<b>Prediction</b>	<b>6%PF</b>
<b>MOE1 (GPa)</b>	<b>6.63</b>	<b>6.34</b>	<b>MOE 2 (GPa)</b>	<b>4.8</b>	<b>4.87</b>
<b>MOR 1 (MPa)</b>	<b>61</b>	<b>60.4</b>	<b>MOR 2 (MPa)</b>	<b>49</b>	<b>51.38</b>
<b>IB 1 (MPa)</b>	<b>0.6</b>	<b>0.435</b>	<b>IB 2 (MPa)</b>	<b>0.5</b>	<b>0.38</b>
<b>2hrs WA (%)</b>	<b>44</b>	<b>38.45</b>	<b>24hrs WA (%)</b>	<b>77</b>	<b>74.1</b>
<b>2hrs TS (%)</b>	<b>16</b>	<b>12.2</b>	<b>24hrs TS (%)</b>	<b>28</b>	<b>28</b>

## **Summary and Conclusions**

This study explored the effect of PF/PVAc ratios and application sequence on wood strand composite performances. Response surface model is applied to understand the changing trends of mechanical and physical properties with varying PF/PVAc ratio and resin application sequences. Based on the results above, several conclusions can be drawn:

- MOE is not significantly affected by change in resin ratio, but is suspected to be influenced by different application sequences
- MOR is slightly improved with increase of PVAc under normal condition
- Small amount of PVAc has a positive effect on MOR under severe RH treatment whereas turns to a negative effect as PVAc is increased beyond 5% because of PVAc's poor moisture resistance
- Internal bond strength under both normal and severe condition continuously increases with addition of PVAc up to 6%

- Addition of PVAc has a significant influence on reducing water absorption and thickness swelling although the effect is much less effective than adding the same amount of PF
- In general, applying PF first lead to better performance
- Application of PVAc first at a proportion of PVAc beyond optimum ratio could be detrimental to panel performance when exposed to severe relative humidity conditions that allowed the panel to undergo shrinking and swelling.
- PF/PVAc ratio is optimized in a range from 1:0.6 to 1:0.77 to obtain desired mechanical properties and dimensional stability of wood strand composites for further study

## References

- Adams, R., and Broline, B. (2006). "A practical overview of resin systems for OSB." *International wood composites symposium*, Seattle, WA.
- Adams, W. (2006). "Handbook for Experimenters, Version 7.3, Stat-Ease." *Inc., Minneapolis, MN, USA*.
- ASTM Standard. (2006). *ASTM D1037 - 99 Standard Test Methods for Evaluating Properties of Wood-Base Fiber and Particle Panel Materials*.
- Bach, L. (1989). "Manufacture of corrugated waferboard." *Forest Products Journal*, 39(10), 58–62.
- Caughey, R. A., Haataja, B. A., Kilpela, T. B., and Hamilton, J. F. (1981). "Pallet having densified edge and method of making same."
- Geimer, R. L., and Christiansen, A. W. (1996). "Critical variables in the rapid cure and bonding of phenolic resins." *Forest Products Journal and Index*, 46(11), 67–72.
- Geimer, R. L., and Lehmann, W. F. (1977). "Combination sheathing support-member building product."
- Hann, R. A., Black, J. M., and Blomquist, R. F. (1962). "How durable is particleboard." *Forest Prod. J*, 12(12), 577–84.
- Hansen, E. (2006). "Structural panel industry evolution: Implications for innovation and new product development." *Forest Policy and Economics*, 8(7), 774–783.
- Hse, C. Y., Koch, P., Mcmillin, C. W., and Price, E. W. (1975). "Laboratory-scale development of a structural exterior flakeboard from hardwoods growing on southern pine sites." *Forest Products Journal*, 25(4), 42-50.
- Hsu, W. E. (1997). "Wood quality requirements for panel products." *Proceeding of CTIA/IUFRO International Wood Quality Workshop, Timber Management toward Wood Quality and End-product Value. Forintek Canada Corp. Québec City, Canada. I-7/10*.
- Kelly, M. (1977). "Critical literature review of relationships between processing parameter and physical properties of particleboard." *General Technical Report FPL*, 10.
- LeBlanc, J., Mass, W., and Miller, R. (1971). "Corrugated Fiberboard."
- Lee, O., and Tahir, P. (2003). "Effects of fine particle content on the properties of five-layered oriented strand board - Google Search." *Congress proceedings*, <<http://www.google.com/search?q=Effects+of+fine+particle+content+on+the+properties+of+five-layered+oriented+strand+board&ie=utf-8&oe=utf-8&aq=t&rls=org.mozilla:en-US:official&client=firefox-a>> (Jul. 12, 2010).
- Lehmann, W. F. (1970). "Resin efficiency in particleboard as influenced by density, atomization, and resin content." *Forest Products Journal*, 20(11), 48–54.
- Linville, J. D. (2000). "The influence of a horizontal density distribution on moisture-related mechanical degradation of oriented strand composites." Ph.D Dissertation, Washington State University, Pullman, WA.
- Marra, A. A. (1992). *Technology of wood bonding*. Van Nostrand Reinhold.
- Pang, W., Sandberg, L., Laks, P., and Forsman, J. (2007). "Corrugated strandboard structural panels." *Forest Products Journal*, 57(3), 48-53.

- Papadopoulos, A. N., Hill, C. A. S., Traboulay, E., and Hague, J. R. B. (2002). "Isocyanate resins for particleboard: PMDI vs EMDI." *European Journal of Wood and Wood Products*, 60(2), 81–83.
- Park, B., Riedl, B., Hsu, E., and Shields, J. (1999). "Hot-pressing process optimization by response surface methodology." *Forest Products Journal*, 49(5), 62–68.
- Phillips, E. (2000). "Yesterday's successes and tomorrow's challenges." *Wood Adhesives Session 3A Composite Panel Resin Systems*, South Lake Tahoe, Nevada.
- Post, P. W. (1958). "Effect of particle geometry and resin content on bending strength of oak flake board." *Forest Products Journal*, 317–322.
- Preechatiwong, W., Yingprasert, W., and Kyokong, B. (2007). "Effects of phenol-formaldehyde/isocyanate hybrid adhesives on properties of oriented strand lumber (OSL) from rubberwood waste." *Songklanakarin Journal of Science and Technology*, 29(5), 1367–1375.
- Qiao, L., and Easteal, A. J. (2001). "Aspects of the performance of PVAc adhesives in wood joints." *Pigment & Resin Technology*, 30(2), 79–87.
- Sellers, T. (2000). "Growing markets for engineered products spurs research." *Wood Technol.*, 127(3), 40–43.
- Shi, J. L., Zhang, S. Y., Riedl, B., and Brunette, G. (2005). "Flexural properties, internal bond strength, and dimensional stability of medium density fiberboard panels made from hybrid poplar clones." *Wood and Fiber Science*, 37(4), 629–637.
- Silknitter, K. O., Wisnowski, J. W., and Montgomery, D. C. (1999). "The analysis of covariance: a useful technique for analysing quality improvement experiments." *Quality and Reliability Engineering International*, 15(4), 303–316.
- Simpson, W., and TenWolde, A. (1999). "Wood handbook-wood as an engineering material." *Gen. Tech. Rep. FPL-GTR-113. Department of Agriculture, Forest Service. Forest Products Laboratory. Madison, WI, EUA*, 463.
- Sivachenko, E. W. (1978). "High strength corrugated metal plate and method of fabricating same."
- Spelter, H., McKeever, D., and Alderman, M. (2006). "Status and trends: Profile of structural panels in the United States and Canada." *Research Paper FPL–RP–636*.
- Stat-ease (2005). *Helps in Stat-ease software*.
- Talabgaew, S., and Laemlaksakul, V. (2007). "Experimental Studies on the Mechanical Property of Laminated Bamboo in Thailand." *International Journal of Mathematical, Physical and Engineering Sciences*, 1, 327–331.
- Vital, B., Lehmann, W. F., and Boone, R. S. (1974). "How species and board densities affect properties of exotic hardwood particleboards." *Forest Products Journal*, 24(12), 37–45.
- Voth, C. R. (2009). "Lightweight sandwich panels using small-diameter timber wood-strands and recycled newsprint cores." Washington State University, Pullman, WA.
- Wang, K., and Lam, F. (1999). "Quadratic RSM Models of Processing Parameters for Three-Layer Oriented Flakeboards." *Wood and Fiber Science*, 31(2), 173–186.
- Wang, S., and Winistorfer, P. M. (2003). "An optical technique for determination of layer thickness swell of MDF and OSB." *Forest Products Journal*, 53(9), 64–71.
- Wang, S. Y., Yang, T. H., Lin, L. T., Lin, C. J., and Tsai, M. J. (2007). "Properties of low-formaldehyde-emission particleboard made from recycled wood-waste chips sprayed with PMDI/PF resin." *Building and Environment*, 42(7), 2472–2479.
- Wang, Y., Yadama, V., Marie, P. L., and Debes, B. (2010). "Cure Kinetics of PF/PVAC hybrid



- adhesive for Manufacturing Profiled Wood-Strand Composites.” *Holzforschung In press*.
- Winistorfer, P. M., Young, T. M., and Walker, E. (1996). “Modeling and comparing vertical density profiles.” *Wood and Fiber Science*, 28(1), 133.
- Wu, Q., and Piao, C. (1999). “Thickness swelling and its relationship to internal bond strength loss of commercial oriented strandboard.” *Forest Products Journal*, 49(7/8), 50–55.
- Wu, Q., and Suchsland, O. (1997). “Effect of moisture on the flexural properties of commercial oriented strandboards.” *Wood and Fiber Science*, 29(1), 47–56.
- Wu, Q., and Lee, J. (2002). “Thickness swelling of oriented strandboard under long-term cyclic humidity exposure condition.” *Wood and Fiber Science*, 34(1), 125-139.
- Xu, W. (1999). “Influence of vertical density distribution on bending modulus of elasticity of wood composite panels: A theoretical consideration.” *Wood and fiber science*, 31(3), 277–282.
- Zhou, D. (1990). “A study of oriented structural board made from hybrid poplar: physical and mechanical properties of OSB.” *Holz als Roh-und Werkstoff*, 48(7-8), 293–296.

## **CHAPTER 4 PROJECT SUMMARY, CONCLUSIONS AND FURTHER WORK**

### **Summary and Conclusions**

Profiled wood composite, a value-added product, is able to realize high performance with fewer raw materials. Manufacturing methods, such as roll-forming, shows promise for profiled wood strand composites because it is in a continuous processing flow which is easier for manufacturing application. However, this kind of methods requires good tackiness to compensate the dislocation of wood strand elements in loose mats during handling. This study evaluated the effectiveness of a multi-functional hybrid adhesive system, phenol-formaldehyde (PF) / polyvinyl acetate emulsion (PVAc) to solve difficulty in such manufacture process. This binary adhesive has an initial tackiness from PVAc that retains mat integrity at room temperature. Durable bonding of wood strand composites can be achieved as the mat go through shape forming process, accompanying with curing of PF under heat and pressure treatment.

This study is based on the cure kinetics study of the PF/PVAc hybrid and its bond development in a multi-step hot-pressing schedule (Wang et al. 2010); and is further investigated regarding PF/PVAc adhesive –wood interactions, as well as its processing parameters, which contributes to developing a continuous manufacturing method for profiled wood strand composites. This thesis project systematically investigated the PF/PVAc binary adhesive interaction with varying proportions at different scales. This research studied the interaction between the PF and PVAc in the resin blend and between the hybrid adhesive and the wood substrate; and also evaluated the performance of the wood strand panels that contained the PF/PVAc hybrid adhesive.

The first part of the study comprehensively characterized the interaction between PF/PVAc hybrid adhesive and the wood at the macro-scale and micro-scale, as well as evaluating the physical properties of the hybrid adhesive. The pH of PF/PVAc hybrid adhesive showed no significant difference from neat PF, remaining strongly alkaline. The viscosity of the binary adhesive decreased at first when a small portion of PVAc was added, and increased dramatically as more than 50% PVAc was added in the blend. Assembly joints glued on both tangential and radial surfaces were manufactured and tested to elucidate adhesive bond performance (shear stress and wood failure), as well as adhesive penetration. Adhesive bond performance on a tangential glued surface of sugar maple was superior to that of a radial glued surface, although no significant difference was found in adhesive penetration. Bond performance and adhesive penetration did not decrease significantly when PVAc content was below 50%, whereas they deteriorated significantly when PVAc made up more than 50% of the resin blend.

The second part of the study investigated the performance of wood strand composites using the hybrid adhesive, in order to identify the interference of PVAc between PF and wood strands in terms of mechanical properties and dimensional stability. The study also evaluated the effects of different adhesive application sequence effects in order to improve manufacturing process. The study found that the addition of PVAc did not contribute to the MOE, but did have an effect on the MOR. Under severe conditions, MOR increased as PVAc content increased as long as PVAc content was less than 5%. However, the MOR decreased once the PVAc content rose beyond 5%. We speculated that a small amount of PVAc improves the bond between wood strands due to its good deformability, whereas too much PVAc weakens this bond due to PVAc's poor moisture resistance. Internal bonding strength was continuously enhanced with the addition

of either PVAc, PF or both. This same trend also occurred in regard to water absorption and thickness swelling. In most cases, applying PF is superior to the other two sequences in terms of both mechanical properties and water resistance. Some interaction between the application sequence and PVAc content in MOR and IB indicates that PVAc at a certain high load level may deteriorate with the bond between PF and wood strands, especially under severe RH treatment. This study provided an optimized resin blend ratio ranging from 1:0.6 to 1:0.77, and also provided predicted properties as a reference for further study.

### **Further Work**

This study provides an important framework for larger projects. However, more research is needed before this hybrid adhesive should be used in commercial application. In terms of hybrid adhesive-wood interaction, studies on adhesive penetration at the nano-scale would provide further information on penetration of this PF/PVAc hybrid adhesive. As PF has been confirmed that can penetrate into wood cell walls (Gindl et al. 2004; Laborie 2002), it is important to understand the interfere of PVAc on penetration at nano-scale. Moreover, to validate the optimization of wood strand composite performance, it is necessary to fabricate wood composites with the suggested blend ratios. Another interesting avenue for future research includes the processing of profiled wood strand composites and the study of other processing parameters.

## References

- Gindl, W., Schöberl, T., and Jeronimidis, G. (2004). "The interphase in phenol-formaldehyde and polymeric methylene di-phenyl-di-isocyanate glue lines in wood." *International Journal of Adhesion and Adhesives*, 24(4), 279–286.
- Laborie, M. (2002). "Investigation of the wood/phenol-formaldehyde adhesive interphase morphology." PhD. Dissertation, Virginia Polytechnic Institute and State University, Blacksburg, Virginia.
- Wang, Y., Yadama, V., Laborie, M., and Bhattacharyya, D. (2010). "Cure Kinetics of PF/PVAC hybrid adhesive for Manufacturing Profiled Wood-Strand Composites." *Holzforschung*, In press.

## APPENDIX A HOT PRESS SCHECULE

**Table A-1 Hot press schedule**

<b>Segment</b>	<b>Control</b>	<b>Setpoint</b>	<b>Seg. Time (s)</b>	<b>End Condition</b>
<b>1</b>	<b>Fastposn</b>	<b>-1.27cm/s</b>	<b>10s</b>	<b>Position &lt;=2.54cm</b>
<b>2</b>	<b>Position</b>	<b>50%</b>	<b>1s</b>	
<b>3</b>	<b>Position</b>	<b>0.66cm</b>	<b>20s</b>	
<b>4</b>	<b>Position</b>	<b>0.66cm</b>	<b>240s</b>	
<b>5</b>	<b>Pressure</b>	<b>0.2MPa</b>	<b>75s</b>	
<b>6</b>	<b>Pressure</b>	<b>0.14MPa</b>	<b>75s</b>	
<b>7</b>	<b>Pressure</b>	<b>0MPa</b>	<b>75s</b>	
<b>8</b>	<b>Fastposn</b>	<b>1.27cm/s</b>	<b>20s</b>	<b>Position&gt;=25.4cm</b>

## APPENDIX B STATISTICS ON BOND PERFORMANCE

**Table B-1 P-values of ANOVA & ANCOVA considering density as covariate on tangential surface**

Pr>F	ANOVA		ANCOVA		
	Shear Stress	Wood Failure	Effective Penetration	Max penetration	# of penetrated lumens
Percentage	0.0009**	<0.0001**	<0.0001**	0.0009**	0.0002**
Density	NA	NA	0.0004**	0.0198**	0.0008**

**Table B-2 P-values of ANOVA & ANCOVA considering density as covariate on radial surface**

Pr>F	ANOVA		ANCOVA		
	Shear Stress	Wood Failure	Effective Penetration	Max penetration	# of penetrated lumens
Percentage	0.0369**	0.4015	0.0023**	0.0599	<0.0001**
Density	NA	NA	0.0092**	0.0104**	0.0007**

**Table B-3 Bond performances of assembly joints with wood on tangential surfaces based on SAS output**

<b>PF Percent (%)</b>	<b>Shear Stress (MPa)</b>	<b>Wood Failure</b>	<b>Effective Penetration (μm)</b>	<b>Max penetration(μm)</b>	<b># of penetrated lumens</b>
<b>100</b>	<b>26.12</b>	<b>58%</b>	<b>75.8</b>	<b>549</b>	<b>32</b>
<b>80</b>	<b>26.03</b>	<b>55%</b>	<b>79.4</b>	<b>523</b>	<b>36</b>
<b>75</b>	<b>27.23</b>	<b>48%</b>	<b>78.3</b>	<b>523</b>	<b>33</b>
<b>67</b>	<b>25.06</b>	<b>51%</b>	<b>63.5</b>	<b>469</b>	<b>31</b>
<b>50</b>	<b>20.35</b>	<b>28%</b>	<b>77.8</b>	<b>375</b>	<b>27</b>
<b>25</b>	<b>22.67</b>	<b>15%</b>	<b>58.6</b>	<b>335</b>	<b>20</b>
<b>0</b>	<b>26.07</b>	<b>1%</b>	<b>50.8</b>	<b>277</b>	<b>14</b>

**Table B-4 Bond performances of assembly joints with wood on radial surfaces based on SAS output**

<b>PF Percent (%)</b>	<b>Shear Stress (MPa)</b>	<b>Wood Failure</b>	<b>Effective Penetration (μm)</b>	<b>Max penetration(μm)</b>	<b># of penetrated lumens</b>
<b>100</b>	<b>21.60</b>	<b>45%</b>	<b>91.6</b>	<b>710</b>	<b>40</b>
<b>75</b>	<b>20.21</b>	<b>49%</b>	<b>77.5</b>	<b>572</b>	<b>34</b>
<b>50</b>	<b>22.08</b>	<b>60%</b>	<b>97.6</b>	<b>684</b>	<b>36</b>
<b>25</b>	<b>16.65</b>	<b>33%</b>	<b>56.9</b>	<b>363</b>	<b>20</b>
<b>0</b>	<b>21.40</b>	<b>33%</b>	<b>54.1</b>	<b>394</b>	<b>17</b>



## APPENDIX C STATISTICS ON PROPERTIES OF WOOD STRAND COMPOSITES

**Table C-1 Statistics of fitted models for each response**

**1- Specimens under normal condition (20°C, 65%RH)**

**2-Specimens under severe condition cycle treatment**

**# Response was adjusted by ANCOVA including density as covariate**

**<sup>^IS^</sup> Data was under inverse square Transformation**

**<sup>^I^</sup> Data was under inverse square Transformation**

**<sup>^P^</sup> Data was under Power Transformation with a Lambda of -1.89**

**\*\*Significant at Alpha=0.05**

**\*Significant at Alpha=0.1**

Responses	Model	P-value					
		model	Predicted R <sup>2</sup>	lack of fit	PF	PVAc	Sequences
MOE1 <sup>#</sup>	Reduced Linear	0.0736*	0.005	0.4711	0.1232	NA	NA
MOE2 <sup>#</sup>	Reduced Linear	0.0174*	0.0776	0.2913	0.0174*	NA	NA
MOR1 <sup>#</sup>	Linear	0.0423**	0.0127	0.7528	0.3024	0.1217	0.0493**
MOR2 <sup>#</sup>	Quadratic	0.0214**	-0.0105	0.629	0.0056**	0.0463**	0.3583
IB1 <sup>#</sup>	2FI	<0.0001**	0.6444	0.8077	0.0069**	<0.0001**	0.0029**
IB2 <sup>#</sup>	Linear	<0.0001**	0.7265	0.6228	0.0385**	<0.0001**	0.0188**
WA <sup>2hrs#</sup>	Linear	0.0075**	0.1769	0.1308	0.0011**	0.0865	0.5403
TS <sup>2hrs<sup>^IS^</sup></sup>	Linear	0.0001**	0.4341	0.2323	<0.0001* *	0.0055**	0.5324
WA <sup>24hrs# <sup>^P^</sup></sup>	2FI	<0.0001**	0.6232	0.2290	<0.0001* *	<0.0001**	0.1546
TS <sup>24hrs# <sup>^I^</sup></sup>	Linear	0.0013**	0.2797	0.5317	0.0004**	0.0255**	0.3665

**Table C-2 Summary of properties of wood strand composites**

<b>Response</b>	<b>Prediction</b>	<b>SE Mean</b>	<b>95% CI low</b>	<b>95% CI high</b>	<b>SE Pred</b>	<b>95% PI low</b>	<b>95% PI high</b>
<b>MOE1 (GPa)</b>	<b>6.63</b>	<b>0.21</b>	<b>6.21</b>	<b>7.05</b>	<b>0.55</b>	<b>5.51</b>	<b>7.75</b>
<b>MOR 1 (MPa)</b>	<b>61</b>	<b>1.69</b>	<b>57.08</b>	<b>64.05</b>	<b>5.36</b>	<b>49.54</b>	<b>71.58</b>
<b>IB 1 (MPa)</b>	<b>0.6</b>	<b>0.031</b>	<b>0.53</b>	<b>0.66</b>	<b>0.095</b>	<b>0.39</b>	<b>0.79</b>
<b>MOE 2 (GPa)</b>	<b>4.8</b>	<b>0.079</b>	<b>4.67</b>	<b>5.00</b>	<b>0.43</b>	<b>3.95</b>	<b>5.72</b>
<b>MOR 2 (MPa)</b>	<b>49</b>	<b>1.19</b>	<b>46.82</b>	<b>51.72</b>	<b>3.74</b>	<b>41.60</b>	<b>56.95</b>
<b>IB 2 (MPa)</b>	<b>0.5</b>	<b>0.028</b>	<b>0.45</b>	<b>0.57</b>	<b>0.087</b>	<b>0.33</b>	<b>0.69</b>
<b>2hrs WA (%)</b>	<b>44</b>	<b>1.29</b>	<b>41.20</b>	<b>46.47</b>	<b>7.03</b>	<b>29.43</b>	<b>58.24</b>
<b>1/Sqrt(2hrs TS (%))</b>	<b>0.248</b>	<b>4.492E-003</b>	<b>0.24</b>	<b>0.26</b>	<b>0.025</b>	<b>0.20</b>	<b>0.30</b>
<b>(24hrs WA (%))-1.89</b>	<b>0.000</b>	<b>9.053E-006</b>	<b>2.514E-004</b>	<b>2.892E-004</b>	<b>2.754E-005</b>	<b>2.128E-004</b>	<b>3.277E-004</b>
<b>1/(24hrs TS (%))</b>	<b>0.036</b>	<b>8.517E-004</b>	<b>0.034</b>	<b>0.038</b>	<b>4.652E-003</b>	<b>0.026</b>	<b>0.045</b>